FACULTY OF SCIENCE
UNIVERSITY OF COPENHAGEN

Master's Thesis

Nonlinear photon interactions in waveguides

Mantas Čepulkovskis

Supervisor: Anders Søndberg Sørensen

Submitted: 04-09-2017

Abstract

In this thesis, a general formalism is developed to investigate effective nonlinear photon-photon interactions for a system of multiple quantum emitters coupled to a waveguide. Two-level quantum emitters and a weak input coherent state field incident on one of the sides of a 1D waveguide is considered. The input field propagates along the waveguide and interferes with the emitted photons, giving rise to a rich range of nonlinear effects. In particular, the second-order correlation function and nonlinear output intensity are calculated, both of which in this method are not restricted by the number and placement of the emitters, nor the combination of light-matter coupling constants, which may differ depending on the propagation direction. The introduced approach is then used to investigate robustness of chiral waveguides due to imperfections – the coupling to the suppressed propagation direction.

Acknowledgements

First of all, I would like to thank my supervisor Anders Søndberg Sørensen for introducing me to this field, explaining various concepts that I did not understand, sharing his ideas and helping me throughout this project. Without him, I would have never been able to do this work. It was truly an honor to work with him.

I would also like to thank Sumanta Kumar Das for our discussions which would always clear things up in my mind and for reviewing this thesis. He gave countless comments, without which this thesis would have been nowhere near a presentable form. Additionally, I would like to thank everyone else at the Theoretical Quantum Optics group for the interesting discussions during the weekly group meetings.

Finally, I would like to thank my fiancée Arūnė Kažemėkaitytė for her emotional support during this project and my dear friend Jack Christopher Hutchinson Rolph, who proofread my thesis and was the best friend to me during my studies in Denmark.

Contents

Chapter 1

Introduction

Strong nonlinear photon interactions are necessary to build new optical devices operating on a level of a single quantum of light, such as a single-photon transistor [1] or a photon-photon gate for optical quantum information processing [2]. In vacuum, photons interact only due to quantum mechanical fluctuations [3], an effect which is far too weak for that purpose. Very well known nonlinear optical effects can be obtained in nonlinear optical media [4] due to the higher-order dependence of electric polarization with respect to the external field. However, these effects are small at low intensities. Recently, tremendous progress has been made in the field of nanophotonics [5], where the electromagnetic field is confined in the length scale of optical wavelengths and results in strong light-matter coupling. Such devices were used to demonstrate a quantum optical switch [6] and a photon-photon gate [7], where the strong light-matter coupling results in effective nonlinear interactions between photons at a single-photon level.

In particular, emitters which couple strongly to nanophotonic waveguides are promising systems for scalable quantum networks. Photons emitted into a guided waveguide mode with a near unity probability [8] can be used as propagating qubits, connecting stationary qubits of a quantum network. Effective nonlinear interactions of photons in a system of a quantum dot coupled to a photonic crystal waveguide was demonstrated [9], as well as a three-level system [10], a hybrid organic molecule-superconductor system [11] and a few quantum emitters coupled to a waveguide were investigated [12] among other works. Also, chiral waveguides – waveguides that couple only to one propagation direction – have been investigated [13, 14] and are promising systems for engineering on-chip quantum networks [15].

Recently, a coupling of a large number of cesium atoms (~2000) to an optical glass fiber waveguide was demonstrated [16, 17]. Theoretically, it is difficult and computationally demanding to investigate the nonlinear properties of a system with such a large number of emitters. A method to do this efficiently is then necessary, as it is interesting to investigate how nonlinear photon interactions scale for a large number of emitters and how that can be useful for further work in the field.

In this thesis, we thus present a general formalism that can be used to investigate effective nonlinear photon interactions for emitters coupled to a waveguide with different parameters, such as the number of emitters, placement of emitters and light-matter couplings. In particular, we consider a weak coherent state input field incident from one of the sides of a 1D waveguide, which is coupled to quantum two-level emitters. The coherent field is a superposition of different photon number states and thus can be used to derive nonlinear properties of the system. We then use that to calculate the second-order correlation function and nonlinear output intensity, both of which are a measure of the effective nonlinear interactions between photons. The presented method is then used to investigate rigidness of chiral waveguides due to imperfections – couplings to the suppressed propagation direction.

The thesis outline is then as follows:

- **Chapter 1**. Presents current status of the field and the motivation of this thesis (current chapter).
- **Chapter 2**. Introduces necessary concepts of quantum mechanics and quantum optics.
- **Chapter 3**. The approach of this thesis is presented, the second-order correlation function is derived and general second-order coherence properties of the system are investigated for different parameters.
- **Chapter 4**. The method of this thesis is modified to calculate nonlinear output intensity and general simulation results are discussed.
- **Chapter 5**. The formalism is applied to parameters of an experimentally viable chiral waveguide system and rigidness of such a system due to imperfections is investigated.
- **Chapter 6**. Conclusions of this work and an outlook is provided.

Chapter 2

Preliminaries

In this chapter, we present concepts of quantum mechanics (section 2.1), quantum optics and properties of waveguides (section 2.2), which are necessary for the understanding of the formalism which we present in later chapters.

2.1 Basic Quantum Mechanics

State Vectors

In quantum mechanics, a state of a physical system is described completely by a state vector in a Hilbert space [18]. The Hilbert space is spanned by a complex number space **C**. In Dirac bracket notation, a state vector of a state ψ is denoted as a ket (bra) – $|\psi\rangle$ ($\langle\psi|$). Bra and ket are related by a conjugate transpose operation: $\langle\psi|^\dagger = |\psi\rangle$. $|\psi\rangle$ multiplied with a complex number c is another ket $c\,|\psi\rangle$. However, it represents the same physical state, so only rays of Hilbert space are of significance. An inner product between states is defined as $\langle\varphi\,|\,\psi\rangle$ and the result is a complex number in **C** (it is analagous with a dot product in vector calculus). The inner product has the following properties:

1) Positivity: $\langle\varphi\,|\,\psi\rangle \geq 0$;

2) Linearity: $\langle\varphi|\,(a\,|\psi_1\rangle + b\,|\psi_2\rangle) = a\,\langle\varphi\,|\,\psi_1\rangle + b\,\langle\varphi\,|\,\psi_1\rangle$;

3) Antisymmetry: $\langle\varphi\,|\,\psi\rangle = \langle\psi\,|\,\varphi\rangle^*$;

4) Completeness: $\langle\psi\,|\,\psi\rangle = |\psi|^2$ (analogous to the magnitude of a vector in vector calculus).

Two kets $|\psi\rangle$ and $|\varphi\rangle$ are said to be orthogonal if

$$\langle\psi\,|\,\varphi\rangle = 0. \tag{2.1}$$

Also, since $|\psi\rangle$ and $c\,|\psi\rangle$ represent the same physical state, it is convenient to consider normalized kets:

$$\left|\tilde{\psi}\right\rangle = \frac{1}{\sqrt{\langle\psi\,|\,\psi\rangle}}\,|\psi\rangle\,. \tag{2.2}$$

Observables

Observables are properties of a quantum system that can, in principle, be measured. In quantum mechanics they are represented as Hermitian operators, which act on kets. Operator $\hat{A}$ acting on a ket $|\psi\rangle$ results in another ket: $\hat{A}\,|\psi\rangle = |\phi\rangle$. Of particular importance are kets which have the property

$$\hat{A}\,|\psi'\rangle = \psi'\,|\psi'\rangle\,, \hat{A}\,|\psi''\rangle = \psi''\,|\psi''\rangle\,, ... \tag{2.3}$$

where $\psi', \psi'', ...$ are numbers (for Hermitian operators they are real). Such kets are called eigenkets of an operator A and the numbers are called eigenvalues. Any other state vector can then be expanded in the basis of eigenkets as:

$$|\varphi\rangle = \sum_{\psi'} c_{\psi'}\,|\psi'\rangle\,, \tag{2.4}$$

where $c_{\psi'}$ are complex coefficients, known as probability amplitudes. Dimension of the Hilbert space is then given by a set of orthonormal eigenkets of an observable:

$$\langle\psi'\,|\,\psi''\rangle = \delta_{\psi'\psi''}. \tag{2.5}$$

An expectation value of an observable is defined as $\left\langle\varphi\,\middle|\,\hat{A}\,\middle|\,\varphi\right\rangle$. Upon measurement, the state of a system collapses to one of the eigenstates of the observable. Expanding a state in eigenkets with eq. (2.4), we get

$$\langle\varphi\,|\,A\,|\,\varphi\rangle = \sum_{\psi'} \psi'\,|c_{\psi'}|^2\,, \tag{2.6}$$

where, for normalized state vectors, $|c_{\psi'}|^2$ is then a probability of measuring the value ψ' in an experiment for an observable A.

Time-Evolution

Time-evolution of a state vector with a time independent Hamiltonian is given by the Schrödinger equation:

$$i\hbar\frac{\mathrm{d}}{\mathrm{d}t}\left|\psi(t)\right\rangle = \hat{H}\left|\psi(t)\right\rangle. \tag{2.7}$$

In this form, all time dependence of the system is included in the state vector and all operators are time independent. This description of system dynamics is known as Schrödinger picture. The state vector at any given time is then

$$\left|\psi(t)\right\rangle = \mathrm{e}^{-\frac{i\hat{H}t}{\hbar}}\left|\psi(0)\right\rangle. \tag{2.8}$$

The expectation value of an operator $\hat{A}$ then evolves as

$$\left\langle\psi(t)\middle|\hat{A}\middle|\psi(t)\right\rangle = \left\langle\psi(0)\middle|\mathrm{e}^{\frac{i\hat{H}t}{\hbar}}\hat{A}\mathrm{e}^{-\frac{i\hat{H}t}{\hbar}}\middle|\psi(0)\right\rangle. \tag{2.9}$$

Note that in above equation we can define $\hat{A}(t) = \mathrm{e}^{\frac{i\hat{H}t}{\hbar}}\hat{A}\mathrm{e}^{-\frac{i\hat{H}t}{\hbar}}$ and evolve the operator instead of the state vector. The case where time-evolution is defined in operators and the state vectors are time independent is known as the Heisenberg picture. Time-evolution of an operator is then given by the Heisenberg equation:

$$i\hbar\frac{\mathrm{d}}{\mathrm{d}t}\hat{A}(t) = \left[\hat{A}(t), \hat{H}\right]. \tag{2.10}$$

Rotating Frame

Consider a state vector $\left|\psi(t)\right\rangle$ in the Schrödinger picture. We define a new state vector

$$\left|\Psi(t)\right\rangle = \hat{U}^\dagger(t)\left|\psi(t)\right\rangle, \tag{2.11}$$

where $\hat{U}^\dagger(t)$ is a unitary operator. We would like to get an equation of motion for the newly defined state vector. Taking the derivative of the state vector:

$$\begin{aligned}
i\hbar\frac{\mathrm{d}}{\mathrm{d}t}\left|\Psi(t)\right\rangle =& i\hbar\frac{\mathrm{d}}{\mathrm{d}t}\left(\hat{U}^\dagger(t)\left|\psi(t)\right\rangle\right) = i\hbar\dot{\hat{U}}^\dagger(t)\left|\psi(t)\right\rangle + i\hbar\hat{U}^\dagger(t)\left|\dot{\psi}(t)\right\rangle & (2.12)\\
=& i\hbar\dot{\hat{U}}^\dagger(t)\hat{U}(t)\hat{U}^\dagger(t)\left|\psi(t)\right\rangle + \hat{U}^\dagger(t)\hat{H}\hat{U}(t)\hat{U}^\dagger(t)\left|\psi(t)\right\rangle & (2.13)\\
=& \left(i\hbar\dot{\hat{U}}^\dagger(t)\hat{U}(t) + \hat{U}^\dagger(t)\hat{H}\hat{U}(t)\right)\left|\Psi(t)\right\rangle & (2.14)\\
=& \hat{\tilde{H}}(t)\left|\Psi(t)\right\rangle. & (2.15)
\end{aligned}$$

So we have obtained a new equation of motion, similar to the Schrödinger equation, but with a new Hamiltonian $\hat{\tilde{H}}(t) = i\hbar\dot{\hat{U}}^\dagger(t)\hat{U}(t) + \hat{U}^\dagger(t)\hat{H}\hat{U}(t)$, for the state $\left|\Psi(t)\right\rangle$. This is known as time-evolution in the rotating frame, in which the phase that would be present in the Schrödinger picture has been absorbed into the new Hamiltonian and state vector. Note that the new Hamiltonian is not necessarily time independent, in which case both the state and the operators have time dependence.

Consider a time-independent Hamiltonian, which can be written as $\hat{H} = \hat{H}_0 + \hat{H}_1$. If in the above rotating frame derivation we use $\hat{U}^\dagger(t) = \mathrm{e}^{-i\hat{H}_0 t}$, then $\hat{\tilde{H}} = \hat{U}^\dagger(t)\hat{H}_1\hat{U}(t)$. That is, we move to a picture that absorbs the time evolution of $\hat{H}_0$ both into state vectors and operators. This special case of the rotating frame is known as the interaction picture. This approach is also valid if $\hat{H}_1$ is time dependent.

Second Quantization

For multiparticle systems, containing identicle particles such as photons, it is inconvenient to keep track of what state each particle is in. Instead, we define a new state vector

$$|n_1, n_2, ..., n_i, ...\rangle \,, \tag{2.16}$$

where n_i specifies how many particles there are with eigenvalue k_i. In this way, we instead follow how many particles there are in a particular state, an approach which is known as second quantization. This new vector space is called Fock space. Two special cases of such states are the vacuum state of the system and the single-particle state with eigenvalue k_i:

$$|0, 0, ..., 0, ...\rangle \equiv |0\rangle \,, \tag{2.17}$$

$$|0, 0, ..., n_i = 1, ...\rangle = |k_i\rangle \,. \tag{2.18}$$

We then introduce the creation and annihilation operators $a_i^\dagger$ and a_i that respectively create and annihilate a particle in a state with eigenvalue k_i:

$$a_i^\dagger |0\rangle = |k_i\rangle \,, \tag{2.19}$$

$$a_i |k_i\rangle = |0\rangle \,, \tag{2.20}$$

so that

$$a_i |k_j\rangle = \delta_{ij} |0\rangle \,. \tag{2.21}$$

For photons and bosons in general, the commutation relation for annihilation and creation operators is then given by:

$$[a_i, a_j] = \left[a_i^\dagger, a_j^\dagger\right], \tag{2.22}$$

$$\left[a_i, a_j^\dagger\right] = \delta_{ij}. \tag{2.23}$$

2.2 Basic Quantum Optics

Quantized Electromagnetic Field

For a cavity with perfectly conducting walls, a single-mode electromagnetic field satisfying Maxwell's equations and boundary conditions, assuming the cavity is along the direction z and the electric (magnetic) field is polarized in x (y) direction, is given by [19]:

$$E_x(z,t) = \sqrt{\frac{2\omega^2}{V\varepsilon_0}}q(t)sin(kz), \tag{2.24}$$

$$B_y(z,t) = \left(\frac{\mu_0\varepsilon_0}{k}\right)\sqrt{\frac{2\omega^2}{V\varepsilon_0}}p(t)cos(kz), \tag{2.25}$$

where the electromagnetic field takes the form of a standing wave and ω is the frequency of the mode, $k = \frac{\omega}{c}$ is the wavenumber, V is the volume of the cavity, ε_0 (μ_0) is the permittivity (permeability) of free space. $q(t)$ and $p(t) = \dot{q}(t)$ are time dependent factors, which respectively correspond to canonical position and momentum. Classical field energy is then given by:

$$H = \frac{1}{2}\left(p^2 + \omega^2 q^2\right), \tag{2.26}$$

which is equivalent to a harmonic oscillator. The quantization is performed by defining q and p as operators $\hat{q}$ and $\hat{p}$, which satisfy the canonical commutation relation:

$$[\hat{q}, \hat{p}] = i\hbar. \tag{2.27}$$

Annihilation and creation operators are defined as:

$$\hat{a}^{(\dagger)} = \sqrt{2\hbar\omega}\left(\omega\hat{q} \pm i\hat{p}\right), \tag{2.28}$$

which have the bosonic commutation relation, given by eq. (2.22) and (2.23), the electric field and the Hamiltonian is given by:

$$\hat{E}_x(z,t) = \mathcal{E}_0\left(\hat{a} + \hat{a}^\dagger\right)sin(kz), \tag{2.29}$$

$$\hat{H} = \hbar\omega\left(\hat{a}^\dagger\hat{a} + \frac{1}{2}\right), \tag{2.30}$$

where $\mathcal{E}_0 = \sqrt{\frac{\hbar\omega}{V\varepsilon_0}}$. We denote $|n\rangle$ as the eigenstate of the Hamiltonian:

$$\hat{H}\,|n\rangle = E_n\,|n\rangle\,, \tag{2.31}$$

where $E_n = \hbar\omega(n+\frac{1}{2})$ and n describes how many photons there are in a state with frequency ω. Then we can define $\hat{a}^\dagger\hat{a} = \hat{n}$ as the photon number operator.

Annihilation and creation operators then act on $|n\rangle$ as

$$\hat{a}\,|n\rangle = \sqrt{n}\,|n-1\rangle\,, \tag{2.32}$$

$$\hat{a}^\dagger\,|n\rangle = \sqrt{n+1}\,|n+1\rangle\,. \tag{2.33}$$

So we see that the annihilation (creation) operator creates (annihilates) one photon in the system with frequency ω, which is an example of second quantization discussed previously. Note that $\langle n\,|\,E_x\,|\,n\rangle = 0$, so this is a highly non-classical state, since, for a classical electric field, we do not predict vacuum if there are photons present in the system.

Coherent States

From eq. (2.29) we see that for an expectation value of an electric field to be non-zero, we define a new state, which is an eigenstate of the annihilation operator. Such states are known as coherent states $|\alpha\rangle$:

$$\hat{a}\,|\alpha\rangle = \alpha\,|\alpha\rangle\,, \tag{2.34}$$

where α is a complex number. The coherent state can be expanded in the previously introduced number states as

$$|\alpha\rangle = \mathrm{e}^{-\frac{1}{2}|\alpha|^2}\sum_{n=0}^{\infty}\frac{\alpha^n}{\sqrt{n!}}\,|n\rangle\,, \tag{2.35}$$

so that a coherent state is a superposition of photon number states. The expectation value of coherent states is (using $\alpha = |\alpha|\,\mathrm{e}^{i\theta}$):

$$\langle\alpha\,|\,E_x(z,t)\,|\,\alpha\rangle = |\alpha|\,\sqrt{2}\mathcal{E}_0 sin(\omega t - kz - \theta), \tag{2.36}$$

which looks similar to a classical field amplitude. In fact, a coherent state is the most "classical" quantum state of electromagnetic field. Also, the average photon number for a coherent state is given by:

$$\langle \alpha \,|\, \hat{n} \,|\, \alpha \rangle = |\alpha|^2 \,, \tag{2.37}$$

so that for $|\alpha|^2 \ll 1$ the coherent state consists mostly of vacuum and single photon number states. The coherent state can also be represented as

$$|\alpha\rangle = \hat{D}(\alpha)\,|0\rangle \,, \tag{2.38}$$

where $\hat{D}(\alpha)$ is a unitary operator, known as displacement operator, given by:

$$\hat{D}(\alpha) = \mathrm{e}^{\alpha\hat{a}^\dagger - \alpha^*\hat{a}}. \tag{2.39}$$

The displacement has the property

$$\hat{D}^\dagger(\alpha)\hat{a}\hat{D}(\alpha) = \hat{a} + \alpha, \tag{2.40}$$

$$\hat{D}(\alpha)\hat{a}\hat{D}^\dagger(\alpha) = \hat{a} - \alpha, \tag{2.41}$$

so that it "displaces" the annihilation operator. A similar property holds for the creation operator.

Jaynes-Cummings Model

Interaction between quantized electromagnetic field and atoms is described by the Jaynes-Cummings model. We consider a single mode electromagnetic field in a cavity and two levels of the atom: ground state $|g\rangle$ and excited state $|e\rangle$. The Jaynes-Cummings Hamiltonian is given by:

$$\hat{H} = \hat{H}_\mathrm{a} + \hat{H}_\mathrm{f} + \hat{H}_\mathrm{int}, \tag{2.42}$$

where $\hat{H}_\mathrm{a}$ is the free atomic Hamiltonian, $\hat{H}_\mathrm{f}$ is the free field Hamiltonian and $\hat{H}_\mathrm{int}$ is the interaction Hamiltonian:

$$\hat{H}_\mathrm{a} = \hbar\omega_\mathrm{eg}\,|e\rangle\,\langle e| \,, \tag{2.43}$$

$$\hat{H}_\mathrm{f} = \hbar\omega\hat{a}^\dagger\hat{a}, \tag{2.44}$$

$$\hat{H}_{\text{int}} = -\hat{d} \cdot \hat{E}, \tag{2.45}$$

with $\hat{H}_{\text{a}}$ given in terms of the transition frequency ω_{eg} between states $|g\rangle$ and $|e\rangle$, and having $\hat{d}$ as the dipole moment operator. Here we assumed that the dipole moment and the electric field polarization is in the same direction. A general approach can be used by considering them as vectors. We can expand the dipole moment operator in the basis of the atom states as:

$$\hat{d} = (|g\rangle\langle g| + |e\rangle\langle e|)\, \hat{d}\, (|g\rangle\langle g| + |e\rangle\langle e|)\,. \tag{2.46}$$

Due to parity considerations (dipole moment is odd under parity transformation), only off-diagonal terms are non-zero: $\left\langle g \middle| \hat{d} \middle| g \right\rangle = \left\langle e \middle| \hat{d} \middle| e \right\rangle = 0$. Defining $d = \left\langle e \middle| \hat{d} \middle| g \right\rangle$, $\hat{\sigma}_{ij} = |i\rangle\langle j|$, assuming that d is real and using eq. (2.29), we can write the interaction Hamiltonian as:

$$\hat{H}_{\text{int}} = \hbar g\, (\hat{\sigma}_{eg} + \hat{\sigma}_{ge}) \left(\hat{a} + \hat{a}^{\dagger}\right), \tag{2.47}$$

where $g = -\frac{d\mathcal{E}_0}{\hbar} sin(kz)$. Note that in the above Hamiltonian we have terms $\hat{\sigma}_{eg}\hat{a}^{\dagger}$ and $\hat{\sigma}_{ge}\hat{a}$, which respectively correspond to emitting a photon while having a transition from ground state to excited state and absorbing a photon while going from excited state to ground state. These terms do not conserve energy and vary in time with a larger frequency than the other terms, so they can be neglected, which is the rotating wave approximation. The interaction Hamiltonian between a quantized electromagnetic field and a two-level atom is then given by:

$$\hat{H}_{\text{int}} = \hbar g \left(\hat{\sigma}_{eg}\hat{a} + \hat{a}^{\dagger}\hat{\sigma}_{ge}\right). \tag{2.48}$$

Correlation Functions

Correlation functions give information about coherence properties of the electric field. The first-order correlation function $g^{(1)}$ can be used to calculate coherence time and length of radiation. In this thesis, however, we are interested in the second-order coherence, which is given by the second-order correlation function $g^{(2)}$. Second-order correlation function gives insight about the statistical properties of the field, since it is a measure of what photon-photon correlations are present. It is defined as:

$$g^{(2)}(\tau) = \frac{G^{(2)}(t+\tau, t)}{G^{(1)}(t,t)G^{(1)}(t+\tau, t+\tau)}, \tag{2.49}$$

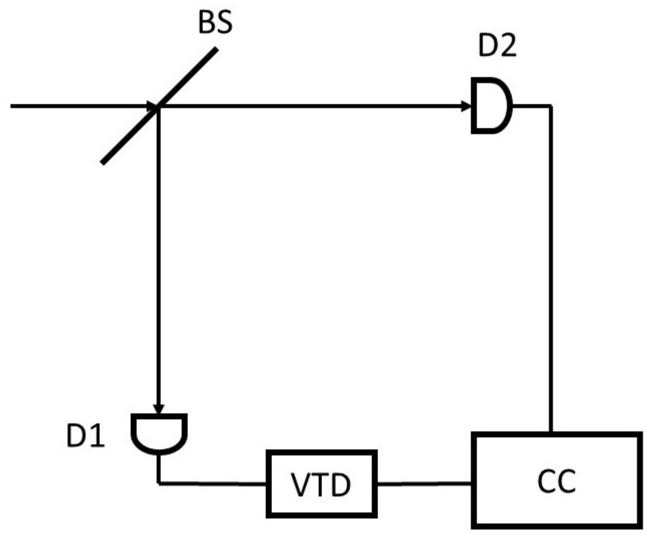

Figure 2.1: Hanbury-Brown and Twiss setup. The incident field is split by the beam splitter (BS). Coincidence rate is measured by a coincidence counter (CC) for detector D2 registering a photon at time t and D1 at time $t+\tau$ with an electronically variable time delay (VTD) τ.

where $G^{(2)}(t+\tau,t) = \langle I(t+\tau)I(t)\rangle$, $G^{(1)}(t,t) = \langle I(t)\rangle$ and τ is some time delay. It shows how intensities at two different time points are correlated. In terms of the annihilation and creation operators, it can be written as:

$$g^{(2)}(\tau) = \frac{\left\langle \hat{a}^\dagger(t)\hat{a}^\dagger(t+\tau)\hat{a}(t+\tau)\hat{a}(t)\right\rangle}{\langle \hat{a}^\dagger(t)\hat{a}(t)\rangle \langle \hat{a}^\dagger(t+\tau)\hat{a}(t+\tau)\rangle}. \tag{2.50}$$

In this form, the $g^{(2)}$ is given specifically for a quantum mechanical state and shows correlations between photons. The $g^{(2)}$ can be measured by having the field split with a beam splitter into two single-photon detectors with an electronically variable time delay, which is known as Hanbury-Brown and Twiss setup (fig. 2.1). This setup measures the coincident detection rate for one detector registering a photon count at time t and the other at time $t+\tau$.

For a quantum mechanical state, the value of $g^{(2)}(0)$ is in the range $0 \leq g^{(2)}(0) < \infty$ (in the classical case, it is in the range $1 \leq g^{(2)}(0) < \infty$) and several cases are of particular importance:

1) $g^{(2)}(0) = g^{(2)}(\tau) = 1$: if the second-order correlation function has the value of 1 at any time delay, it is equivalent to factorization of the numerator as $\left\langle \hat{a}^\dagger(t)\hat{a}^\dagger(t+\tau)\hat{a}(t+\tau)\hat{a}(t)\right\rangle = \left\langle \hat{a}^\dagger(t)\hat{a}(t)\right\rangle \left\langle \hat{a}^\dagger(t+\tau)\hat{a}(t+\tau)\right\rangle$, so that photons are not correlated and they reach the detectors at random time intervals. An example of this is light in a coherent state.

2) $g^{(2)}(0) > g^{(2)}(\tau)$: photons tend to arrive in pairs, which is known as photon bunching: for example, this effect is seen for $g^{(2)}$ measurements of chaotic light.

3) $g^{(2)}(0) < g^{(2)}(\tau)$: a quantum mechanical effect – photons arrive evenly spaced in time. The probability to measure coincident photons is less than for a coherent state. For a single-mode field in a number state $|n\rangle$, $g^{(2)}(0) = 1 - \frac{1}{n}$ (excluding vacuum), so a value of $g^{(2)}(0) = 0$ constitutes a true single-photon source.

Enhancement of Light-Matter Interactions in 1D Waveguides

The spontaneous emission rate of emitters is not an intrinsic property of the emitter and it can be enhanced by the emitter's surroundings, which is known as the Purcell effect. One way of seeing this is considering Fermi's golden rule for transition from excited to ground state of the emitter, which is proportional to the density of final states. By confining the electromagnetic field, the density of final states can be enhanced. The enhancement, in general, can be given as [5]:

$$\rho(\boldsymbol{r}, \omega, \hat{\boldsymbol{e}}_{\boldsymbol{d}}) = \frac{n\omega^2}{3\pi^2 c^3} F_{\mathrm{P}}(\boldsymbol{r}, \omega, \hat{\boldsymbol{e}}_{\boldsymbol{d}}), \tag{2.51}$$

where ρ is the local density of states for an emitter at position $\boldsymbol{r}$, electric field frequency ω and dipole moment direction $\hat{\boldsymbol{e}}_{\boldsymbol{d}}$, n is the refractive index of the material and F_{P} is the Purcell factor. The Purcell factor is then given by:

$$F_{\mathrm{P}}(\boldsymbol{r}, \omega, \hat{\boldsymbol{e}}_{\boldsymbol{d}}) = \frac{\mathit{\Gamma}_{\mathrm{rad}}(\boldsymbol{r}, \omega, \hat{\boldsymbol{e}}_{\boldsymbol{d}})}{\mathit{\Gamma}_{\mathrm{rad}}^{\mathrm{hom}}(\omega)}, \tag{2.52}$$

where the Purcell factor is a ratio between spontaneous emission rates for radiative decay of the inhomogeneously designed material to the spontaneous emission of the same emitter in a homogeneous material with a refractive index n. In a 1D waveguide, an emitter that is optimally positioned with a dipole moment in the direction of the electric field has a maximum Purcell factor of:

$$F_{\mathrm{P}}^{\mathrm{max}}(\omega) = \left(\frac{3}{4\pi n} \frac{\lambda^2/n^2}{V_{\mathrm{eff}}/a} \right) n_{\mathrm{g}}(\omega), \tag{2.53}$$

where λ is the wavelength of the electric field, V_{eff} is the effective mode volume per unit cell, a is the lattice period and $n_{\mathrm{g}}(\omega) = c/v_{\mathrm{g}}(\omega)$ specifies the retardation of group velocity v_{g}. From the above expression, it can be seen that two effects contribute to the enhancement of spontaneous emission: a slow group velocity and a small effective mode volume. A slow group velocity can be achieved due to the highly dispersive nature of some waveguides and a small effective mode volume is achieved by confining light in two dimensions. The emitter upon decay then can reach a near unity probability of emitting a photon into the guided mode of the waveguide, which results in strong light-matter coupling.

Moreover, when the electric field is confined in two dimensions, a longitudinal polarization is present for the field [14]. The longitudinal polarization has a $\pm\pi/2$ phase shift compared to the transverse modes, and the sign depends on the propagation direction. The resulting field has an elliptical polarization and possesses a spin angular momentum. The spin angular momentum flips sign depending on the propagation direction. Upon decay of an emitter, spin angular momentum has to be conserved, so the emitted photon would have either propagation direction depending on the dipole orientation.

Using this effect, a waveguide can be designed in a way that would suppress coupling to photons propagating in a certain direction, resulting in chirality of the waveguide. In the Jaynes-Cummings Hamiltonian, given by eq. (2.48), this would result in different coupling constants g depending on the propagation direction.

Chapter 3

Second-Order Quantum Coherence

In this chapter, the method for calculating the second-order correlation function ($g^{(2)}$) is explained for any number of two-level quantum emitters in a 1D waveguide. For simplicity, we start with the investigation of a single emitter in a waveguide in section 3.1. The method is then expanded for any number of emitters in section 3.2. Finally, in section 3.3 we simulate the dynamics of the emitters numerically and present our findings on the second order coherence.

3.1 Single Emitter in a 1D Waveguide

To investigate nonlinear photon interactions in a 1D waveguide and discuss the method used for calculating the system dynamics, it is first better to consider a single emitter. A single emitter in a waveguide is sketched in figure 3.1. In this thesis, a coherent state input field is investigated. The field is incident from one of the sides of the waveguide. Since the input field travels along the waveguide, the emitted photons can interfere with it, giving rise to interesting effects. Upon decay of the emitter's excited state $|\mathrm{e}\rangle$ to the ground state $|\mathrm{g}\rangle$, a photon can be either emitted into the mode supported by the waveguide (decay into the waveguide) or into any other modes (decay outside the waveguide). These are described by decay rates $\mathit{\Gamma}_{\mathrm{1D,R}}$, $\mathit{\Gamma}_{\mathrm{1D,L}}$ and $\mathit{\Gamma}'$. Here $\mathit{\Gamma}'$ is the decay rate for emitting a photon outside the waveguide and, since decay rate into the waveguide can be dependent upon the direction that the photon is emitted, $\mathit{\Gamma}_{\mathrm{1D,R}}$ ($\mathit{\Gamma}_{\mathrm{1D,L}}$) corresponds to a decay rate of emitting a right (left)-propagating photon into the waveguide.

The System Hamiltonian

Interaction between the emitter and a quantized electromagnetic field is described by the Jaynes-Cummings model as described in Chapter 2. The corresponding Hamiltonian in the Schrödinger picture is

$$\hat{H}_{\mathrm{int}} = -\hbar g \int \mathrm{d}k \left(\hat{\sigma}_{\mathrm{eg}} \hat{a}_k \mathrm{e}^{ikz_{\mathrm{a}}} + \hat{a}_k^{\dagger} \hat{\sigma}_{\mathrm{ge}} \mathrm{e}^{-ikz_{\mathrm{a}}} \right), \tag{3.1}$$

where z_{a} is the emitter position, g is the coupling constant, $\hat{a}_k$ ($\hat{a}_k^{\dagger}$) is the annihilation (creation) operator for a mode with a wavenumber k and $\hat{\sigma}_{\mathrm{ij}} = |i\rangle \langle j|$. The full Hamiltonian of the system in the Schrödinger picture then can be written as

$$\hat{H}_{\mathrm{S}} = \hat{H}_{\mathrm{side}} + \hat{H}_{\mathrm{a}} + \hat{H}_{\mathrm{f}} + \hat{H}_{\mathrm{int}}, \tag{3.2}$$

where $\hat{H}_{\mathrm{side}}$ is the term describing decay outside the waveguide, $\hat{H}_{\mathrm{a}}$ is the free atomic excitation Hamiltonian and $\hat{H}_{\mathrm{f}}$ is the free field Hamiltonian:

$$\hat{H}_{\mathrm{side}} = -\hbar \frac{i\Gamma'}{2} \hat{\sigma}_{\mathrm{ee}}, \tag{3.3}$$

$$\hat{H}_{\mathrm{a}} = \hbar \omega_{\mathrm{eg}} \hat{\sigma}_{\mathrm{ee}}, \tag{3.4}$$

$$\hat{H}_{\mathrm{f}} = \hbar \int \mathrm{d}k \omega_k \hat{a}_k^{\dagger} \hat{a}_k. \tag{3.5}$$

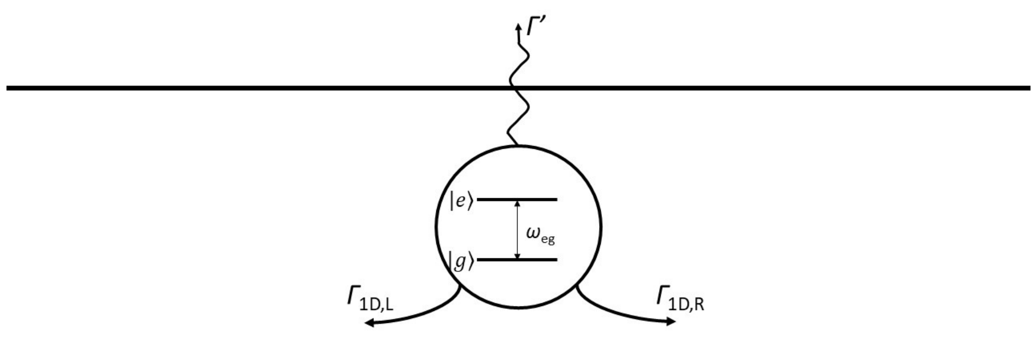

Figure 3.1: Single two-level emitter in a 1D waveguide with the transition frequency between ground and excited states as ω_{eg}. Upon decay of the excited state, the emitter emits a left or right-propagating photon into the waveguide, or a photon is lost from the system by emission outside the waveguide. The corresponding decay rates are respectively $\Gamma_{\mathrm{1D,R}}$, $\Gamma_{\mathrm{1D,L}}$ and Γ'.

Here $\omega_{\rm eg}$ is the transition frequency between states $|{\rm e}\rangle$ and $|{\rm g}\rangle$ of the emitter and ω_k is the frequency of photons with wavenumber k. Note that for now we treat the decay outside the waveguide as a non-Hermitian Hamiltonian term $\hat{H}_{\rm side}$. As will be seen later in the derivation of the equations of motion, this non-Hermitian term will result in a decay for excited emitter states. This is sufficient for $g^{(2)}$ calculations as long as we do not need to follow the amount of photons being emitted outside the waveguide. Also, only field frequencies close to the emitter transition frequency will be considered, so it is assumed that the linear dispersion relation holds over those frequencies: $\omega_k = v_{\rm g}\,|k|$, where $v_{\rm g}$ is the group velocity of the field.

Any further analysis of the system is simplified by transforming into the interaction picture. The unitary operator used for transformation is given as

$$\hat{U} = {\rm e}^{-\frac{i}{\hbar}(\hat{H}_{\rm a}+\hat{H}_{\rm f})t}. \tag{3.6}$$

The details of the transformation of the Hamiltonian from the Schrödinger to the interaction picture are described in Appendix A.1, with the resulting Hamiltonian given as:

$$\hat{H} = -\hbar\frac{i\Gamma'}{2}\hat{\sigma}_{\rm ee} - \hbar g\int {\rm d}k(\hat{\sigma}_{\rm eg}\hat{a}_k{\rm e}^{-i\Delta_k t+ikz_{\rm a}} + \hat{a}_k^\dagger\hat{\sigma}_{\rm ge}{\rm e}^{i\Delta_k t-ikz_{\rm a}}), \tag{3.7}$$

where $\Delta_k = \omega_k - \omega_{\rm eg}$ is the detuning of the photon frequency with respect to the emitter transition frequency. Since we are interested only in near-resonant photons, we can treat left- and right-propagating photons as separate quantum fields [1], such that $\hat{a}_k{\rm e}^{ikz_{\rm a}} \to \hat{a}_{{\rm R},k}{\rm e}^{ikz_{\rm a}} + \hat{a}_{{\rm L},k}{\rm e}^{-ikz_{\rm a}}$, $\hat{a}_k^\dagger{\rm e}^{-ikz_{\rm a}} \to \hat{a}_{{\rm R},k}^\dagger{\rm e}^{-ikz_{\rm a}} + \hat{a}_{{\rm L},k}^\dagger{\rm e}^{ikz_{\rm a}}$. Also, we consider detuning with respect to the central frequency of the incoming electromagnetic field for near-resonant photons: $\Delta_k \to \Delta$, with $\Delta = \omega - \omega_0$, where ω is the central frequency of the incoming field. With these considerations, the Hamiltonian in the interaction picture is then given by:

$$\begin{aligned} \hat{H} \quad &= \quad -\hbar\frac{i\Gamma'}{2}\hat{\sigma}_{\rm ee} - \hbar\int {\rm d}k\Big[\hat{\sigma}_{\rm eg}(g_{\rm R}\hat{a}_{{\rm R},k}{\rm e}^{-i\Delta t+ikz_{\rm a}} + g_{\rm L}\hat{a}_{{\rm L},k}{\rm e}^{-i\Delta t-ikz_{\rm a}}) \\ &+ \quad (g_{\rm R}\hat{a}_{{\rm R},k}^\dagger{\rm e}^{i\Delta t-ikz_{\rm a}} + g_{\rm L}\hat{a}_{{\rm L},k}^\dagger{\rm e}^{i\Delta t+ikz_{\rm a}})\hat{\sigma}_{\rm ge})\Big], \end{aligned} \tag{3.8}$$

where we also include separate coupling constants for right (left)-propagating photons $g_{\rm R(L)}$.

It is most convenient to analyze this system with respect to real space operators, so we define the following slowly-varying operators:

$$\hat{E}_{\rm R}(z) = \frac{1}{\sqrt{2\pi}}\int {\rm d}k\hat{a}_{{\rm R},k}{\rm e}^{i(k-k_0)z}, \tag{3.9}$$

$$\hat{E}_{\rm L}(z) = \frac{1}{\sqrt{2\pi}}\int {\rm d}k\hat{a}_{{\rm L},k}{\rm e}^{-i(k-k_0)z}, \tag{3.10}$$

where $k_0 = \frac{\omega_{\mathrm{eg}}}{v_{\mathrm{g}}}$. The commutation relation for these operators is then given by:

$$\left[\hat{E}_{\mathrm{L}}(z), \hat{E}^{\dagger}_{\mathrm{L}}(z)\right] = \left[\hat{E}_{\mathrm{R}}(z), \hat{E}^{\dagger}_{\mathrm{R}}(z)\right] = \delta(z - z'), \tag{3.11}$$

$$\left[\hat{E}_{\mathrm{R}}(z), \hat{E}^{\dagger}_{\mathrm{L}}(z)\right] = \left[\hat{E}_{\mathrm{L}}(z), \hat{E}^{\dagger}_{\mathrm{R}}(z)\right] = 0, \tag{3.12}$$

while the interaction picture Hamiltonian in real space can be written as:

$$\begin{aligned}\hat{H} \quad &= \quad -\hbar\frac{i\Gamma'}{2}\hat{\sigma}_{\mathrm{ee}} - \hbar\sqrt{2\pi}\int \mathrm{d}z\delta(z - z_{\mathrm{a}})\Big[\hat{\sigma}_{\mathrm{eg}}\left(g_{\mathrm{R}}\hat{E}_{\mathrm{R}}(z)\mathrm{e}^{-i\Delta t + ik_0 z} + g_{\mathrm{L}}\hat{E}_{\mathrm{L}}(z)\mathrm{e}^{-i\Delta t - ik_0 z}\right) \\ &+ \quad \left(g_{\mathrm{R}}\hat{E}^{\dagger}_{\mathrm{R}}(z)\mathrm{e}^{i\Delta t - ik_0 z} + g_{\mathrm{L}}\hat{E}^{\dagger}_{\mathrm{L}}(z)\mathrm{e}^{i\Delta t + ik_0 z}\right)\hat{\sigma}_{\mathrm{ge}}\Big].\end{aligned} \tag{3.13}$$

Since the initial state of the system is a steady input coherent field (α_k is time independent), which is represented in the interaction picture as

$$|\Psi(t = -\infty)\rangle = \hat{D}(\alpha_k)\,|\mathrm{g}0\rangle\,, \tag{3.14}$$

where, assuming the input field is incident from the left side of the waveguide:

$$\hat{D}(\alpha_k) = \mathrm{e}^{\left(\int \mathrm{d}k\left(\hat{a}^{\dagger}_{\mathrm{R},k}\alpha_k - \alpha^*_k\hat{a}_{\mathrm{R},k}\right)\right)}, \tag{3.15}$$

it is convenient to change the initial wavefunction state as

$$\left|\tilde{\Psi}(t)\right\rangle = \hat{D}^{\dagger}(\alpha)\,|\Psi(t)\rangle\,, \tag{3.16}$$

while performing a rotating frame Hamiltonian transformation as described in Appendix A.2, resulting in the final Hamiltonian:

$$\begin{aligned}\tilde{\hat{H}} \quad &= \quad -\hbar\frac{i\Gamma'}{2}\hat{\sigma}_{\mathrm{ee}} - \hbar\sqrt{2\pi}\int \mathrm{d}z\delta(z - z_{\mathrm{a}})\Big[\hat{\sigma}_{\mathrm{eg}}\Big(g_{\mathrm{R}}\hat{E}_{\mathrm{R}}(z)\mathrm{e}^{-i\Delta t + ik_0 z} \\ &+ \quad g_{\mathrm{R}}\mathcal{E}\mathrm{e}^{-i\Delta t + ik_0 z} + g_{\mathrm{L}}\hat{E}_{\mathrm{L}}(z)\mathrm{e}^{-i\Delta t - ik_0 z}\Big) + \Big(g_{\mathrm{R}}\hat{E}^{\dagger}_{\mathrm{R}}(z)\mathrm{e}^{i\Delta t - ik_0 z} \\ &+ \quad g_{\mathrm{R}}\mathcal{E}^*\mathrm{e}^{i\Delta t - ik_0 z} + g_{\mathrm{L}}\hat{E}^{\dagger}_{\mathrm{L}}(z)\mathrm{e}^{i\Delta t + ik_0 z}\Big)\hat{\sigma}_{\mathrm{ge}}\Big],\end{aligned} \tag{3.17}$$

with $\mathcal{E} = \int \mathrm{d}k\alpha_k\mathrm{e}^{i(k-k_0)z}$. Essentially, this change of basis maps the initial state of the system to vacuum, while the right-propagating photon operator transforms as $\hat{E}_{\mathrm{R}}(z) \rightarrow$

$\hat{E}_{\mathrm{R}}(z) + \mathcal{E}$. This simplifies the wavefunction ansatz, as we do not need to include states containing the input field.

Dynamics of the System

To derive all the dynamics of the system that we are interested in, the following method is used: first, we make a wavefuction ansatz, containing all the relevant possible states of the system; time-evolution equations are then derived for all the states; equations of motion are solved numerically and finally, all the quantities we are interested in can be calculated from the dynamics of the states, as long as the necessary states are included in the antsatz.

In this thesis, we are interested in photon-photon interactions. We investigate how two excitations in the system evolve, resulting in two photons being emitted. Correspondingly, we need to include states with two excitations in the wavefunction ansatz to follow such dynamics. However, we consider only weak input fields: $\bar{n} = |\mathcal{E}|^2 \ll 1$. Therefore, we do not need to include states with three or more excitations, because the probability for having that many excitations in the system is very low. Taking this into consideration, we construct the following wavefunction ansatz for a single emitter in a 1D waveguide:

$$\begin{aligned}
\left|\tilde{\Psi}(t)\right\rangle \;=\;& c_{\mathrm{g}}(t)\left|\mathrm{g}0\right\rangle + c_{\mathrm{e}}(t)\left|\mathrm{e}0\right\rangle + \int \mathrm{d}t_{\mathrm{e}} \phi_{\mathrm{gR}}(t, t_{\mathrm{e}}) \hat{E}^{\dagger}_{\mathrm{R}}(v_{\mathrm{g}}(t - t_{\mathrm{e}}) + z_{\mathrm{a}})\left|\mathrm{g}0\right\rangle \\
+\;& \int \mathrm{d}t_{\mathrm{e}} \phi_{\mathrm{eR}}(t, t_{\mathrm{e}}) \hat{E}^{\dagger}_{\mathrm{R}}(v_{\mathrm{g}}(t - t_{\mathrm{e}}) + z_{\mathrm{a}})\left|\mathrm{e}0\right\rangle \\
+\;& \int \mathrm{d}t_{\mathrm{e}2} \int \mathrm{d}t_{\mathrm{e}1} \phi_{\mathrm{RR}}(t, t_{\mathrm{e}2}, t_{\mathrm{e}1}) \hat{E}^{\dagger}_{\mathrm{R}}(v_{\mathrm{g}}(t - t_{\mathrm{e}2}) + z_{\mathrm{a}}) \hat{E}^{\dagger}_{\mathrm{R}}(v_{\mathrm{g}}(t - t_{\mathrm{e}1}) + z_{\mathrm{a}})\left|\mathrm{g}0\right\rangle \\
+\;& \int \mathrm{d}t_{\mathrm{e}2} \int \mathrm{d}t_{\mathrm{e}1} \phi_{\mathrm{RL}}(t, t_{\mathrm{e}2}, t_{\mathrm{e}1}) \hat{E}^{\dagger}_{\mathrm{R}}(v_{\mathrm{g}}(t - t_{\mathrm{e}2}) + z_{\mathrm{a}}) \hat{E}^{\dagger}_{\mathrm{L}}(v_{\mathrm{g}}(t - t_{\mathrm{e}1}) + z_{\mathrm{a}})\left|\mathrm{g}0\right\rangle \\
+\;& \mathrm{R} \leftrightarrow \mathrm{L},
\end{aligned} \tag{3.18}$$

where $\mathrm{R} \leftrightarrow \mathrm{L}$ indicates similar states to the ones presented, with left and right-propagating photon creation operators and corresponding state amplitudes exchanged. The probability amplitudes in the ansatz correspond to: $c_{\mathrm{g(e)}}$ – ground (excited) emitter state amplitude; $\phi_{\mathrm{gR(L)}}(t, t_{\mathrm{e}})$ – a state amplitude at a time t where a right (left)-propagating photon was emitted at time t_{e}, with the emitter in the ground state; $\phi_{\mathrm{eR(L)}}(t, t_{\mathrm{e}})$ – same as $\phi_{\mathrm{gR(L)}}$, but with the emitter in the excited state; $\phi_{\mathrm{RR(LL)}}(t, t_{\mathrm{e}2}, t_{\mathrm{e}1})$ – two right (left)-propagating photons emitted at times $t_{\mathrm{e}2}$ and $t_{\mathrm{e}1}$; ϕ_{RL} and ϕ_{LR} – two-photon state amplitude, where both photons were emitted in different directions, corresponding to either the left or the right-propagating photon being emitted first. Note that the wavefunction consists of state amplitudes, which have dependence on emission time t_e. We include this parameter, because when we evaluate the wavefunction, it would look different depending on when the emission occured. For example, if $t < t_\mathrm{e}$, emission has not occured yet, so any state amplitudes containing emitted photons are equal to 0. The wavefunction at any point in time is then given by considering all emission times (mathematically it means that we integrate over t_e).

Time-evolution of the wavefunction, in the basis of eq. (3.16), is given by

$$i\hbar \left|\dot{\tilde{\Psi}}(t)\right\rangle = \hat{\tilde{H}} \left|\tilde{\Psi}(t)\right\rangle. \tag{3.19}$$

Using this, we derive the equations of motion for ansatz states by projecting into a corresponding state in the following way:

$$\begin{aligned} i\hbar \left\langle \mathrm{g}0 \middle| \dot{\tilde{\Psi}}(t)\right\rangle \quad &= \quad \left\langle \mathrm{g}0 \middle| \hat{\tilde{H}} \middle| \tilde{\Psi}(t)\right\rangle \\ = i\hbar \dot{c}_\mathrm{g}(t) \quad &= \quad -\hbar g_\mathrm{R}\sqrt{2\pi}\mathcal{E}^* \mathrm{e}^{i\Delta t - ik_0 z} c_\mathrm{e}(t). \end{aligned} \tag{3.20}$$

Similarly, we derive the equations of motion for all the other states:

$$\dot{c}_\mathrm{g}(t) = i g_\mathrm{R}\sqrt{2\pi}\mathcal{E}^* \mathrm{e}^{i\Delta t} c_\mathrm{e}(t), \tag{3.21}$$

$$\begin{aligned} \dot{c}_\mathrm{e}(t) =& i g_\mathrm{R}\sqrt{2\pi}\mathcal{E} \mathrm{e}^{-i\Delta t} c_\mathrm{g}(t) - \frac{\Gamma'}{2} c_\mathrm{e}(t) + \frac{i g_\mathrm{R}\sqrt{2\pi}}{v_\mathrm{g}} \phi_\mathrm{gR}(t,t) \mathrm{e}^{-i\Delta t} \\ &+ \frac{i g_\mathrm{L}\sqrt{2\pi}}{v_\mathrm{g}} \phi_\mathrm{gL}(t,t) \mathrm{e}^{-i\Delta t}, \end{aligned} \tag{3.22}$$

$$\dot{\phi}_\mathrm{gR}(t,t_\mathrm{e}) = i g_\mathrm{R}\sqrt{2\pi} c_\mathrm{e}(t_\mathrm{e}) \delta(t - t_\mathrm{e}) \mathrm{e}^{i\Delta t_\mathrm{e}} + i g_\mathrm{R}\sqrt{2\pi}\mathcal{E}^* \mathrm{e}^{i\Delta t} \phi_\mathrm{eR}(t,t_\mathrm{e}), \tag{3.23}$$

$$\begin{aligned} \dot{\phi}_\mathrm{eR}(t,t_\mathrm{e}) =& i g_\mathrm{R}\sqrt{2\pi}\mathcal{E} \mathrm{e}^{-i\Delta t} \phi_\mathrm{gR}(t,t_\mathrm{e}) - \frac{\Gamma'}{2} \phi_\mathrm{eR}(t,t_\mathrm{e}) \\ &+ \frac{i g_\mathrm{R}\sqrt{2\pi}}{v_\mathrm{g}} \phi_\mathrm{RR}(t,t,t_\mathrm{e}) \mathrm{e}^{-i\Delta t} + \frac{i g_\mathrm{R}\sqrt{2\pi}}{v_\mathrm{g}} \phi_\mathrm{RR}(t,t_\mathrm{e},t) \mathrm{e}^{-i\Delta t} \\ &+ \frac{i g_\mathrm{L}\sqrt{2\pi}}{v_\mathrm{g}} \phi_\mathrm{RL}(t,t_\mathrm{e},t) \mathrm{e}^{-i\Delta t} + \frac{i g_\mathrm{L}\sqrt{2\pi}}{v_\mathrm{g}} \phi_\mathrm{LR}(t,t,t_\mathrm{e}) \mathrm{e}^{-i\Delta t}, \end{aligned} \tag{3.24}$$

$$\dot{\phi}_\mathrm{gL}(t,t_\mathrm{e}) = i g_\mathrm{L}\sqrt{2\pi} c_\mathrm{e}(t_\mathrm{e}) \delta(t - t_\mathrm{e}) \mathrm{e}^{i\Delta t_\mathrm{e}} + i g_\mathrm{R}\sqrt{2\pi}\mathcal{E}^* \mathrm{e}^{i\Delta t} \phi_\mathrm{eL}(t,t_\mathrm{e}), \tag{3.25}$$

$$\begin{aligned} \dot{\phi}_\mathrm{eL}(t,t_\mathrm{e}) =& i g_\mathrm{R}\sqrt{2\pi}\mathcal{E} \mathrm{e}^{-i\Delta t} \phi_\mathrm{gL}(t,t_\mathrm{e}) - \frac{\Gamma'}{2} \phi_\mathrm{eL}(t,t_\mathrm{e}) \\ &+ \frac{i g_\mathrm{L}\sqrt{2\pi}}{v_\mathrm{g}} \phi_\mathrm{LL}(t,t,t_\mathrm{e}) \mathrm{e}^{-i\Delta t} + \frac{i g_\mathrm{L}\sqrt{2\pi}}{v_\mathrm{g}} \phi_\mathrm{LL}(t,t_\mathrm{e},t) \mathrm{e}^{-i\Delta t} \\ &+ \frac{i g_\mathrm{R}\sqrt{2\pi}}{v_\mathrm{g}} \phi_\mathrm{RL}(t,t,t_\mathrm{e}) \mathrm{e}^{-i\Delta t} + \frac{i g_\mathrm{R}\sqrt{2\pi}}{v_\mathrm{g}} \phi_\mathrm{LR}(t,t_\mathrm{e},t) \mathrm{e}^{-i\Delta t}, \end{aligned} \tag{3.26}$$

$$\dot{\phi}_{\mathrm{RR}}(t,t_{\mathrm{e2}},t_{\mathrm{e1}}) = ig_{\mathrm{R}}\sqrt{2\pi}\phi_{\mathrm{eR}}(t_{\mathrm{e2}},t_{\mathrm{e1}})\delta(t-t_{\mathrm{e2}})\mathrm{e}^{i\Delta t_{\mathrm{e2}}}, \tag{3.27}$$

$$\dot{\phi}_{\mathrm{LR}}(t,t_{\mathrm{e2}},t_{\mathrm{e1}}) = ig_{\mathrm{L}}\sqrt{2\pi}\phi_{\mathrm{eR}}(t_{\mathrm{e2}},t_{\mathrm{e1}})\delta(t-t_{\mathrm{e2}})\mathrm{e}^{i\Delta t_{\mathrm{e2}}}, \tag{3.28}$$

$$\dot{\phi}_{\mathrm{RL}}(t,t_{\mathrm{e2}},t_{\mathrm{e1}}) = ig_{\mathrm{R}}\sqrt{2\pi}\phi_{\mathrm{eL}}(t_{\mathrm{e2}},t_{\mathrm{e1}})\delta(t-t_{\mathrm{e2}})\mathrm{e}^{i\Delta t_{\mathrm{e2}}}, \tag{3.29}$$

$$\dot{\phi}_{\mathrm{LL}}(t,t_{\mathrm{e2}},t_{\mathrm{e1}}) = ig_{\mathrm{L}}\sqrt{2\pi}\phi_{\mathrm{eL}}(t_{\mathrm{e2}},t_{\mathrm{e1}})\delta(t-t_{\mathrm{e2}})\mathrm{e}^{i\Delta t_{\mathrm{e2}}}. \tag{3.30}$$

The position of the emitter in the above derivation was set to $z_{\mathrm{a}} = 0$. To simplify the equations, we change to a dimensionless time variable $\zeta = \mathit{\Gamma} t$ (where emission times are also dimensionless $\zeta_{\mathrm{e}} = \mathit{\Gamma} t_{\mathrm{e}}$), where $\mathit{\Gamma} = \mathit{\Gamma}_{\mathrm{1D,R}} + \mathit{\Gamma}_{\mathrm{1D,L}} + \mathit{\Gamma}'$ is the total emitter decay rate, with decays into the waveguide defined as $\mathit{\Gamma}_{\mathrm{1D,R(L)}} = \frac{2\pi g^2_{\mathrm{R(L)}}}{v_{\mathrm{g}}}$, and specify the following other dimensionless variables: $\tilde{\mathcal{E}} = \frac{\Gamma}{v_{\mathrm{g}}}\mathcal{E}$, $\phi_{\mathrm{gR(L)}} = \sqrt{\Gamma v_{\mathrm{g}}}\tilde{\phi}_{\mathrm{gR(L)}}$, $\phi_{\mathrm{eR(L)}} = \sqrt{\Gamma v_{\mathrm{g}}}\tilde{\phi}_{\mathrm{eR(L)}}$, $\phi_{\mathrm{R(L)R(L)}} = \Gamma v_{\mathrm{g}}\tilde{\phi}_{\mathrm{R(L)R(L)}}$, $\tilde{\Delta} = \frac{\Delta}{\mathit{\Gamma}}$,$\beta_{\mathrm{R(L)}} = \frac{\mathit{\Gamma}_{\mathrm{1D,R(L)}}}{\mathit{\Gamma}}$, $\beta_{side} = \frac{\mathit{\Gamma}'}{\mathit{\Gamma}}$, noting that $\beta_{\mathrm{R}} + \beta_{\mathrm{L}} + \beta_{side} = 1$. The equations of motion are then changed to the ones given in Appendix A.3.

We consider the emitter to be initially in the ground state, so that $c_{\mathrm{g}} = 1$. Note that ϕ_{gR} and ϕ_{gL} have a term containing $c_{\mathrm{e}}(t_{\mathrm{e}})\delta(t-t_{\mathrm{e}})$, as seen in eq. (3.23) and (3.25). So the derivative of these two state amplitudes get a contribution only after evolution time t has crossed the emission time t_{e}. All the other state amplitudes, which describe states with emitted photons, then evolve as $\phi_{\mathrm{gR(L)}} \to \phi_{\mathrm{eR(L)}} \to \phi_{\mathrm{R(L)R(L)}}$. This can be used to split the time-evolution of the system into two time windows: $0 < \zeta < \zeta_{\mathrm{e}}+\varepsilon$ and $\zeta_{\mathrm{e}}+\varepsilon < \zeta < \infty$ where ε is an infinitesimal dimensionless time period. These two time windows then correspond to: $0 < \zeta < \zeta_{\mathrm{e}} + \varepsilon$ – from the initial state to the evolution time right after the emission of the first photon; $\zeta_{\mathrm{e}} + \varepsilon < \zeta < \infty$ – everything after the first photon emission. As will be seen, the equations of motion for emitter states and for the states containing emitted photons can then be uncoupled. For $0 < \zeta < \zeta_{\mathrm{e}} + \varepsilon$, where we use the dimensionless variables introduced previously:

$$\begin{aligned} \dot{\tilde{\phi}}_{\mathrm{gR}}(\zeta,\zeta_{\mathrm{e}}) &= i\sqrt{\beta_{\mathrm{R}}}c_{\mathrm{e}}(\zeta_{\mathrm{e}})\delta(\zeta-\zeta_{\mathrm{e}})\mathrm{e}^{i\tilde{\Delta}\zeta_{\mathrm{e}}}, \\ \dot{\tilde{\phi}}_{\mathrm{gL}}(\zeta,\zeta_{\mathrm{e}}) &= i\sqrt{\beta_{\mathrm{L}}}c_{\mathrm{e}}(\zeta_{\mathrm{e}})\delta(\zeta-\zeta_{\mathrm{e}})\mathrm{e}^{i\tilde{\Delta}\zeta_{\mathrm{e}}}. \end{aligned} \tag{3.31}$$

These equations can be formally integrated with respect to ζ and give

$$\begin{aligned} \tilde{\phi}_{\mathrm{gR}}(\zeta,\zeta_{\mathrm{e}}) &= i\sqrt{\beta_{\mathrm{R}}}c_{\mathrm{e}}(\zeta)\theta(\zeta-\zeta_{\mathrm{e}})\mathrm{e}^{i\tilde{\Delta}\zeta}, \\ \tilde{\phi}_{\mathrm{gL}}(\zeta,\zeta_{\mathrm{e}}) &= i\sqrt{\beta_{\mathrm{L}}}c_{\mathrm{e}}(\zeta)\theta(\zeta-\zeta_{\mathrm{e}})\mathrm{e}^{i\tilde{\Delta}\zeta}. \end{aligned} \tag{3.32}$$

Plugging in this result for the evolution of excited emitter state, we get

$$
\begin{aligned}
\dot{c}_{\mathrm{e}}(\zeta) &= i\sqrt{\beta_{\mathrm{R}}}\tilde{\mathcal{E}}\mathrm{e}^{-i\tilde{\Delta}\zeta}c_{\mathrm{g}}(\zeta) - \frac{\beta_{side}}{2}c_{\mathrm{e}}(\zeta) + i\sqrt{\beta_{\mathrm{R}}}\tilde{\phi}_{\mathrm{gR}}(\zeta,\zeta)\mathrm{e}^{-\tilde{\Delta}\zeta} + i\sqrt{\beta_{\mathrm{L}}}\tilde{\phi}_{\mathrm{gL}}(\zeta,\zeta)\mathrm{e}^{-i\tilde{\Delta}\zeta} \\
&= i\sqrt{\beta_{\mathrm{R}}}\tilde{\mathcal{E}}\mathrm{e}^{-i\tilde{\Delta}\zeta}c_{\mathrm{g}}(\zeta) - \frac{\beta_{side}}{2}c_{\mathrm{e}}(\zeta) - \beta_{\mathrm{R}}c_{\mathrm{e}}(\zeta)\theta(\zeta-\zeta_{\mathrm{e}}) - \beta_{\mathrm{L}}c_{\mathrm{e}}(\zeta)\theta(\zeta-\zeta_{\mathrm{e}}) \\
&= i\sqrt{\beta_{\mathrm{R}}}\tilde{\mathcal{E}}\mathrm{e}^{-i\tilde{\Delta}\zeta}c_{\mathrm{g}}(\zeta) - \frac{1}{2}c_{\mathrm{e}}(\zeta),
\end{aligned}
\tag{3.33}
$$

where we have used $\theta(0) = \frac{1}{2}$ and $\beta_{\mathrm{R}} + \beta_{\mathrm{L}} + \beta_{side} = 1$. Summarizing, for $0 < \zeta < \zeta_{\mathrm{e}} + \varepsilon$, the time-evolution of the system is given by the following coupled equations of motion:

$$
\begin{aligned}
\dot{c}_{\mathrm{g}}(\zeta) &= i\sqrt{\beta_{\mathrm{R}}}\tilde{\mathcal{E}}^{*}\mathrm{e}^{i\tilde{\Delta}\zeta}c_{\mathrm{e}}(\zeta), \\
\dot{c}_{\mathrm{e}}(\zeta) &= i\sqrt{\beta_{\mathrm{R}}}\tilde{\mathcal{E}}\mathrm{e}^{-i\tilde{\Delta}\zeta}c_{\mathrm{g}}(\zeta) - \frac{1}{2}c_{\mathrm{e}}(\zeta).
\end{aligned}
\tag{3.34}
$$

This result is simply interpreted as follows. There are two processes that affect the evolution of emitter states right up until the point when an emission occurs: excitation of the ground state by the input field (the terms proportional to $\mathcal{E}$ in eq (3.34)) or decay of the excited state into any channel, given by $-\frac{1}{2}c_{\mathrm{e}}$.

Similar derivation is done for the time span $\zeta_{\mathrm{e}} + \varepsilon < \zeta < \infty$. Formal integration of the two photon states, containing a right-propagating photon, gives

$$
\begin{aligned}
\tilde{\phi}_{\mathrm{RR}}(\zeta,\zeta_{\mathrm{e2}},\zeta_{\mathrm{e1}}) &= i\sqrt{\beta_{\mathrm{R}}}\tilde{\phi}_{\mathrm{eR}}(\zeta,\zeta_{\mathrm{e1}})\theta(\zeta-\zeta_{\mathrm{e2}})\mathrm{e}^{i\tilde{\Delta}\zeta}, \\
\tilde{\phi}_{\mathrm{LR}}(\zeta,\zeta_{\mathrm{e2}},\zeta_{\mathrm{e1}}) &= i\sqrt{\beta_{\mathrm{L}}}\tilde{\phi}_{\mathrm{eR}}(\zeta,\zeta_{\mathrm{e1}})\theta(\zeta-\zeta_{\mathrm{e2}})\mathrm{e}^{i\tilde{\Delta}\zeta}, \\
\tilde{\phi}_{\mathrm{RL}}(\zeta,\zeta_{\mathrm{e2}},\zeta_{\mathrm{e1}}) &= i\sqrt{\beta_{\mathrm{R}}}\tilde{\phi}_{\mathrm{eL}}(\zeta,\zeta_{\mathrm{e1}})\theta(\zeta-\zeta_{\mathrm{e2}})\mathrm{e}^{i\tilde{\Delta}\zeta}.
\end{aligned}
\tag{3.35}
$$

Plugging this in for the $\tilde{\phi}_{\mathrm{eR}}$ equation of motion, we get

$$
\begin{aligned}
\dot{\tilde{\phi}}_{\mathrm{eR}}(\zeta,\zeta_{\mathrm{e}}) &= i\sqrt{\beta_{\mathrm{R}}}\tilde{\mathcal{E}}\mathrm{e}^{-i\tilde{\Delta}\zeta}\tilde{\phi}_{\mathrm{gR}}(\zeta,\zeta_{\mathrm{e}}) - \frac{\beta_{side}}{2}\tilde{\phi}_{\mathrm{eR}}(\zeta,\zeta_{\mathrm{e}}) + i\sqrt{\beta_{\mathrm{R}}}\tilde{\phi}_{\mathrm{RR}}(\zeta,\zeta,\zeta_{\mathrm{e}})\mathrm{e}^{-i\tilde{\Delta}\zeta} \\
&+ i\sqrt{\beta_{\mathrm{R}}}\tilde{\phi}_{\mathrm{RR}}(\zeta,\zeta_{\mathrm{e}},\zeta)\mathrm{e}^{-i\tilde{\Delta}\zeta} + i\sqrt{\beta_{\mathrm{L}}}\tilde{\phi}_{\mathrm{RL}}(\zeta,\zeta_{\mathrm{e}},\zeta)\mathrm{e}^{-i\tilde{\Delta}\zeta} + i\sqrt{\beta_{\mathrm{L}}}\tilde{\phi}_{\mathrm{LR}}(\zeta,\zeta,\zeta_{\mathrm{e}})\mathrm{e}^{-i\tilde{\Delta}\zeta} \\
&= i\sqrt{\beta_{\mathrm{R}}}\tilde{\mathcal{E}}\mathrm{e}^{-i\tilde{\Delta}\zeta}\tilde{\phi}_{\mathrm{gR}}(\zeta,\zeta_{\mathrm{e}}) - \frac{1}{2}\tilde{\phi}_{\mathrm{eR}}(\zeta,\zeta_{\mathrm{e}}).
\end{aligned}
\tag{3.36}
$$

Note that in the above equation $\tilde{\phi}_{\mathrm{RR}}(\zeta,\zeta_{\mathrm{e}},\zeta) = \tilde{\phi}_{\mathrm{RL}}(\zeta,\zeta_{\mathrm{e}},\zeta) = 0$, which can be seen from eq. (3.35), because $\tilde{\phi}_{\mathrm{eR}}(\zeta,\zeta) = \tilde{\phi}_{\mathrm{eR}}(\zeta,\zeta) = 0$ (right at the emission time these state amplitudes are 0, as were given by initial condition). Now the time-evolution is described by the following system of equations of motion:

$$\begin{aligned} \dot{\tilde{\phi}}_{\mathrm{gR}}(\zeta,\zeta_{\mathrm{e}}) &= i\sqrt{\beta_{\mathrm{R}}}\tilde{\mathcal{E}}^{*}\mathrm{e}^{i\tilde{\Delta}\zeta}\tilde{\phi}_{\mathrm{eR}}(\zeta,\zeta_{\mathrm{e}}), \\ \dot{\tilde{\phi}}_{\mathrm{eR}}(\zeta,\zeta_{\mathrm{e}}) &= i\sqrt{\beta_{\mathrm{R}}}\tilde{\mathcal{E}}\mathrm{e}^{-i\tilde{\Delta}\zeta}\tilde{\phi}_{\mathrm{gR}}(\zeta,\zeta_{\mathrm{e}}) - \frac{1}{2}\tilde{\phi}_{\mathrm{eR}}(\zeta,\zeta_{\mathrm{e}}). \end{aligned} \tag{3.37}$$

Notice that this is exactly the same set of coupled equations as in eq. (3.34). That is to be expected, because, once an emitter decays and a photon is emitted, the emitter states for one emitter evolve the same way until the second photon emission. Also, note that the initial condition for eq. (3.37) is given by eq. (3.32).

The equations of motion for $0 < \zeta < \zeta_{\mathrm{e}} + \varepsilon$, given by eq. (3.34), will reach a nearly steady-state after some time because we are considering a steady input field. We describe it as a nearly steady-state, because, in this description, the input field is treated as being infinitely long, and there is a constant decay of the excited state. This means that after reaching a steady-state, the states have a slow linear decay, proportional to a higher order of the input field $\tilde{\mathcal{E}}$. This problem will be discussed in detail in Chapter 4 for calculating output intensity. Second order coherence, however, is normalized, so any higher-order errors can be ignored by going to sufficiently low input fields without loss of generalization. In such a limit, we can assume that all states of the system reach a steady-state at some point. After a steady-state is reached, the initial condition for photon-states, given by eq. (3.32), is independent of the emission time. This means that to calculate dymanics of the system for all emission times, it is enough to consider just one emission time, which is sufficiently large so that the emitter state amplitudes c_{g} and c_{e} have reached a steady-state. This, of course, significantly reduces simulation time, since it is not necessary to repeat the calculation multiple times with different ζ_{e}. Taking this into cosideration, we continue with the $g^{(2)}$ calculation.

The second-order coherence function for the state, described by eq. (3.16), at the output of the waveguide for a field incident from the left, is given by:

$$g^{(2)}(t_{\mathrm{d}'},t_{\mathrm{d}}) = \frac{G^{(2)}(t_{\mathrm{d}'},t_{\mathrm{d}})}{G^{(1)}(t_{\mathrm{d}},t_{\mathrm{d}})G^{(1)}(t_{\mathrm{d}'},t_{\mathrm{d}'})}, \tag{3.38}$$

where

$$\begin{aligned} G^{(2)}(t_{\mathrm{d}'},t_{\mathrm{d}}) &= \left|\left(\hat{E}_{\mathrm{R}}(z_{t_{\mathrm{d}}}) + \mathcal{E}\right)\left(\hat{E}_{\mathrm{R}}(z_{t_{\mathrm{d}'}}) + \mathcal{E}\right)\left|\tilde{\Psi}(T)\right\rangle\right|^{2}, \\ G^{(1)}(t_{\mathrm{d}},t_{\mathrm{d}}) &= \left|\left(\hat{E}_{\mathrm{R}}(z_{t_{\mathrm{d}}}) + \mathcal{E}\right)\left|\tilde{\Psi}(T)\right\rangle\right|^{2}. \end{aligned} \tag{3.39}$$

Here $z_{t_{\mathrm{d}}} = v_{\mathrm{g}}\left(T - t_{\mathrm{d}}\right) + L$, which can be understood as follows. We evaluate the wave-function at time T, which is big enough so that all the two photon processes have occured and the photons have already left the waveguide. Then, this photon “wave packet “ travels in free-space until it reaches the detector at position L. Depending on the detection time t_{d}, we would see different parts of the "wave packet". This way we measure the intensity fluctuations at time $t_{\mathrm{d}} - T$.

$$\begin{aligned}\left(\hat{E}_{\mathrm{R}}(z_{t_{\mathrm{d}}}) + \mathcal{E}\right)\left(\hat{E}_{\mathrm{R}}(z_{t_{\mathrm{d}'}}) + \mathcal{E}\right)\left|\tilde{\Psi}(T)\right\rangle = \Bigg(\frac{1}{v_{\mathrm{g}}^2}\phi_{\mathrm{RR}}(T, t'_{\mathrm{e}}, t_{\mathrm{e}}) + \frac{1}{v_{\mathrm{g}}}\mathcal{E}\phi_{\mathrm{gR}}(T, t_{\mathrm{e}}) \\ + \frac{1}{v_{\mathrm{g}}}\mathcal{E}\phi_{\mathrm{gR}}(T, t'_{\mathrm{e}}) + c_{\mathrm{g}}(T)|\mathcal{E}|^2\Bigg)|\mathrm{g}0\rangle + O(\mathcal{E}^3),\end{aligned} \tag{3.40}$$

where $t_{\mathrm{e}} = t_{\mathrm{d}} - \frac{L}{v_{\mathrm{g}}}$.

An example of terms proportional to third order in the input field $O(\mathcal{E}^3)$ in the above equation is: $\left(\frac{1}{v_{\mathrm{g}}}\mathcal{E}\phi_{\mathrm{eR}}(T, t_{\mathrm{e}}) + \frac{1}{v_{\mathrm{g}}}\mathcal{E}\phi_{\mathrm{eR}}(T, t'_{\mathrm{e}}) + c_{\mathrm{e}}(T)|\mathcal{E}|^2\right)|\mathrm{e}0\rangle$. There are other terms in the higher-order of the input field, but since we consider only a weak input field ($|\mathcal{E}|^2 \ll 1$), those terms can be safely neglected for the $g^{(2)}$ calculation. Similarly,

$$\left(\hat{E}_{\mathrm{R}}(z_{t_{\mathrm{d}}}) + \mathcal{E}\right)\left|\tilde{\Psi}(T)\right\rangle = \left(\frac{1}{v_{\mathrm{g}}}\phi_{\mathrm{gR}}(T, t_{\mathrm{e}}) + c_{\mathrm{g}}(T)\mathcal{E}\right)|\mathrm{g}0\rangle + O(\mathcal{E}^2), \tag{3.41}$$

the absolute square of which is $G^{(1)}(t_{\mathrm{d}}, t_{\mathrm{d}})$. Switching to dimensionless variables, $g^{(2)}$ can be written as:

$$g^{(2)}(\zeta'_{\mathrm{e}}, \zeta_{\mathrm{e}}) = \frac{\left|\tilde{\phi}_{\mathrm{RR}}(\zeta_T, \zeta'_{\mathrm{e}}, \zeta_{\mathrm{e}}) + \tilde{\mathcal{E}}\tilde{\phi}_{\mathrm{gR}}(\zeta_T, \zeta_{\mathrm{e}}) + \tilde{\mathcal{E}}\tilde{\phi}_{\mathrm{gR}}(\zeta_T, \zeta'_{\mathrm{e}}) + c_{\mathrm{g}}(\zeta_T)|\tilde{\mathcal{E}}|^2\right|^2}{\left|\tilde{\phi}_{\mathrm{gR}}(\zeta_T, \zeta_{\mathrm{e}}) + c_{\mathrm{g}}(\zeta_T)\tilde{\mathcal{E}}\right|^2\left|\tilde{\phi}_{\mathrm{gR}}(\zeta_T, \zeta'_{\mathrm{e}}) + c_{\mathrm{g}}(\zeta_T)\tilde{\mathcal{E}}\right|^2}, \tag{3.42}$$

where $\zeta_T = \Gamma T$. Using the previously derived equations (3.34), (3.35) and (3.37), it is seen that there are all the terms necessary to calculate $g^{(2)}$ from eq. (3.42). Beforehand, however, note that photon coherence is independent of the first photon emission time, since we look at the steady-state solution for the emitter states, as was mentioned previously. So we can write $g^{(2)}(\zeta'_{\mathrm{e}}, \zeta_{\mathrm{e}})$ as $g^{(2)}(\zeta')$, where $\zeta' = \Gamma\tau$, with $\tau = t'_{\mathrm{e}} - t_{\mathrm{e}}$.

Numerical simulation results for a single emitter in a 1D waveguide are presented in fig. 3.2. It may be immediately seen that the results match for a chiral case and a non-chiral case. This is to be expected, because for one emitter there are no interference effects for left-propagating photons and they can be treated as losses with respect to the output field. Thus, for one emitter it is enough to consider a chiral waveguide with one parameter β_{R} to get the full overview of possible coherences in such a system. We see that for $\beta_{\mathrm{R}} \leq 0.25$ photon anti-bunching occurs. This can be interpreted as follows. For such low emitter

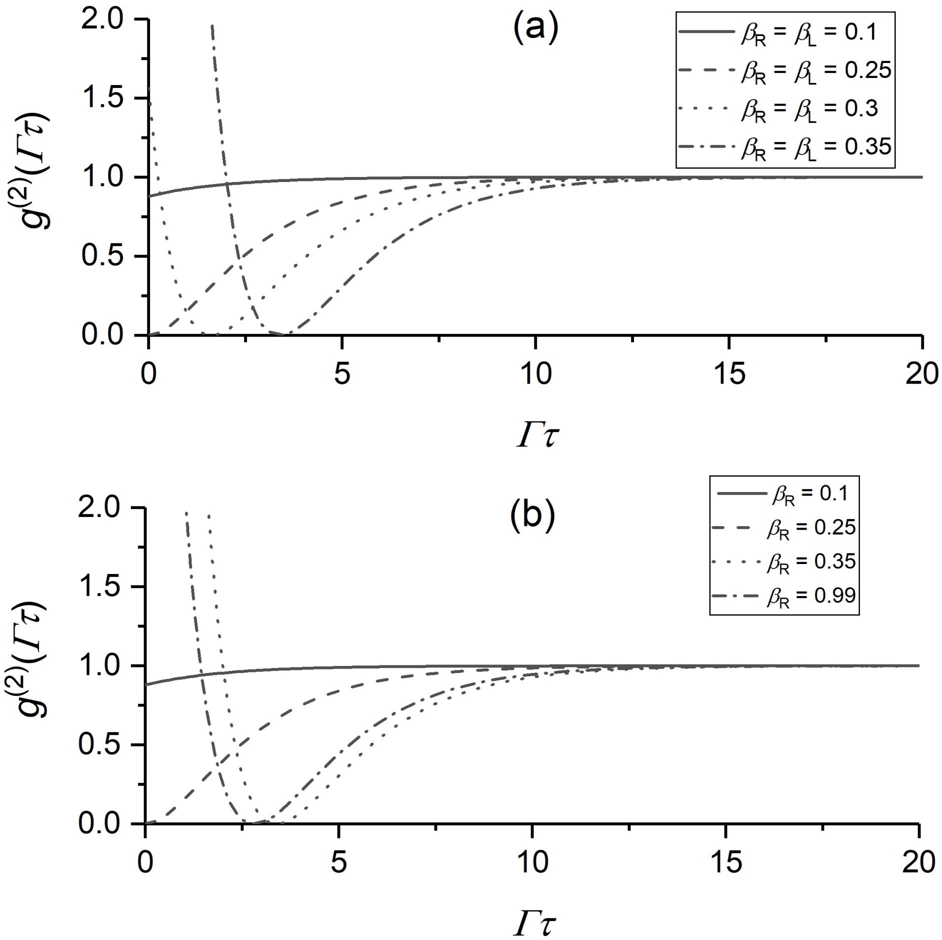

Figure 3.2: $g^{(2)}$ simulation results for one emitter coupled to a 1D waveguide ($\Delta = 0$). a) – equal coupling factors for both the left and right emission directions $\beta_L = \beta_R$; b) – chiral ($\beta_L = 0$) waveguide. Results for chiral and non-chiral waveguide simulations match, because decay to the left can be treated as losses for a single emitter with respect to the transmitted field.

to waveguide coupling, only few of the incoming photons would interact with the emitter. Those that do interact would take some time to be emitted, so this would result in a time delay between the photons, even if a two-photon number state is incident. Note for $\beta_\mathrm{R} = 0.25$ that $g^{(2)}(0) = 0$, which is most likely due to interference effects between the emitted photons and the input field. Such interference effects are difficult to interpret, which only shows that even one emitter in a 1D waveguide produces non-trivial coherences between photons. For higher values of β_R, initial bunching occurs, which is followed by anti-bunching. Value of $g^{(2)}(0) \sim 1$ is observed for low coupling factors, dropping to 0 at $\beta_\mathrm{R} = 0.25$ (anti-coherence mentioned previously). For stronger couplings, $g^{(2)}(0) \gg 1$, peaking at $\beta_\mathrm{R} = 0.5$.

In the next section, we generalize the description presented here for any number of emitters.

3.2 Multiple Emitters

Now that we are familiar with the method used for calculating $g^{(2)}$ for one emitter in a 1D waveguide, we can generalize the approach for any number of emitters. It will be seen that even two emitters produce a range of completely different effects than in one emitter case. This is due to the fact that emitters can get excited by a photon that was emitted by another emitter. We can therefore expect that photon coherences will be highly dependent upon the distance between emitters, because a photon acquires a phase while propagating, and the coupling for left-propagating photons.

Dynamics for N Emitters

We start the derivation by specifying the Hamiltonian for the number of emitters, N. We omit the "~" for operators and the wavefunction, which was used to distinguish the basis, keeping in mind that from now on we work in the basis given by eq. (3.16):

$$
\begin{aligned}
\hat{H} \;=\; & -\hbar\frac{i\Gamma'}{2}\sum_{i=1}^{N}\hat{\sigma}^{i}_{\mathrm{ee}} - \hbar\sqrt{2\pi}\sum_{i=1}^{N}\int \mathrm{d}z\,\delta(z-z_i)\Big[\hat{\sigma}^{i}_{\mathrm{eg}}\Big(g_\mathrm{R}\hat{E}_\mathrm{R}(z)\mathrm{e}^{-i\Delta t+ik_0 z} \\
+ \; & g_\mathrm{R}\mathcal{E}\mathrm{e}^{-i\Delta t+ik_0 z} + g_\mathrm{L}\hat{E}_\mathrm{L}(z)\mathrm{e}^{-i\Delta t-ik_0 z}\Big) + \Big(g_\mathrm{R}\hat{E}^{\dagger}_\mathrm{R}(z)\mathrm{e}^{i\Delta t-ik_0 z} \\
+ \; & g_\mathrm{R}\mathcal{E}^{*}\mathrm{e}^{i\Delta t-ik_0 z} + g_\mathrm{L}\hat{E}^{\dagger}_\mathrm{L}(z)\mathrm{e}^{i\Delta t+ik_0 z}\Big)\hat{\sigma}^{i}_{\mathrm{ge}}\Big].
\end{aligned}
\tag{3.43}
$$

We also construct a new wavefunction ansatz, containing all the possible system states truncated up to two excitations:

$$
\begin{aligned}
\left|\tilde{\Psi}(t)\right\rangle &= c_{\mathrm{g}}(t)\left|\mathrm{g}^N 0\right\rangle + \sum_{i=1}^{N} c_{\mathrm{e}}^{i}(t)\left|\mathrm{e}_i \mathrm{g}^{N-1} 0\right\rangle + \sum_{i<j}^{N} c_{\mathrm{ee}}^{ij}(t)\left|\mathrm{e}_i \mathrm{e}_j \mathrm{g}^{N-2} 0\right\rangle \\
&+ \int \mathrm{d}z_{\mathrm{e}} \int \mathrm{d}t_{\mathrm{e}} \phi_{\mathrm{gR}}(t, t_{\mathrm{e}}, z_{\mathrm{e}}) \hat{E}_{\mathrm{R}}^{\dagger}(v_{\mathrm{g}}(t-t_{\mathrm{e}})+z_{\mathrm{e}})\left|\mathrm{g}^N 0\right\rangle \\
&+ \sum_{i=1}^{N} \int \mathrm{d}z_{\mathrm{e}} \int \mathrm{d}t_{\mathrm{e}} \phi_{\mathrm{eR}}^{i}(t, t_{\mathrm{e}}, z_{\mathrm{e}}) \hat{E}_{\mathrm{R}}^{\dagger}(v_{\mathrm{g}}(t-t_{\mathrm{e}})+z_{\mathrm{e}})\left|\mathrm{e}_i \mathrm{g}^{N-1} 0\right\rangle \\
&+ \int \mathrm{d}z_{\mathrm{e}2} \int \mathrm{d}z_{\mathrm{e}1} \int \mathrm{d}t_{\mathrm{e}2} \int \mathrm{d}t_{\mathrm{e}1} \phi_{\mathrm{RR}}(t, t_{\mathrm{e}2}, t_{\mathrm{e}1}, z_{\mathrm{e}2}, z_{\mathrm{e}1}) \\
&\cdot \hat{E}_{\mathrm{R}}^{\dagger}(v_{\mathrm{g}}(t-t_{\mathrm{e}2})+z_{\mathrm{e}2}) \hat{E}_{\mathrm{R}}^{\dagger}(v_{\mathrm{g}}(t-t_{\mathrm{e}1})+z_{\mathrm{e}1})\left|\mathrm{g}^N 0\right\rangle \\
&+ \int \mathrm{d}z_{\mathrm{e}2} \int \mathrm{d}z_{\mathrm{e}1} \int \mathrm{d}t_{\mathrm{e}2} \int \mathrm{d}t_{\mathrm{e}1} \phi_{\mathrm{RL}}(t, t_{\mathrm{e}2}, t_{\mathrm{e}1}, z_{\mathrm{e}2}, z_{\mathrm{e}1}) \\
&\cdot \hat{E}_{\mathrm{R}}^{\dagger}(v_{\mathrm{g}}(t-t_{\mathrm{e}2})+z_{\mathrm{e}2}) \hat{E}_{\mathrm{L}}^{\dagger}(v_{\mathrm{g}}(t-t_{\mathrm{e}1})+z_{\mathrm{e}1})\left|\mathrm{g}^N 0\right\rangle \\
&+ \mathrm{R} \leftrightarrow \mathrm{L}.
\end{aligned} \tag{3.44}
$$

Note the following changes from the wavefunction ansatz of one emitter: 1) state c_{ee}^{ij} is included, since two emitters can be excited at the same time by two photons from the input field; 2) states that include emitted photons now have to be integrated over the emission positions, to describe where a photon was emitted from.

Equations of motion for each probability amplitude are presented in Appendix A.4. As in the single emitter case, we define two time windows $0 < \zeta < \zeta_{\mathrm{e}} + \varepsilon$ and $\zeta_{\mathrm{e}} + \varepsilon < \zeta < \infty$ to uncouple some of the equations. For $0 < \zeta < \zeta_{\mathrm{e}} + \varepsilon$, the detailed derivation is done in Appendix A.4. The resulting equations of motion that govern the dynamics of the system in the time window $0 < \zeta < \zeta_{\mathrm{e}} + \varepsilon$, using dimensionless variables introduced previously, are given by:

$$
\dot{c}_{\mathrm{g}}(\zeta) = i\sqrt{\beta_{\mathrm{R}}} \sum_{i=1}^{N} \tilde{\mathcal{E}}^{*} \mathrm{e}^{i\tilde{\Delta}\zeta - ik_0 z_i} c_{\mathrm{e}}^{i}(\zeta), \tag{3.45}
$$

$$
\begin{aligned}
\dot{c}_{\mathrm{e}}^{i}(\zeta) =& i\sqrt{\beta_{\mathrm{R}}} \tilde{\mathcal{E}} \mathrm{e}^{-i\tilde{\Delta}\zeta + ik_0 z_i} c_{\mathrm{g}}(\zeta) - \frac{1}{2} c_{\mathrm{e}}^{i}(\zeta) + i\sqrt{\beta_{\mathrm{R}}} \sum_{j<i} \tilde{\mathcal{E}}^{*} \mathrm{e}^{i\tilde{\Delta}\zeta - ik_0 z_j} c_{\mathrm{ee}}^{ji}(\zeta) \\
&+ i\sqrt{\beta_{\mathrm{R}}} \sum_{i<j} \tilde{\mathcal{E}}^{*} \mathrm{e}^{i\tilde{\Delta}\zeta - ik_0 z_j} c_{\mathrm{ee}}^{ij}(\zeta) - \beta_{\mathrm{R}} \sum_{j<i} c_{\mathrm{e}}^{j}(\zeta) \mathrm{e}^{ik_0(z_i - z_j)} - \beta_{\mathrm{L}} \sum_{j>i} c_{\mathrm{e}}^{j}(\zeta) \mathrm{e}^{ik_0(z_j - z_i)},
\end{aligned} \tag{3.46}
$$

$$
\begin{aligned}
\dot{c}_{\mathrm{ee}}^{ij}(\zeta) =& i\sqrt{\beta_{\mathrm{R}}} \tilde{\mathcal{E}} \mathrm{e}^{-i\tilde{\Delta}\zeta + ik_0 z_j} c_{\mathrm{e}}^{i}(\zeta) + i\sqrt{\beta_{\mathrm{R}}} \tilde{\mathcal{E}} \mathrm{e}^{-i\tilde{\Delta}\zeta + ik_0 z_i} c_{\mathrm{e}}^{j}(\zeta) - c_{\mathrm{ee}}^{ij}(\zeta) \\
&- \beta_{\mathrm{R}} \sum_{j'<i} c_{\mathrm{ee}}^{j'i}(\zeta) \mathrm{e}^{ik_0(z_j - z_{j'})} - \beta_{\mathrm{R}} \sum_{j'<j, j'>i} c_{\mathrm{ee}}^{ij'}(\zeta) \mathrm{e}^{ik_0(z_j - z_{j'})} \\
&- \beta_{\mathrm{R}} \sum_{i'<i,} c_{\mathrm{ee}}^{i'j}(\zeta) \mathrm{e}^{ik_0(z_i - z_{i'})} - \beta_{\mathrm{L}} \sum_{j'>j} c_{\mathrm{ee}}^{ij'}(\zeta) \mathrm{e}^{ik_0(z_{j'} - z_j)}
\end{aligned}
$$

$$- \beta_{\mathrm{L}} \sum_{i'>i, i'<j}^{N} c_{\mathrm{ee}}^{i'j}(\zeta) \mathrm{e}^{ik_0(z_{i'}-z_i)} - \beta_{\mathrm{L}} \sum_{i'>j}^{N} c_{\mathrm{ee}}^{ji'}(\zeta) \mathrm{e}^{ik_0(z_{i'}-z_i)}. \tag{3.47}$$

Having the equations of motion in this final form, we can investigate what processes are present that were not in the single emitter case. We see that time-evolution of c_{g} is unchanged – the only process is the excitation of emitters by the input field. For c_{e} states, however, apart from excitation from c_{g} and the decay term (first two terms), we observe new processes: since there is more than one emitter, another emitter can get excited with the system changing to one of the c_{ee} states (terms proportional to c_{ee}); one of the emitters can decay emitting a photon, which is absorbed by another emitter (last two terms), with a phase difference that the photon acquires during propagation between the two emitters – $\mathrm{e}^{ik_0(z_i-z_j)}$. Note that due to the last process described, depending on the distance between the emitters, there can be many distinct interference effects that can completely change the coherence between photons. This will be illustrated by considering a two emitter case at the end of this section. Also, note that similar processes are seen for c_{ee} time-evolution: excitation from c_{e} states and decay (first three terms); reabsorption of a photon, emitted by another emitter (all the other terms).

For the time window $\zeta_{\mathrm{e}} + \varepsilon < \zeta < \infty$, we perform a similar derivation for the state amplitudes, which contain right-propagating photons and are given in Appendix A.4. We formally integrate the state amplitudes $\tilde{\phi}_{\mathrm{RR}}$, $\tilde{\phi}_{\mathrm{RL}}$, $\tilde{\phi}_{\mathrm{LR}}$ and plug in the result to the equations of motion for $\tilde{\phi}_{\mathrm{eR}}$. The system dynamics for $\zeta_{\mathrm{e}} + \varepsilon < \zeta < \infty$ are then described by the following time-evolution equations:

$$\dot{\tilde{\phi}}_{\mathrm{gR}}(\zeta, \zeta_{\mathrm{e}}, z_{\mathrm{e}}) = i\sqrt{\beta_{\mathrm{R}}} \sum_{i=1}^{N} \tilde{\mathcal{E}}^* \mathrm{e}^{i\tilde{\Delta}\zeta - ik_0 z_i} \tilde{\phi}_{\mathrm{eR}}^{i}(\zeta, \zeta_{\mathrm{e}}, z_{\mathrm{e}}), \tag{3.48}$$

$$\begin{aligned} \dot{\tilde{\phi}}_{\mathrm{eR}}^{i}(\zeta, \zeta_{\mathrm{e}}, z_{\mathrm{e}}) &= i\sqrt{\beta_{\mathrm{R}}} \tilde{\mathcal{E}} \mathrm{e}^{-i\tilde{\Delta}\zeta + ik_0 z_i} \tilde{\phi}_{\mathrm{gR}}(\zeta, \zeta_{\mathrm{e}}, z_{\mathrm{e}}) - \frac{1}{2} \tilde{\phi}_{\mathrm{eR}}^{i}(\zeta, \zeta_{\mathrm{e}}, z_{\mathrm{e}}) \\ &- \beta_{\mathrm{R}} \sum_{j<i} \tilde{\phi}_{\mathrm{eR}}^{j}(\zeta, \zeta_{\mathrm{e}}, z_{\mathrm{e}}) \mathrm{e}^{ik_0(z_i - z_j)} - \beta_{\mathrm{L}} \sum_{j>i} \tilde{\phi}_{\mathrm{eR}}^{j}(\zeta, \zeta_{\mathrm{e}}, z_{\mathrm{e}}) \mathrm{e}^{ik_0(z_j - z_i)}. \end{aligned} \tag{3.49}$$

Here, again, notable changes from the single emitter case are the last two terms in eq. (3.49), which describe interaction between emitters by emission and reabsorption of photons.

When looking at the output field of the waveguide, we are interested in the total photon "wave-packet", which can consist of photons emitted at various positions. Mathematically, this means that we should integrate over all emission positions z_{e}. In order to do this, we now define new variables, distinguished by a superscript "z", which indicates position integrated variables: $\tilde{\phi}^{z}_{\mathrm{g(e)R}}(\zeta, \zeta_{\mathrm{e}}) = \int \mathrm{d}z_{\mathrm{e}} \tilde{\phi}_{\mathrm{g(e)R}}(\Gamma t, \zeta_{\mathrm{e}}, z_{\mathrm{e}})$, $\tilde{\phi}^{z}_{\mathrm{RR}}(\zeta, \zeta_{\mathrm{e2}}, \zeta_{\mathrm{e1}}) =$

$\int \mathrm{d}z_{\mathrm{e}2} \int \mathrm{d}z_{\mathrm{e}1} \tilde{\phi}_{\mathrm{RR}}(\zeta, \zeta_{\mathrm{e}2}, \zeta_{\mathrm{e}1}, z_{\mathrm{e}2}, z_{\mathrm{e}1})$. In terms of these new variables the equations of motion for time window $\zeta_{\mathrm{e}} + \varepsilon < \zeta < \infty$ can be rewritten without dependence of z_{e} as:

$$
\begin{aligned}
\dot{\tilde{\phi}}^{z}_{\mathrm{gR}}(\zeta, \zeta_{\mathrm{e}}) &= i\sqrt{\beta_{\mathrm{R}}} \sum_{i=1}^{N} \tilde{\mathcal{E}}^{*} \mathrm{e}^{i\tilde{\Delta}\zeta - ik_0 z_i} \tilde{\phi}^{z,i}_{\mathrm{eR}}(\zeta, \zeta_{\mathrm{e}}), && (3.50)\\
\dot{\tilde{\phi}}^{z,i}_{\mathrm{eR}}(\zeta, \zeta_{\mathrm{e}}) &= i\sqrt{\beta_{\mathrm{R}}} \tilde{\mathcal{E}} \mathrm{e}^{-i\tilde{\Delta}\zeta + ik_0 z_i} \tilde{\phi}^{z}_{\mathrm{gR}}(\zeta, \zeta_{\mathrm{e}}) - \frac{1}{2} \tilde{\phi}^{z,i}_{\mathrm{eR}}(\zeta, \zeta_{\mathrm{e}}) \\
&- \beta_{\mathrm{R}} \sum_{j<i} \tilde{\phi}^{z,j}_{\mathrm{eR}}(\zeta, \zeta_{\mathrm{e}}) \mathrm{e}^{ik_0(z_i - z_j)} - \beta_{\mathrm{L}} \sum_{j>i} \phi^{z,j}_{\mathrm{eR}}(\zeta, \zeta_{\mathrm{e}}) \mathrm{e}^{ik_0(z_j - z_i)}, && (3.51)\\
\tilde{\phi}^{z}_{\mathrm{RR}}(\zeta, \zeta_{\mathrm{e}2}, \zeta_{\mathrm{e}1}) &= i\sqrt{\beta_{\mathrm{R}}} \sum_{i=1}^{N} \tilde{\phi}^{z,i}_{\mathrm{eR}}(\zeta_{\mathrm{e}2}, \zeta_{\mathrm{e}1}) \theta(\zeta - \zeta_{\mathrm{e}2}) \mathrm{e}^{i\tilde{\Delta}\zeta - ik_0 z_i}. && (3.52)
\end{aligned}
$$

The initial condition for these equations are then given by:

$$
\begin{aligned}
\tilde{\phi}^{z}_{\mathrm{gR}}(\zeta_{\mathrm{e}} + \varepsilon, \zeta_{\mathrm{e}}) &= i\sqrt{\beta_{\mathrm{R}}} \sum_{i=1}^{N} c^{i}_{\mathrm{e}}(\zeta_{\mathrm{e}}) \mathrm{e}^{i\tilde{\Delta}\zeta_{\mathrm{e}} - ik_0 z_i}, && (3.53)\\
\tilde{\phi}^{z,i}_{\mathrm{eR}}(\zeta_{\mathrm{e}} + \varepsilon, \zeta_{\mathrm{e}}) &= i\sqrt{\beta_{\mathrm{R}}} \sum_{j<i}^{N} c^{ji}_{\mathrm{ee}}(\zeta_{\mathrm{e}}) \mathrm{e}^{i\tilde{\Delta}\zeta_{\mathrm{e}} - ik_0 z_j} + i\sqrt{\beta_{\mathrm{R}}} \sum_{j>i}^{N} c^{ij}_{\mathrm{ee}}(\zeta_{\mathrm{e}}) \mathrm{e}^{i\tilde{\Delta}\zeta_{\mathrm{e}} - ik_0 z_j}. && (3.54)
\end{aligned}
$$

Also, note that the calculation of these integrated variables is faster numerically because we do not need to consider a separate state amplitude for each emission position. Having derived all the equations of motion, we can proceed with the $g^{(2)}$ calculation for N emitters.

$g^{(2)}$ is given by the same form as in eq. (3.38) and (3.39). Using the N emitter wavefunction ansatz (eq. (3.44)), calculating $G^{(2)}$, $G^{(1)}$ and omitting higher order terms we get:

$$
\begin{aligned}
G^{(2)}(\zeta'_{\mathrm{d}}, \zeta_{\mathrm{d}}) &= \Bigg| \int \mathrm{d}z_{\mathrm{e}2} \int \mathrm{d}z_{\mathrm{e}1} \tilde{\phi}_{\mathrm{RR}}(\zeta_T, \zeta'_{\mathrm{d}} - \Gamma \frac{L - z_{\mathrm{e}2}}{v_{\mathrm{g}}}, \zeta_{\mathrm{d}} - \Gamma \frac{L - z_{\mathrm{e}1}}{v_{\mathrm{g}}}, z_{\mathrm{e}2}, z_{\mathrm{e}1}) \\
&+ \int \mathrm{d}z_{\mathrm{e}} \tilde{\mathcal{E}} \tilde{\phi}_{\mathrm{gR}}(\zeta_T, \zeta_{\mathrm{d}} - \Gamma \frac{L - z_{\mathrm{e}}}{v_{\mathrm{g}}}, z_{\mathrm{e}}) && (3.55)\\
&+ \int \mathrm{d}z_{\mathrm{e}} \tilde{\mathcal{E}} \tilde{\phi}_{\mathrm{gR}}(\zeta_T, \zeta'_{\mathrm{d}} - \Gamma \frac{L - z_{\mathrm{e}}}{v_{\mathrm{g}}}) + c_{\mathrm{g}}(\zeta_T) |\tilde{\mathcal{E}}|^2 \Bigg|^2, \\
G^{(1)}(\zeta_{\mathrm{d}}, \zeta_{\mathrm{d}}) &= \Bigg| \int \mathrm{d}z_{\mathrm{e}} \tilde{\phi}_{\mathrm{gR}}(\zeta_T, \zeta_{\mathrm{d}} - \Gamma \frac{L - z_{\mathrm{e}}}{v_{\mathrm{g}}}) + c_{\mathrm{g}}(\zeta_T) \tilde{\mathcal{E}} \Bigg|^2. && (3.56)
\end{aligned}
$$

Note that the above equations contain emissions times like $\zeta_{\mathrm{d}} - \Gamma \frac{L - z_{\mathrm{e}}}{v_{\mathrm{g}}}$. Since we will be considering distances between the emitters around the wavelength of photons, the maximum time difference (in dimensionless units) for a photon to travel through the waveguide is $\Gamma\frac{N\lambda_0}{v_{\mathrm{g}}}$. It is easily seen that $\Gamma\frac{N\lambda_0}{v_{\mathrm{g}}} = \frac{N\Gamma}{\nu_0}$, where $\nu_0 = \frac{\omega_0}{2\pi}$. The electronic transition frequencies for atoms are usually near the optical range - hundreds of THz, while the decay rates are in the range of MHz. So $\Gamma\frac{z_N - z_1}{v_{\mathrm{g}}} \ll 1$ as long as we do not consider millions of emitters, and we can safely discard terms such as $\Gamma\frac{z_{\mathrm{e}}}{v_{\mathrm{g}}}$. In doing so, we can change to position integrated variables that were introduced before and write $G^{(2)}$ and $G^{(1)}$ as:

$$
\begin{aligned}
G^{(2)}(\zeta_{\mathrm{e}}', \zeta_{\mathrm{e}}) &= \left|\tilde{\phi}^z_{\mathrm{RR}}(\zeta_T, \zeta_{\mathrm{e}}', \zeta_{\mathrm{e}}) + \tilde{\mathcal{E}}\tilde{\phi}^z_{\mathrm{gR}}(\zeta_T, \zeta_{\mathrm{e}}) + \tilde{\mathcal{E}}\tilde{\phi}^z_{\mathrm{gR}}(\zeta_T, \zeta_{\mathrm{e}}') + c_{\mathrm{g}}(\zeta_T)|\tilde{\mathcal{E}}|^2\right|^2, \quad (3.57)\\
G^{(1)}(\zeta_{\mathrm{e}}, \zeta_{\mathrm{e}}) &= \left|\tilde{\phi}^z_{\mathrm{gR}}(\zeta_T, \zeta_{\mathrm{e}}) + c_{\mathrm{g}}(\zeta_T)\tilde{\mathcal{E}}\right|^2, \quad (3.58)
\end{aligned}
$$

where $\zeta_{\mathrm{e}} = \zeta_{\mathrm{d}} - \Gamma\frac{L}{v_{\mathrm{g}}}$ as in the single emitter case. Now that $g^{(2)}$ can be calculated, we first present the results for two emitters in a waveguide to get an intuitive idea of what to expect for N emitters, and in the next section the results are presented for large numbers of emitters in many different cases.

Photon-Photon Coherences for Two Emitters in a Waveguide

As mentioned before, to illustrate how photon-photon coherences are influenced by interactions between emitters, which are mediated by emitted and reabsorbed photons, we now consider a two emitter case. For $0 < \zeta < \zeta_{\mathrm{e}} + \varepsilon$, we use eq. (3.46) to construct the following system of equations presented in a matrix form:

$$
\dot{\vec{C}} = M_C \vec{C}, \tag{3.59}
$$

where

$$
\vec{C} = \begin{pmatrix} c_{\mathrm{g}} \\ c^1_{\mathrm{e}} \\ c^2_{\mathrm{g}} \\ c^{12}_{\mathrm{ee}} \end{pmatrix}, \tag{3.60}
$$

$$
M_C = \begin{pmatrix}
0 & i\sqrt{\beta_{\mathrm{R}}}\tilde{\mathcal{E}}^*\mathrm{e}^{i\tilde{\Delta}\zeta - ik_0z_1} & i\sqrt{\beta_{\mathrm{R}}}\tilde{\mathcal{E}}^*\mathrm{e}^{i\tilde{\Delta}\zeta - ik_0z_2} & 0 \\
i\sqrt{\beta_{\mathrm{R}}}\mathcal{E}\mathrm{e}^{-i\tilde{\Delta}\zeta + ik_0z_1} & -\frac{1}{2} & -\beta_{\mathrm{L}}\mathrm{e}^{ik_0(z_2 - z_1)} & i\sqrt{\beta_{\mathrm{R}}}\tilde{\mathcal{E}}^*\mathrm{e}^{i\tilde{\Delta}\zeta - ik_0z_2} \\
i\sqrt{\beta_{\mathrm{R}}}\mathcal{E}\mathrm{e}^{-i\tilde{\Delta}\zeta + ik_0z_2} & -\beta_{\mathrm{R}}\mathrm{e}^{ik_0(z_2 - z_1)} & -\frac{1}{2} & i\sqrt{\beta_{\mathrm{R}}}\tilde{\mathcal{E}}^*\mathrm{e}^{i\tilde{\Delta}\zeta - ik_0z_1} \\
0 & i\sqrt{\beta_{\mathrm{R}}}\tilde{\mathcal{E}}\mathrm{e}^{-i\tilde{\Delta}\zeta + ik_0z_2} & i\sqrt{\beta_{\mathrm{R}}}\tilde{\mathcal{E}}\mathrm{e}^{-i\tilde{\Delta}\zeta + ik_0z_1} & -1
\end{pmatrix}. \tag{3.61}
$$

We clearly see from these equations the effect that was mentioned before: the excited state of the first emitter c_{e}^{1} is coupled to the second emitter with coupling factor β_{L} and the other way around with β_{R}, with the phase that a photon acquires during propagation. For $\zeta_{\mathrm{e}}+\varepsilon<\zeta<\infty$ we use eq. (3.49) to construct a matrix equation describing the system after the first photon was emitted:

$$\dot{\overrightarrow{P}} = M_P \overrightarrow{P}, \tag{3.62}$$

where

$$\overrightarrow{P} = \begin{pmatrix} \tilde{\phi}^{z}_{\mathrm{gR}} \\ \tilde{\phi}^{z,1}_{\mathrm{eR}} \\ \tilde{\phi}^{z,2}_{\mathrm{eR}} \end{pmatrix}, \tag{3.63}$$

$$M_P = \begin{pmatrix} 0 & i\sqrt{\beta_{\mathrm{R}}}\tilde{\mathcal{E}}^{*}\mathrm{e}^{i\tilde{\Delta}\zeta-ik_0z_1} & i\sqrt{\beta_{\mathrm{R}}}\tilde{\mathcal{E}}^{*}\mathrm{e}^{i\tilde{\Delta}\zeta-ik_0z_2} \\ i\sqrt{\beta_{\mathrm{R}}}\tilde{\mathcal{E}}\mathrm{e}^{-i\tilde{\Delta}\zeta+ik_0z_1} & -\frac{1}{2} & -\beta_{\mathrm{L}}\mathrm{e}^{ik_0(z_2-z_1)} \\ i\sqrt{\beta_{\mathrm{R}}}\tilde{\mathcal{E}}\mathrm{e}^{-i\tilde{\Delta}\zeta+ik_0z_2} & -\beta_{\mathrm{R}}\mathrm{e}^{ik_0(z_2-z_1)} & -\frac{1}{2} \end{pmatrix}, \tag{3.64}$$

with initial condition given by:

$$\tilde{\phi}^{z}_{\mathrm{gR}}(\zeta_{\mathrm{e}}+\varepsilon,\zeta_{\mathrm{e}}) = i\sqrt{\beta_{\mathrm{R}}}\left(c_{\mathrm{e}}^{1}(\zeta_{\mathrm{e}})\mathrm{e}^{i\tilde{\Delta}\zeta_{\mathrm{e}}-ik_0z_1} + c_{\mathrm{e}}^{2}(\Gamma t_{\mathrm{e}})\mathrm{e}^{i\tilde{\Delta}\zeta_{\mathrm{e}}-ik_0z_2}\right), \tag{3.65}$$

$$\tilde{\phi}^{z,1}_{\mathrm{eR}}(\zeta_{\mathrm{e}}+\varepsilon,\zeta_{\mathrm{e}}) = i\sqrt{\beta_{\mathrm{R}}}c_{\mathrm{ee}}^{12}(\zeta_{\mathrm{e}})\mathrm{e}^{i\tilde{\Delta}\zeta_{\mathrm{e}}-ik_0z_2}, \tag{3.66}$$

$$\tilde{\phi}^{z,2}_{\mathrm{eR}}(\zeta_{\mathrm{e}}+\varepsilon,\zeta_{\mathrm{e}}) = i\sqrt{\beta_{\mathrm{R}}}c_{\mathrm{ee}}^{12}(\zeta_{\mathrm{e}})\mathrm{e}^{i\tilde{\Delta}\zeta_{\mathrm{e}}-ik_0z_1}. \tag{3.67}$$

Notice that the matrix M_P is the same as M_C apart from the terms describing evolution of the two-emitter excited state amplitude. That is, of course, due to the truncation of our wavefunction to second-order in excitation – if a photon is emitted and two emitters are excited, it would give three excitations in the system, which we neglect. By using eq. (3.57), eq. (3.58) and

$$\begin{aligned}\tilde{\phi}^{z}_{\mathrm{RR}}(\zeta,\zeta_{\mathrm{e2}},\zeta_{\mathrm{e1}}) =& i\sqrt{\beta_{\mathrm{R}}}\tilde{\phi}^{z,1}_{\mathrm{eR}}(\zeta_{\mathrm{e2}},\zeta_{\mathrm{e1}})\theta(\zeta-\zeta_{\mathrm{e2}})\mathrm{e}^{i\tilde{\Delta}\zeta-ik_0z_1} \\ &+ i\sqrt{\beta_{\mathrm{R}}}\tilde{\phi}^{z,2}_{\mathrm{eR}}(\zeta_{\mathrm{e2}},\zeta_{\mathrm{e1}})\theta(\zeta-\zeta_{\mathrm{e2}})\mathrm{e}^{i\tilde{\Delta}\zeta-ik_0z_1},\end{aligned} \tag{3.68}$$

we calculate $g^{(2)}$ and present the results in fig. 3.3 and 3.4.

We first discuss the chiral waveguide case (fig. 3.3, panel (a)). Note that for a chiral waveguide, photon correlations are independent of the distance between emitters. For a

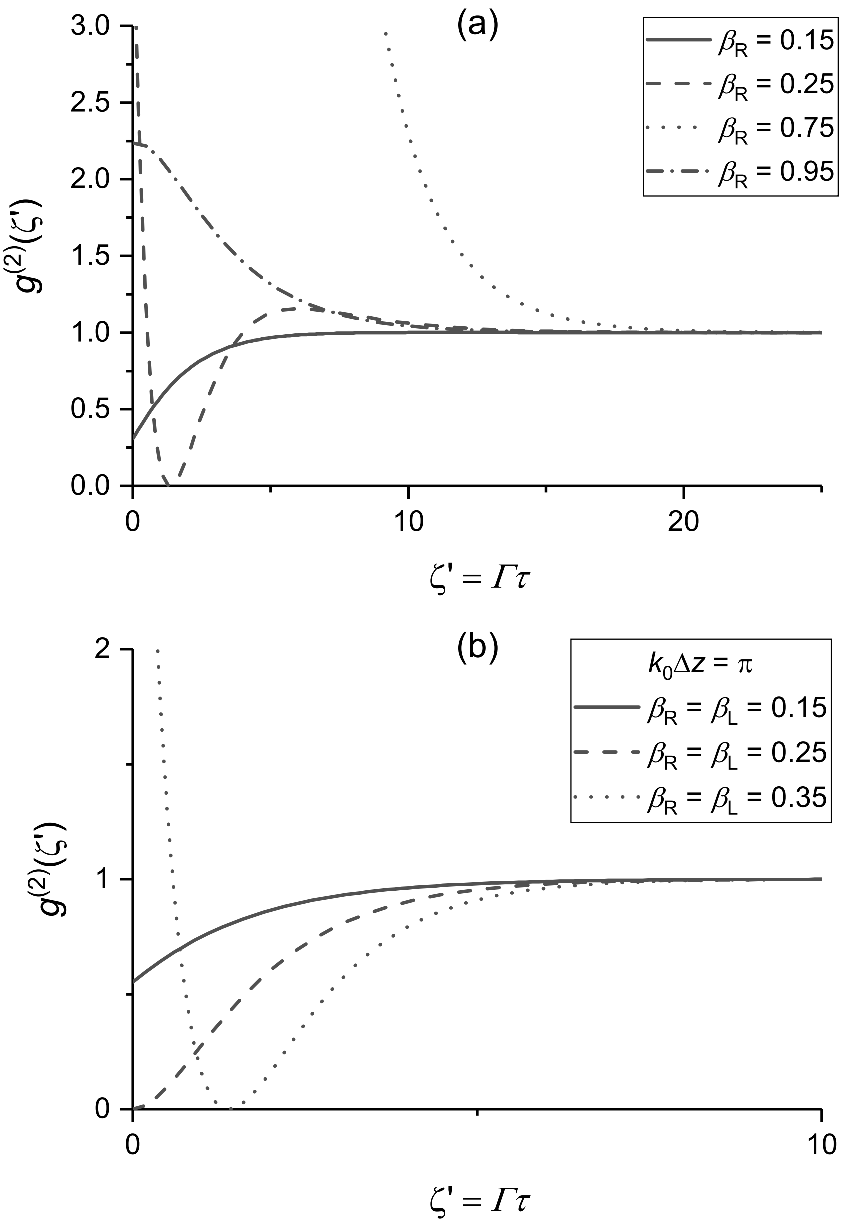

Figure 3.3: $g^{(2)}$ simulation results for two emitters in a waveguide ($\Delta = 0$): (a) – chiral waveguide; (b) – waveguide with coupling β factor equal in both directions (and with distance between emitters in phase $k_0\Delta z = \pi$).

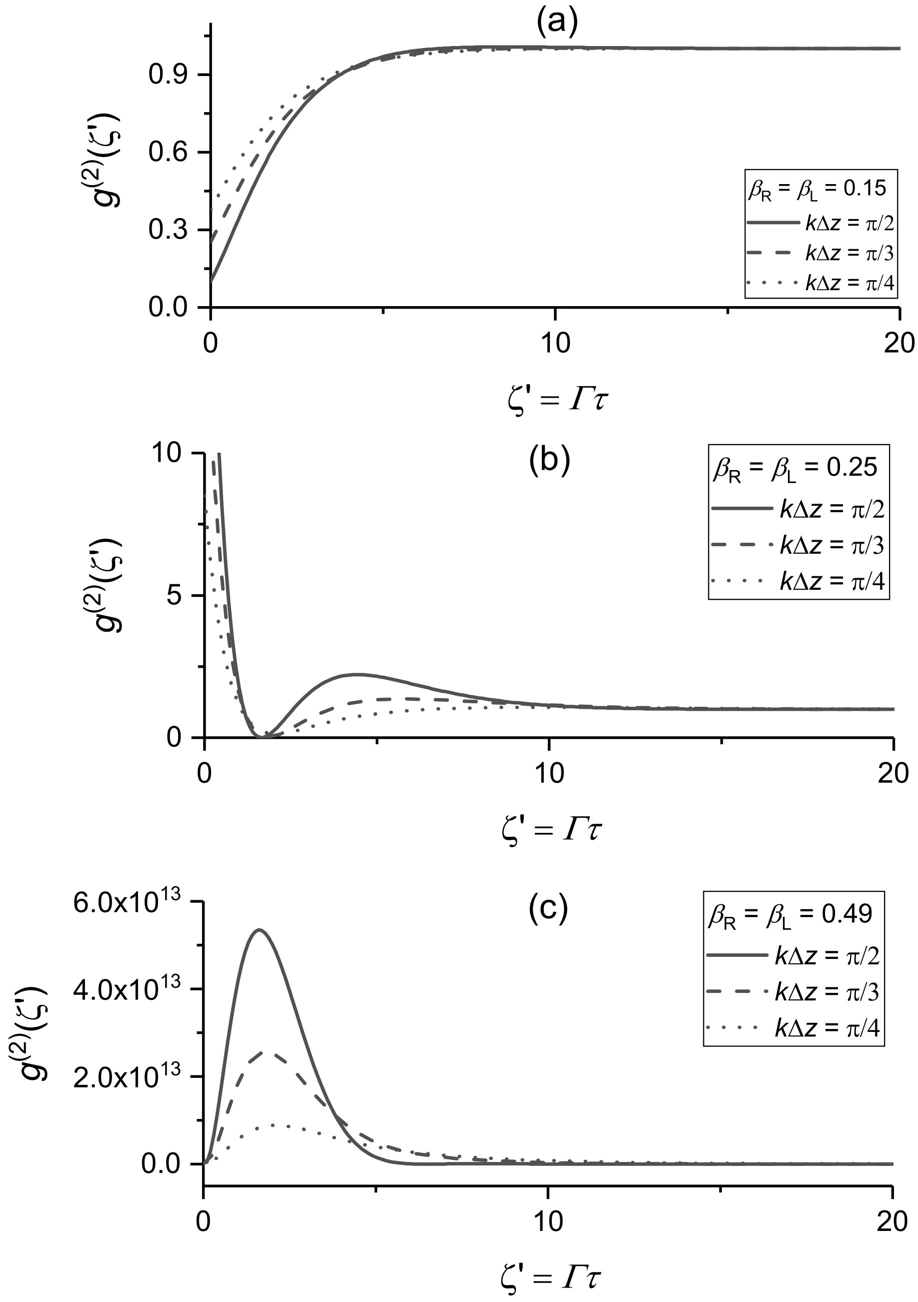

Figure 3.4: $g^{(2)}$ simulation results for two emitters in a waveguide with different parameters ($\Delta = 0$): (a) – $\beta_{\mathrm{R}} = \beta_{\mathrm{L}} = 0.15$; (b) – $\beta_{\mathrm{R}} = \beta_{\mathrm{L}} = 0.25$; (c) – $\beta_{\mathrm{R}} = \beta_{\mathrm{L}} = 0.49$.

small coupling ($\beta_{\mathrm{R}} = 0.15$), we get a similar result as in the single emitter case – antibunching. However, a different and interesting result is observed for $\beta_{\mathrm{R}} = 0.25$. Initial bunching is followed by a short period of antibunching and then another slight increase in correlations, while in the single emitter case, complete initial anti-corellation was observed ($g^{(2)} = 0$). This suggests that the destructive interference between emitted and transmitted photons in the single emitter case is altered by the second emitter. The slight second increase in coherence might be a result of a process where the first emitter emits a photon and the second emitter absorbs and reemits. Stronger couplings result in a strong initial bunching (peaking at $\beta_{\mathrm{R}} = 0.5$, not shown).

We next discuss cases with equal coupling for the left and right-propagating photons. A good example of interactions between emitters, mediated by emitted photons is for a distance between emitters $k_0\Delta z = \pi$ (fig. 3.3, panel (b)). We see that coherences are very similar to the single emitter case. That is because photons, emitted from different emitters, interfere constructively. Due to this, the system for such spacing between emitters behaves like an atomic Bragg mirror [20].

For small β_{R} and β_{L} couplings (fig. 3.4, panel (a)), anti-bunching is observed, independent of the distance between emitters. For $\beta_{\mathrm{R}} = \beta_{\mathrm{L}} = 0.25$, a bunching is followed by anti-bunching and slight increase in coherence again, as in the chiral case, with higher amplitude. For $\beta_{\mathrm{R}} = \beta_{\mathrm{L}} = 0.49$, strong initial bunching is observed, with correlations peaking around $2\Gamma\tau$.

In the next section, numerical $g^{(2)}$ simulation results are presented for higher number of emitters.

3.3 Simulation Results

In this section, we discuss $g^{(2)}$ numerical simulation results for multiple emitters. In the previous section it was seen that photon coherences are non-trivial even for a single emitter. Also, for two emitters, interference effects were shown to give a rich range of distinct photon-photon correlations. It is interesting to see how these effects scale for a large number of emitters.

We start with the results for a waveguide with equal β factors for both directions – fig. 3.5. First of all, note that for $k_0\Delta z = \pi$ (fig. 3.5, panels (a) and (b)), we observe the same effect as in the two emitter case – due to constructive interference between emitted photons, the system behaves as a single emitter. However, $g^{(2)}$ reaches a steady value faster for a larger number of emitters – it takes around $0.3\Gamma\tau$ for 50 emitters. It is interesting to note that an emitter decays with a total rate of Γ – a frequency, which characterizes

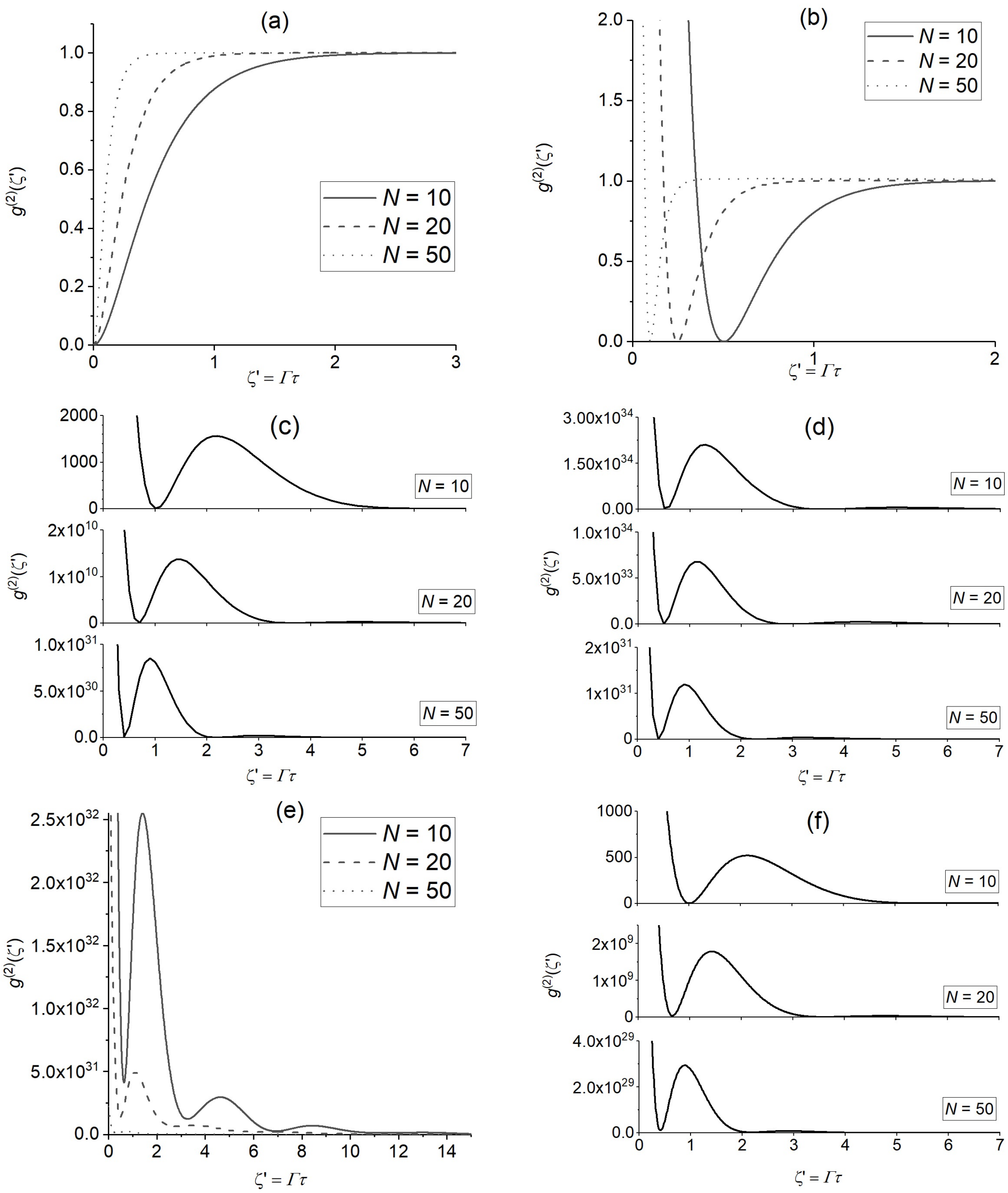

Figure 3.5: $g^{(2)}$ simulation results for multiple emitters in a non-chiral waveguide ($\Delta = 0$). (a) – $\beta_R = \beta_L = 0.25$ with a distance between emitters of $k_0\Delta z = \pi$; (b) – $\beta_R = \beta_L = 0.45$ and $k_0\Delta z = \pi$; (c) – $\beta_R = \beta_L = 0.15$ and $k_0\Delta z = \pi/2$; (d) – $\beta_R = \beta_L = 0.45$ and $k_0\Delta z = \pi/2$; (e) – $\beta_R = \beta_L = 0.45$ and $k_0\Delta z = \pi/4$; (f) – $\beta_R = \beta_L = 0.15$ and $k_0\Delta z = \pi/4$. A system with $k_0\Delta z = \pi$ shows nonlinear properties similar to the single emitter case. Smaller distances between emitters result in strong bunching of photons and oscillations of the second-order correlation function.

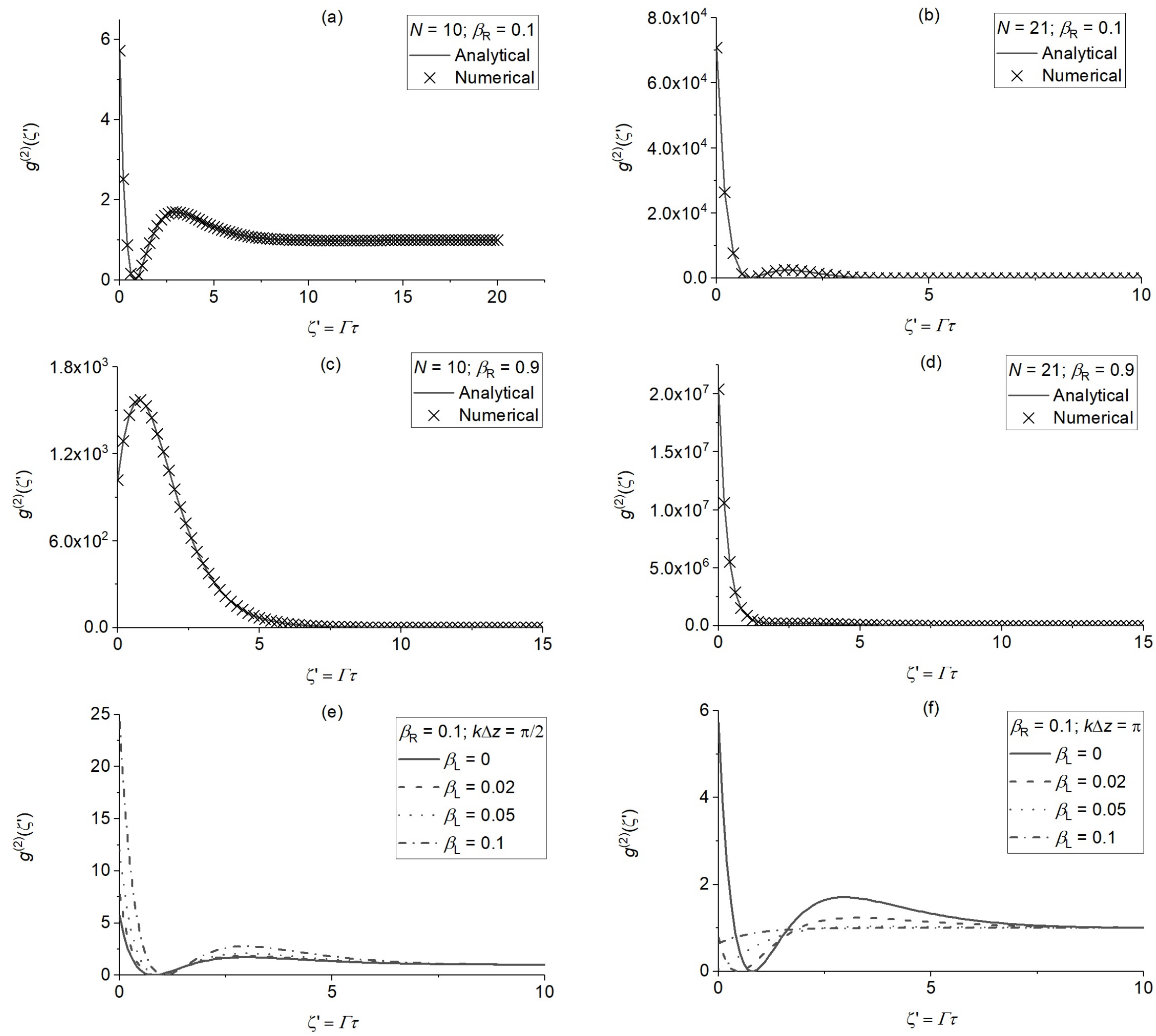

Figure 3.6: $g^{(2)}$ simulation results for multiple emitters in a chiral waveguide ($\Delta = 0$). (a)-(d) – comparison between analytical results [21] and numerical simulation results; (e)-(f) – small coupling is added for the left-propagating photons in a chiral waveguide with uniform emitter placement, showing that this changes the chiral waveguide behaviour.

system dynamics, but we get an effect in a higher frequency than that. Another interesting scaling effect can be seen for low coupling factors $\beta_{\mathrm{R}} = \beta_{\mathrm{L}} = 0.15$, both for $k_0\Delta z = \pi/2$ and $k_0\Delta z = \pi/4$ (fig. 3.5, panels (c) and (f)). In the single and two emitter cases, low coupling resulted in anti-bunching, independent of the distance between emitters because the input field would rarely interact with emitters. Here, however, multiple periods of strong coherence are seen. This can be explained as follows – as the input field propagates through more emitters, there is a higher probability for interaction, even for a small light-matter coupling. The peaks in coherence after initial bunching are most likely the delayed photon emission due to reabsorption. Finally, for $k_0\Delta z = \pi/4$ and strong coupling ($\beta_{\mathrm{R}} = \beta_{\mathrm{L}} = 0.45$, fig. 3.5, panel (e)), distinctly rapid and high amplitude oscillations occur in $g^{(2)}$. Note that in all cases correlations oscillate faster for a larger number of emitters, suggesting that collectively emitters are more effective at "squeezing" photons in time.

In fig. 3.6, the second-order correlation function results for a chiral waveguide are presented. In panels (a)-(d), numerical simulation results are compared against analytical results [21]. The results match, showing strong initial bunching ocurring in all cases, with secondary peaks in correlations for a smaller coupling ($\beta_{\mathrm{R}} = 0.1$). For a higher coupling ($\beta_{\mathrm{R}} = 0.9$), only a single coherence peak is observed. It is interesting to see how correlations change if a coupling for left-propagating photons is added (panels (e)-(f)). The results are then dependent upon the distance between emitters. For $k_0\Delta z = \pi/2$, similar oscillations occur in $g^{(2)}$ with a smaller amplitude, however, the secondary peak in correlations vanishes for higher values of β_{L}. For $k_0\Delta z = \pi$, the coupling to the left completely changes the second-order coherence, leading to initial anti-bunching instead of bunching. Thus, the coherence effects for a chiral waveguide are susceptible for small couplings to the other propagation direction for uniform emitter placement.

Chapter 4

Output Intensity

In this chapter, we discuss how output intensity can be calculated for any number of two-level emitters, with a similar method that was used for second-order coherence calculation. It is not straightforward for a few reasons, which will be discussed in this chapter. In section 4.1, the dynamics of the system will be derived. In section 4.2, a workaround method used for speeding up numerical simulation time will be discussed. Finally, in section 4.3, numerical simulation results will be presented.

4.1 System Dynamics for Output Intensity

Apart from second-order coherence, investigating output intensity gives additional insight into the nonlinear response of the system. We expect transmission for single photons to follow the optical depth relation $T \sim \mathrm{e}^{-\beta N}$. However, it is interesting to see how nonlinear transmission scales for multiple emitters. Since we truncate our system up to two excitations, we can only investigate the two-photon component in the input coherent field expansion. That is sufficient for a weak input field, since the probability of three or more photon states would be small. However, when we were calculating the second-order coherence function, not all of the processes that can contribute to intensity were not included. An example of such a process is illustrated in fig. 4.1, where one photon is lost to the environment, while another right-propagating photon is emitted into the waveguide. This photon still contributes to the output intensity, so it is necessary to include such states if we want to calculate transmission for the two-photon state.

Hamiltonian and Wavefunction Ansatz

To derive dynamics of state amplitudes with a photon emitted outside the waveguide, we first need to modify the Hamiltonian, given by eq. (3.43):

$$\begin{aligned}\hat{H} &= -\hbar\sqrt{2\pi}\sum_{i=1}^{N}\int \mathrm{d}y\delta(y)\int \mathrm{d}z\delta(z-z_i)\Big[\hat{\sigma}^i_{\mathrm{eg}}\Big(g_{\mathrm{R}}\hat{E}_{\mathrm{R}}(z)\mathrm{e}^{-i\Delta t+ik_0z}+g_{\mathrm{R}}\mathcal{E}\mathrm{e}^{-i\Delta t+ik_0z}\\ &+ +g_{\mathrm{L}}\hat{E}_{\mathrm{L}}(z)\mathrm{e}^{-i\Delta t-ik_0z}+g_{\mathrm{side}}\hat{E}_{\mathrm{S},m}(y)\mathrm{e}^{-i\Delta t}\Big)+\Big(g_{\mathrm{R}}\hat{E}^{\dagger}_{\mathrm{R}}(z)\mathrm{e}^{i\Delta t-ik_0z}\\ &+ g_{\mathrm{R}}\mathcal{E}^*\mathrm{e}^{i\Delta t-ik_0z}+g_{\mathrm{L}}\hat{E}^{\dagger}_{\mathrm{L}}(z)\mathrm{e}^{i\Delta t+ik_0z}+g_{\mathrm{side}}\hat{E}^{\dagger}_{\mathrm{S},m}(y)\mathrm{e}^{i\Delta t}\Big)\hat{\sigma}^i_{\mathrm{ge}}\Big].\end{aligned} \tag{4.1}$$

As can be seen, instead of an effective non-Hermitian term $-i\frac{\Gamma}{2}$ as before, we specify decay outside the waveguide as coupling between the emitter and the side-propagating field ($\hat{E}^{(\dagger)}_{\mathrm{S}}$) with a coupling constant g_{side}. To follow which emitter decayed outside the waveguide, we use an index m for the separate side-propagating photon annihilation (creation) operators $\hat{E}^{(\dagger)}_{\mathrm{S},m}$ for each emitter m. Also, note that we introduce another propagation direction y for photons that decayed outside the waveguide. The commutation relations for these operators are then given by:

$$\Big[\hat{E}_{\mathrm{S},m}(y),\hat{E}^{\dagger}_{\mathrm{S},m'}(y')\Big]=\delta_{m,m'}\delta(y-y'). \tag{4.2}$$

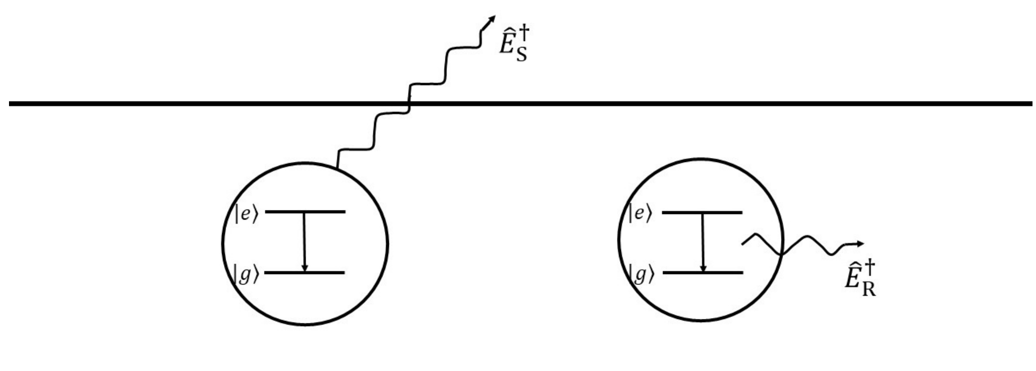

Figure 4.1: Illustration of a process when one photon is emitted outside the waveguide ($\hat{E}^{\dagger}_{\mathrm{S}}$), while the other one is emitted into the waveguide as a right-propagating photon ($\hat{E}^{\dagger}_{\mathrm{R}}$). The right-propagating photon still contributes to the total output intensity, so it is necessary to include such two-photon states in the description of system dynamics.

To describe decay outside the waveguide properly, we must henceforth include all possible states of the system that have photons emitted to the side in the wavefunction ansatz and, as was mentioned in Chapter 3, we truncate it up to two excitations in the system. Taking this into consideration, we can write the new wavefunction ansatz as

$$\begin{aligned}
|\Psi(t)\rangle = |\Psi_0(t)\rangle &+ \sum_{m=1}^{N} \int \mathrm{d}t_\mathrm{s} \phi_{\mathrm{gS},m}(t,t_\mathrm{s}) \hat{E}^\dagger_{\mathrm{S},m}(v_\mathrm{g}(t-t_\mathrm{s})) \left| \mathrm{g}^N 0 \right\rangle \\
&+ \sum_{m=1}^{N} \sum_{i=1}^{N} \int \mathrm{d}t_\mathrm{s} \phi^i_{\mathrm{eS},m}(t,t_\mathrm{s}) \hat{E}^\dagger_{\mathrm{S},m}(v_\mathrm{g}(t-t_\mathrm{s})) \left| \mathrm{e}_i \mathrm{g}^{N-1} 0 \right\rangle \\
&+ \sum_{m'=1}^{N} \sum_{m=1}^{N} \int \mathrm{d}t_\mathrm{s2} \int \mathrm{d}t_\mathrm{s1} \phi_{\mathrm{S,m'S},m}(t,t_\mathrm{s2},t_\mathrm{s1}) \hat{E}^\dagger_{\mathrm{S},m'}(v_\mathrm{g}(t-t_\mathrm{s2})) \hat{E}^\dagger_{\mathrm{S},m}(v_\mathrm{g}(t-t_\mathrm{s1})) \left| \mathrm{g}^N 0 \right\rangle \\
&+ \sum_{m=1}^{N} \int \mathrm{d}t_\mathrm{s} \int \mathrm{d}t_\mathrm{e} \phi_{\mathrm{RS},m}(t,t_\mathrm{s},t_\mathrm{e},z_\mathrm{e}) \hat{E}^\dagger_{\mathrm{S},m}(v_\mathrm{g}(t-t_\mathrm{s})) \hat{E}^\dagger_{\mathrm{R}}(v_\mathrm{g}(t-t_\mathrm{e})+z_\mathrm{e}) \left| \mathrm{g}^N 0 \right\rangle \\
&+ \sum_{m=1}^{N} \int \mathrm{d}t_\mathrm{s} \int \mathrm{d}t_\mathrm{e} \phi_{\mathrm{LS},m}(t,t_\mathrm{s},t_\mathrm{e},z_\mathrm{e}) \hat{E}^\dagger_{\mathrm{S},m}(v_\mathrm{g}(t-t_\mathrm{s})) \hat{E}^\dagger_{\mathrm{L}}(v_\mathrm{g}(t-t_\mathrm{e})+z_\mathrm{e}) \left| \mathrm{g}^N 0 \right\rangle, \quad (4.3)
\end{aligned}$$

where $|\Psi_0(t)\rangle$ is the wavefunction ansatz that was used in the second-order coherence calculation, given by eq. (3.44). The newly introduced probability amplitudes correspond to the following states: $\phi_{\mathrm{gS},m}(t,t_\mathrm{s})$ – emitters in the ground state and a photon emitted outside the waveguide at t_s; $\phi^i_{\mathrm{eS},m}(t,t_\mathrm{s})$ – same as $\phi_{\mathrm{gS},m}(t,t_\mathrm{s})$, but with emitter i in the excited state; $\phi_{\mathrm{S,m'S},m}(t,t_\mathrm{s2},t_\mathrm{s1})$ – two photons emitted outside the waveguide at emission times t_s1 and t_s2; $\phi_{\mathrm{R(L)S},m}(t,t_\mathrm{s},t_\mathrm{e},z_\mathrm{e})$ – one photon emitted outside the waveguide at t_s and another emitted into the waveguide as (left) right-propagating photon at time t_e and position z_e (corresponding to the example in fig. 4.1).

Equations of Motion

The time-evolution of probability amplitudes is given by:

$$i\hbar \left| \dot{\Psi}(t) \right\rangle = \hat{H} \left| \Psi(t) \right\rangle, \quad (4.4)$$

where the Hamiltonian is given by eq. (4.1) and the wavefunction by eq. (4.3). We define dimensionless variables, so that $\phi_{\mathrm{gS},m}(t,t_\mathrm{s}) = \sqrt{v_\mathrm{g}\mathit{\Gamma}}\tilde{\phi}_{\mathrm{gS},m}(t,t_\mathrm{s})$, $\phi_{\mathrm{eS},m}(t,t_\mathrm{s}) = \sqrt{v_\mathrm{g}\mathit{\Gamma}}\tilde{\phi}_{\mathrm{eS},m}(t,t_\mathrm{s})$, $\phi_{\mathrm{S,m'S},m} = v_\mathrm{g}\mathit{\Gamma}\tilde{\phi}_{\mathrm{S,m'S},m}(t,t_\mathrm{s})$, $\phi_{\mathrm{RS},m} = v_\mathrm{g}\mathit{\Gamma}\tilde{\phi}_{\mathrm{RS},m}(t,t_\mathrm{s})$, $\beta_\mathrm{side} = \frac{\mathit{\Gamma}'}{\mathit{\Gamma}}$, where $\mathit{\Gamma}' = \frac{2\pi g^2_\mathrm{side}}{v_\mathrm{g}}$, and we use the same dimensionless time ($\zeta = \mathit{\Gamma}t$, $\zeta_\mathrm{s} = \mathit{\Gamma}t_\mathrm{s}$, $\zeta_\mathrm{e} = \mathit{\Gamma}t_\mathrm{e}$) and other variables, as were defined in Chapter 3. We then derive the equations of motion for the probability amplitudes, which contain photons emitted outside the waveguide:

$$
\begin{aligned}
\dot{\tilde{\phi}}_{\mathrm{gS},m}(\zeta,\zeta_{\mathrm{s}}) &= i\sqrt{\beta_{\mathrm{side}}}c_{\mathrm{e}}^{m}(\zeta_{\mathrm{s}})\delta(\zeta-\zeta_{\mathrm{s}})\mathrm{e}^{i\tilde{\Delta}\zeta_{\mathrm{s}}} + i\sqrt{\beta_{\mathrm{R}}}\sum_{i=1}^{N}\tilde{\mathcal{E}}^{*}\mathrm{e}^{i\tilde{\Delta}\zeta-ik_0z_i}\tilde{\phi}_{\mathrm{eS},m}^{i}(\zeta,\zeta_{\mathrm{s}}), &(4.5)\\
\dot{\tilde{\phi}}_{\mathrm{eS},m}^{i}(\zeta,\zeta_{\mathrm{s}}) &= i\sqrt{\beta_{\mathrm{side}}}c_{\mathrm{ee}}^{im}(\zeta_{\mathrm{s}})\delta(\zeta-\zeta_{\mathrm{s}})\mathrm{e}^{i\tilde{\Delta}\zeta_{\mathrm{s}}} + i\sqrt{\beta_{\mathrm{side}}}\tilde{\phi}_{\mathrm{S,iS},m}(\zeta,\zeta,\zeta_{\mathrm{s}})\mathrm{e}^{-i\tilde{\Delta}\zeta}\\
&\quad + i\sqrt{\beta_{\mathrm{side}}}\tilde{\phi}_{\mathrm{S,iS},m}(\zeta,\zeta_{\mathrm{s}},\zeta)\mathrm{e}^{-i\tilde{\Delta}\zeta} + i\sqrt{\beta_{\mathrm{R}}}\tilde{\mathcal{E}}\mathrm{e}^{-i\tilde{\Delta}\zeta+ik_0z_i}\tilde{\phi}_{\mathrm{gS},m}(\zeta,\zeta_{\mathrm{s}})\\
&\quad + i\sqrt{\beta_{\mathrm{R}}}\int \mathrm{d}z_{\mathrm{e}}\tilde{\phi}_{\mathrm{RS},m}(\zeta,\zeta_{\mathrm{s}},\zeta+\mathit{\Gamma}\frac{z_{\mathrm{e}}-z_i}{v_{\mathrm{g}}},z_{\mathrm{e}})\mathrm{e}^{-i\tilde{\Delta}\zeta+ik_0z_i}\\
&\quad + i\sqrt{\beta_{\mathrm{R}}}\int \mathrm{d}z_{\mathrm{e}}\tilde{\phi}_{\mathrm{LS},m}(\zeta,\zeta_{\mathrm{s}},\zeta-\mathit{\Gamma}\frac{z_{\mathrm{e}}-z_i}{v_{\mathrm{g}}},z_{\mathrm{e}})\mathrm{e}^{-i\tilde{\Delta}\zeta-ik_0z_i}, &(4.6)\\
\dot{\tilde{\phi}}_{\mathrm{S,m'S},m}(\zeta,\zeta_{\mathrm{s2}},\zeta_{\mathrm{s1}}) &= i\sqrt{\beta_{\mathrm{side}}}\tilde{\phi}_{\mathrm{eS},m}^{m'}(\zeta_{\mathrm{s2}},\zeta_{\mathrm{s1}})\delta(\zeta-\zeta_{\mathrm{s2}})\mathrm{e}^{i\tilde{\Delta}\zeta_{\mathrm{s2}}}, &(4.7)\\
\dot{\tilde{\phi}}_{\mathrm{RS},m}(\zeta,\zeta_{\mathrm{s}},\zeta_{\mathrm{e}},z_{\mathrm{e}}) &= i\sqrt{\beta_{\mathrm{R}}}\sum_{i=1}^{N}\tilde{\phi}_{\mathrm{eS},m}^{i}(\zeta_{\mathrm{e}},\zeta_{\mathrm{s}})\delta(\zeta-\zeta_{\mathrm{e}})\mathrm{e}^{i\tilde{\Delta}\zeta_{\mathrm{s}}-ik_0z_i}\\
&\quad + i\sqrt{\beta_{\mathrm{side}}}\tilde{\phi}_{\mathrm{eR}}^{m}(\zeta_{\mathrm{s}},\zeta_{\mathrm{e}},z_{\mathrm{e}})\delta(\zeta-\zeta_{\mathrm{s}})\mathrm{e}^{i\tilde{\Delta}\zeta_{\mathrm{e}}}, &(4.8)\\
\dot{\tilde{\phi}}_{\mathrm{LS},m}(\zeta,\zeta_{\mathrm{s}},\zeta_{\mathrm{e}},z_{\mathrm{e}}) &= i\sqrt{\beta_{\mathrm{L}}}\sum_{i=1}^{N}\tilde{\phi}_{\mathrm{eS},m}^{i}(\zeta_{\mathrm{e}},\zeta_{\mathrm{s}})\delta(\zeta-\zeta_{\mathrm{e}})\mathrm{e}^{i\tilde{\Delta}\zeta_{\mathrm{s}}+ik_0z_i}\\
&\quad\; i\sqrt{\beta_{\mathrm{side}}}\tilde{\phi}_{\mathrm{eL}}^{m}(\zeta_{\mathrm{s}},\zeta_{\mathrm{e}},z_{\mathrm{e}})\delta(\zeta-\zeta_{\mathrm{s}})\mathrm{e}^{i\tilde{\Delta}\zeta_{\mathrm{e}}}. &(4.9)
\end{aligned}
$$

Similarly to the second-order coherence derivation done previously, we define two dimensionless time windows $0 < \zeta < \zeta_{\mathrm{s}}+\varepsilon$ and $\zeta_{\mathrm{s}}+\varepsilon < \zeta < \infty$. Note that these time windows are for emission time outside the waveguide ζ_{s}, instead of emission time into the waveguide ζ_{e}, which was used previously. Since emission outside the waveguide can occur before emission into the waveguide, we need separate time windows to uncouple the equations of motion given above. In Appendix B.1, it is shown that for $0 < \zeta < \zeta_{\mathrm{s}}+\varepsilon$, the time-evolution equations for excited emitter state amplitudes (c_{e} and c_{ee}) are the same as were derived in the second-order coherence calculation, which are given in Appendix A.4. This shows that the non-Hermitian Hamiltonian term $\hat{H}_{\mathrm{side}} = -\hbar\frac{i\mathit{\Gamma}'}{2}\sum_{i=1}^{N}\hat{\sigma}_{\mathrm{ee}}^{i}$ in the previous chapter was chosen correctly to give an effective description of decay outside the waveguide.

In the second-order coherence calculation, for a time window of $\zeta_{\mathrm{e}}+\varepsilon < \zeta < \infty$, we formally integrated the equation of motion of the two-photon probability amplitude ($\tilde{\phi}_{\mathrm{RR}}$) and plugged that in to the equation of motion for $\tilde{\phi}_{\mathrm{eR}}^{i}$, which resulted in the decay and interactions terms of the excited emitter states (eq. (3.49)). We would like to carry out a similar procedure in this case as well with probability amplitudes containing photons emitted outside the waveguide for the time-window $\zeta_{\mathrm{s}}+\varepsilon < \zeta < \infty$, i.e., formally integrate time-evolution equations of $\phi_{\mathrm{S,m'S},m}$, $\tilde{\phi}_{\mathrm{RS},m}$ and $\tilde{\phi}_{\mathrm{LS},m}$, and use the result for the $\tilde{\phi}_{\mathrm{eS},m}^{i}$ equation of motion. However, notice that the time-evolution equation for $\tilde{\phi}_{\mathrm{RS},m}$ and $\tilde{\phi}_{\mathrm{LS},m}$

(eq. (4.8) and (4.9), respectively) have two distinct in time delta functions $\delta(\zeta-\zeta_{\mathrm{e}})$ and $\delta(\zeta-\zeta_{\mathrm{s}})$. These terms result from the fact that a state that has one photon emitted outside and one emitted into the waveguide can occur in two ways – either we first have decay outside the waveguide and then into the waveguide or the other way around. As will be shown later in this section, it is enough to only consider the first case, when emission outside the waveguide occurs before emission into the waveguide. We can then only investigate a time window $\zeta_{\mathrm{s}}+\varepsilon<\zeta<\zeta_{\mathrm{e}}+\varepsilon$ instead of $\zeta_{\mathrm{s}}+\varepsilon<\zeta<\infty$. Then the terms containing $\tilde{\phi}^{m}_{\mathrm{eR}}$ and $\tilde{\phi}^{m}_{\mathrm{eL}}$ in eq. (4.8) and (4.9), are not present and we can formally integrate the equations of motion for $\tilde{\phi}_{\mathrm{S,m'S},m}$, $\tilde{\phi}_{\mathrm{RS},m}$ and $\tilde{\phi}_{\mathrm{LS},m}$ as:

$$
\begin{aligned}
\tilde{\phi}_{\mathrm{S,m'S},m}(\zeta,\zeta_{\mathrm{s2}},\zeta_{\mathrm{s1}}) &= i\sqrt{\beta_{\mathrm{side}}}\tilde{\phi}^{m'}_{\mathrm{eS},m}(\zeta,\zeta_{\mathrm{s1}})\theta(\zeta-\zeta_{\mathrm{s2}})\mathrm{e}^{i\tilde{\Delta}\zeta}, && (4.10)\\
\tilde{\phi}_{\mathrm{RS},m}(\zeta,\zeta_{\mathrm{s}},\zeta_{\mathrm{e}},z_{\mathrm{e}}) &= i\sqrt{\beta_{\mathrm{R}}}\sum_{i=1}^{N}\tilde{\phi}^{i}_{\mathrm{eS},m}(\zeta,\zeta_{\mathrm{s}})\theta(\zeta-\zeta_{\mathrm{e}})\mathrm{e}^{i\tilde{\Delta}\zeta-ik_0z_i}, && (4.11)\\
\tilde{\phi}_{\mathrm{LS},m}(\zeta,\zeta_{\mathrm{s}},\zeta_{\mathrm{e}},z_{\mathrm{e}}) &= i\sqrt{\beta_{\mathrm{L}}}\sum_{i=1}^{N}\tilde{\phi}^{i}_{\mathrm{eS},m}(\zeta,\zeta_{\mathrm{s}})\theta(\zeta-\zeta_{\mathrm{e}})\mathrm{e}^{i\tilde{\Delta}\zeta+ik_0z_i}. && (4.12)
\end{aligned}
$$

Plugging this into the derived equations of motion for $\tilde{\phi}_{\mathrm{gS},m}$ and $\tilde{\phi}^{i}_{\mathrm{eS},m}$, we get the following:

$$
\begin{aligned}
\dot{\tilde{\phi}}_{\mathrm{gS},m}(\zeta,\zeta_{\mathrm{s}}) &= i\sqrt{\beta_{\mathrm{R}}}\sum_{i=1}^{N}\tilde{\mathcal{E}}^{*}\mathrm{e}^{i\tilde{\Delta}\zeta-ik_0z_i}\tilde{\phi}^{i}_{\mathrm{eS},m}(\zeta,\zeta_{\mathrm{s}}), && (4.13)\\
\dot{\tilde{\phi}}^{i}_{\mathrm{eS},m}(\zeta,\zeta_{\mathrm{s}}) &= i\sqrt{\beta_{\mathrm{R}}}\tilde{\mathcal{E}}\mathrm{e}^{-i\tilde{\Delta}\zeta+ik_0z_i}\tilde{\phi}_{\mathrm{gS},m}(\zeta,\zeta_{\mathrm{s}})-\frac{\beta_{\mathrm{side}}}{2}\tilde{\phi}^{i}_{\mathrm{eS},m}(\zeta,\zeta_{\mathrm{s}})\\
&\quad-\beta_{\mathrm{R}}\sum_{j=1}^{N}\tilde{\phi}^{j}_{\mathrm{eS},m}(\zeta,\zeta_{\mathrm{s}})\theta(\mathit{\Gamma}\frac{z_{\mathrm{e}}-z_i}{v_{\mathrm{g}}})\mathrm{e}^{ik_0(z_i-z_j)}\\
&\quad-\beta_{\mathrm{L}}\sum_{j=1}^{N}\tilde{\phi}^{j}_{\mathrm{eS},m}(\zeta,\zeta_{\mathrm{s}})\theta(-\mathit{\Gamma}\frac{z_{\mathrm{e}}-z_i}{v_{\mathrm{g}}})\mathrm{e}^{ik_0(z_j-z_i)}, && (4.14)
\end{aligned}
$$

with the initial condition given by

$$
\begin{aligned}
\tilde{\phi}_{\mathrm{gS},m}(\zeta_{\mathrm{s}}+\varepsilon,\zeta_{\mathrm{s}}) &= i\sqrt{\beta_{\mathrm{side}}}c^{m}_{\mathrm{e}}(\zeta)\mathrm{e}^{i\tilde{\Delta}\zeta},\\
\tilde{\phi}^{i}_{\mathrm{eS},m}(\zeta+\varepsilon,\zeta_{\mathrm{s}}) &= i\sqrt{\beta_{\mathrm{side}}}c^{im}_{\mathrm{ee}}(\zeta)\mathrm{e}^{i\tilde{\Delta}\zeta}.
\end{aligned}
$$

Using $\theta(0)=\frac{1}{2}$, we simplify eq. (4.14) and get the coupled equations that govern the system dynamics for $\zeta_{\mathrm{s}}+\varepsilon<\zeta<\zeta_{\mathrm{e}}+\varepsilon$:

$$\begin{aligned}
\dot{\tilde{\phi}}_{\mathrm{gS},m}(\zeta,\zeta_{\mathrm{s}}) =& i\sqrt{\beta_{\mathrm{R}}}\sum_{i=1}^{N}\tilde{\mathcal{E}}^{*}\mathrm{e}^{i\tilde{\Delta}\zeta-ik_0z_i}\tilde{\phi}^{i}_{\mathrm{eS},m}(\zeta,\zeta_{\mathrm{s}}), && (4.15)\\
\dot{\tilde{\phi}}^{i}_{\mathrm{eS},m}(\zeta,\zeta_{\mathrm{s}}) =& i\sqrt{\beta_{\mathrm{R}}}\tilde{\mathcal{E}}\mathrm{e}^{-i\tilde{\Delta}\zeta+ik_0z_i}\tilde{\phi}_{\mathrm{gS},m}(\zeta,\zeta_{\mathrm{s}})-\frac{1}{2}\tilde{\phi}^{i}_{\mathrm{eS},m}(\zeta,\zeta_{\mathrm{s}})\\
&-\beta_{\mathrm{R}}\sum_{j<i}^{N}\tilde{\phi}^{j}_{\mathrm{eS},m}(\zeta,\zeta_{\mathrm{s}})\mathrm{e}^{ik_0(z_i-z_j)}-\beta_{\mathrm{L}}\sum_{j>i}^{N}\tilde{\phi}^{j}_{\mathrm{eS},m}(\zeta,\zeta_{\mathrm{s}})\mathrm{e}^{ik_0(z_j-z_i)}. && (4.16)
\end{aligned}$$

From the above equations, we see similar processes that were observed for probability amplitudes $\tilde{\phi}^{i}_{\mathrm{eR}}$ in the second-order coherence derivation: since $\tilde{\phi}^{i}_{\mathrm{eS},m}$ is a probability amplitude for an emitter in the excited state and one photon emitted outside the waveguide, the excited state can decay into any channel, which is described by the term $-\frac{1}{2}\tilde{\phi}^{i}_{\mathrm{eS},m}(\zeta,\zeta_{\mathrm{s}})$; an emitter can emit a photon into the waveguide, which can be reabsorbed by another emitter, and this process is described by the last two terms in eq. (4.16).

Output Intensity

Output intensity in photons per second, for an input field incident from the left, is given by:

$$I_{out}(\zeta_{\mathrm{d}}) = v_{\mathrm{g}}\left|\left(\hat{E}_{\mathrm{R}}(z_{\zeta_{\mathrm{d}}})+\mathcal{E}\right)|\Psi(t)\rangle\right|^{2}, \tag{4.17}$$

where $z_{\zeta_{\mathrm{d}}} = v_{\mathrm{g}}\left(\zeta_T-\zeta_{\mathrm{d}}\right)+L$, with $\zeta_T = \mathit{\Gamma} T$ and $\zeta_{\mathrm{d}} = \mathit{\Gamma} t_{\mathrm{d}}$, so that we "freeze" the wavefunction at some large time ζ_T, where all two-photon processes have occurred and the resulting photon "wave-packet" propagates in free-space until it reaches the detector at position L and detection time ζ_{d}, which is same as the way that second-order coherence was calculated. It is most convenient to expand the above equation as:

$$I_{out} = I_{E_{\mathrm{R}}E_{\mathrm{R}}}+I_{E_{\mathrm{R}}\mathcal{E}}+I_{\mathcal{E}E_{\mathrm{R}}}+I_{\mathcal{E}\mathcal{E}}, \tag{4.18}$$

where

$$\begin{aligned}
I_{E_{\mathrm{R}}E_{\mathrm{R}}} =& v_{\mathrm{g}}\left\langle\Psi(t)\middle|\hat{E}^{\dagger}_{\mathrm{R}}(z_{\zeta_{\mathrm{d}}})\hat{E}_{\mathrm{R}}(z_{\zeta_{\mathrm{d}}})\middle|\Psi(t)\right\rangle, && (4.19)\\
I_{E_{\mathrm{R}}\mathcal{E}} =& v_{\mathrm{g}}\left\langle\Psi(t)\middle|\hat{E}^{\dagger}_{\mathrm{R}}(z_{\zeta_{\mathrm{d}}})\mathcal{E}\middle|\Psi(t)\right\rangle, && (4.20)\\
I_{\mathcal{E}E_{\mathrm{R}}} =& v_{\mathrm{g}}\left\langle\Psi(t)\middle|\mathcal{E}^{*}\hat{E}_{\mathrm{R}}(z_{\zeta_{\mathrm{d}}})\middle|\Psi(t)\right\rangle, && (4.21)\\
I_{\mathcal{E}\mathcal{E}} =& v_{\mathrm{g}}\left\langle\Psi(t)\,|\,\mathcal{E}^{*}\mathcal{E}\,|\,\Psi(t)\right\rangle = v_{\mathrm{g}}\left|\mathcal{E}\right|^{2}, && (4.22)
\end{aligned}$$

as it will simplify some derivations later on. As was mentioned before, since we truncate the wavefunction ansatz up to two excitations, we only consider terms with fourth-order in the input field $\mathcal{E}$ for output intensity. We also define a dimensionless output intensity $\tilde{I} = I/\Gamma$, which gives the number of photons in a time period $1/\Gamma$. The output intensity for each component in dimensionless units (except $\tilde{I}_{\mathcal{E}\mathcal{E}}$, since that is always just $\left|\tilde{\mathcal{E}}\right|^2$) is then given by:

$$\begin{aligned}
\tilde{I}_{E_\mathrm{R}E_\mathrm{R}}(\zeta_\mathrm{e}) = &\left|\tilde{\phi}^z_\mathrm{gR}(\zeta_T,\zeta_\mathrm{e})\right|^2 + \sum_{i=1}^{N}\left|\tilde{\phi}^{z,i}_\mathrm{eR}(\zeta_T,\zeta_\mathrm{e})\right|^2 + \int \mathrm{d}\zeta'_\mathrm{e}\left|\tilde{\phi}^z_\mathrm{RR}(\zeta_T,\zeta_\mathrm{e},\zeta'_\mathrm{e})\right|^2 \\
&+ + \int \mathrm{d}\zeta'_\mathrm{e}\left|\tilde{\phi}^z_\mathrm{RR}(\zeta_T,\zeta'_\mathrm{e},\zeta_\mathrm{e})\right|^2 + \int \mathrm{d}\zeta'_\mathrm{e}\left|\tilde{\phi}^z_\mathrm{RL}(\zeta_T,\zeta_\mathrm{e},\zeta'_\mathrm{e})\right|^2 \\
&+ + \int \mathrm{d}\zeta'_\mathrm{e}\left|\tilde{\phi}^z_\mathrm{LR}(\zeta_T,\zeta'_\mathrm{e},\zeta_\mathrm{e})\right|^2 + \int \mathrm{d}\zeta_\mathrm{s}\sum_{m=1}^{N}\left|\tilde{\phi}^z_{\mathrm{RS},m}(\zeta_T,\zeta_\mathrm{s},\zeta_\mathrm{e})\right|^2, \qquad (4.23)
\end{aligned}$$

$$\begin{aligned}
\tilde{I}_{E_\mathrm{R}\mathcal{E}}(\zeta_\mathrm{e}) \quad =&\tilde{\phi}^{z*}_\mathrm{gR}(\zeta_T,\zeta_\mathrm{e})\tilde{\mathcal{E}}c_\mathrm{g}(\zeta_T) + \sum_{i=1}^{N}\tilde{\phi}^{z,i}_\mathrm{eR}(\zeta_T,\zeta_\mathrm{e})\tilde{\mathcal{E}}c^i_\mathrm{e}(\zeta_T) \\
&+ \int \mathrm{d}\zeta'_\mathrm{e}\tilde{\phi}^z_\mathrm{RR}(\zeta_T,\zeta_\mathrm{e},\zeta'_\mathrm{e})\tilde{\mathcal{E}}\tilde{\phi}^z_\mathrm{gR}(\zeta_T,\zeta'_\mathrm{e}) + \int \mathrm{d}\zeta'_\mathrm{e}\tilde{\phi}^z_\mathrm{RR}(\zeta_T,\zeta'_\mathrm{e},\zeta_\mathrm{e})\tilde{\mathcal{E}}\tilde{\phi}^z_\mathrm{gR}(\zeta_T,\zeta'_\mathrm{e}) \\
&+ \int \mathrm{d}\zeta'_\mathrm{e}\tilde{\phi}^z_\mathrm{RL}(\zeta_T,\zeta_\mathrm{e},\zeta'_\mathrm{e})\tilde{\mathcal{E}}\tilde{\phi}_\mathrm{gL}(\zeta_T,\zeta'_\mathrm{e}) + \int \mathrm{d}\zeta'_\mathrm{e}\tilde{\phi}^z_\mathrm{LR}(\zeta_T,\zeta'_\mathrm{e},\zeta_\mathrm{e})\tilde{\mathcal{E}}\tilde{\phi}_\mathrm{gL}(\zeta_T,\zeta'_\mathrm{e}) \\
&+ \int \mathrm{d}\zeta_\mathrm{s}\sum_{m=1}^{N}\tilde{\phi}^z_{\mathrm{RS},m}(\zeta_T,\zeta_\mathrm{s},\zeta_\mathrm{e})\tilde{\mathcal{E}}\tilde{\phi}^z_{\mathrm{gS},m}(\zeta_T,\zeta_\mathrm{s}) + O(\tilde{\mathcal{E}}^6), \qquad (4.24)
\end{aligned}$$

$$\tilde{I}_{\mathcal{E}E_\mathrm{R}}(\zeta_\mathrm{e}) \quad =\tilde{I}^*_{E_\mathrm{R}\mathcal{E}}, \qquad (4.25)$$

where the additional superscript "z" is used to indicate emission position integrated ($\int \mathrm{d}z_\mathrm{e}$) variables and $\zeta_\mathrm{e} = \zeta_\mathrm{d} - \Gamma\frac{L}{v_\mathrm{g}}$, as was introduced in Chapter 3. For two-photon probability amplitudes, we see terms with integration in the first or second photon emission time. These terms can be understood as follows. We evaluate instantaneous output intensity by fixing the emission time of one of the photons to ζ_e. The second photon can then be emitted either before or after ζ_e. We then need to consider all possible emission times of the other photon, which corresponds to integration over either first or second photon emission.

In Appendix B.2, it is shown that $\frac{\mathrm{d}}{\mathrm{d}\zeta_T}I_{out} = 0$, for $\zeta_T \geq \zeta_\mathrm{e} + \varepsilon$ (for simplicity, it is shown for a single emitter in a chiral waveguide). This means that we have a steady-state value of intensity as long as the "freeze" time of the wavefunction ζ_T is larger than the emission time ζ_e; this is illustrated in fig. 4.2. Since the value of the intensity does not change, we do not need to follow what happens after the fixed photon emission ζ_e and can set $\zeta_T = \zeta_\mathrm{e} + \varepsilon$. In this way, we integrate over $\int \mathrm{d}\zeta'_\mathrm{e}$ and $\int \mathrm{d}\zeta_\mathrm{s}$ in eq. (4.23), (4.24) and (4.25) until the emission time ζ_e. This corresponds to the following: for two-photon probability amplitudes,

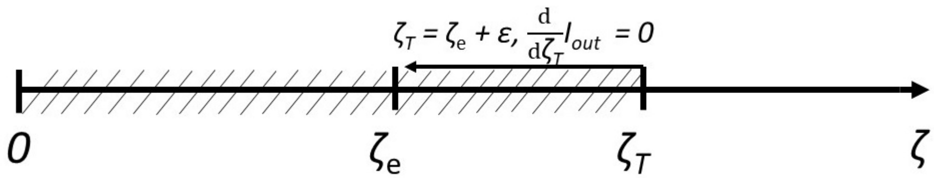

Figure 4.2: For $\zeta_T \geq \zeta_e + \varepsilon$, $\frac{d}{d\zeta_T} I_{out} = 0$, so it is enough to consider $\zeta_T = \zeta_e + \varepsilon$. The shaded region shows how much we need to integrate over $\int d\zeta_e'$ and $\int d\zeta_s$ in eq. (4.23), (4.24) and (4.25). Since $\zeta_T = \zeta_e + \varepsilon$, it is enough to consider decay outside the waveguide before emission into the waveguide.

one photon is emitted at ζ_e and we only need to consider the other photon having been emitted before it.

Intensity Extrapolation

We now have everything that is necessary to evaluate output intensity to second-order in input field and this formalism holds as long as $\tilde{\mathcal{E}} \ll 1$. However, there is another problem that requires attention. In all previous derivations, we do the following: 1) evolve emitter probability amplitudes until the first photon emission; 2) evolve emitter states again, but with new probability amplitudes, which have the previously emitted photon; 3) find the two-photon probability amplitudes and calculate the expectation values that we are interested in. In this way, we ignore the system dynamics after two-photons are emitted in the system. This was not a problem in the second-order coherence calculation, since it is normalized and we can decrease the input field as long as it makes sense numerically without loss of generalization. However, as we start increasing the input field, even for $\tilde{\mathcal{E}} \ll 1$, there comes a point when the system is constantly emitting photons and getting reexcited again, since we consider an infinitely long steady input field. When we reach this point, it is physically incorrect to ignore the system dynamics after two photons are emitted. Numerically, it means that we see the behaviour of probability amplitudes, which is seen in fig 4.3. The probability amplitudes decay without reaching even a nearly steady-state, so calculating steady-state output intensity requires a different approach.

This can be overcome by evaluating output intensity at sufficiently low input fields, so that the probability amplitudes reach a nearly steady-state and extrapolating the results to higher input intensities. The output intensity can be expanded as:

$$I_{out} = AI_{in} + BI_{in}^2, \tag{4.26}$$

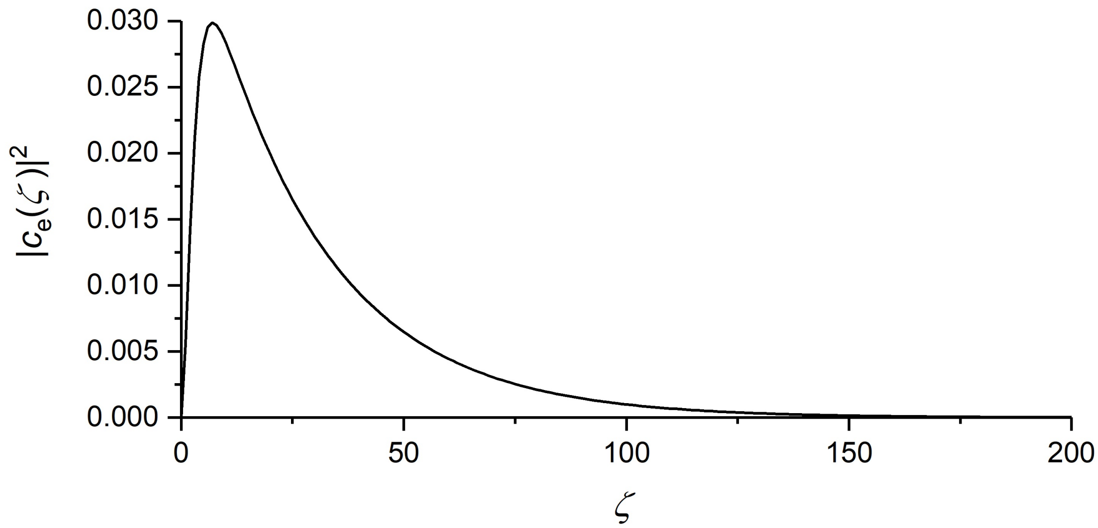

Figure 4.3: Probability of the excited emitter state for a single emitter. $\left|\tilde{\mathcal{E}}\right|^2 = 0.01$ ($\beta_R = 0.9$, $\beta_L = 0$), so the condition $\left|\tilde{\mathcal{E}}\right|^2 \ll 1$ still holds. However, the probability amplitude decays without reaching even a nearly steady-state. It shows that, for stronger input fields, dynamics of the system cannot be ignored after two photons have been emitted.

where $I_{in} = \Gamma \left|\tilde{\mathcal{E}}\right|^2$ is the input intensity in photons per second, while A and B repsectively correspond to transmission of single and two-photon number states of the input coherent field. We then evaluate output intensity as a function of input intensity. We do this at sufficiently low input fields so that the probability amplitudes reach a nearly steady-state and extract parameters A and B by fitting the data to eq. (4.26). We can then use the extracted parameters to extrapolate output intensity for higher input intensitites. This extrapolation is correct as long as $\tilde{\mathcal{E}} \ll 1$, so that three-photon processes are not probable in the system.

Also, previously we showed that we can set $\zeta_T = \zeta_e + \varepsilon$ for the "freeze" time of wavefunction. However, output intensity is still a function of emission time ζ_e, as seen from eq. (4.23), (4.24) and (4.25). ζ_e should be sufficiently large so that the intensity reaches a nearly steady-state, as illustrated in fig. 4.4. Even for large ζ_e, output intensity has a slow decay of the order $O(\mathcal{E}^6)$, which appears due to the truncation of the wavefunction ansatz up to two excitations, however, this can be discarded for $\tilde{\mathcal{E}} \ll 1$. Taking this into consideration, we can evaluate output intensity by choosing a large ζ_e, setting $\zeta_T = \zeta_e + \varepsilon$ and solving the equations of motion numerically and then using eq. (4.23), (4.24) and (4.25).

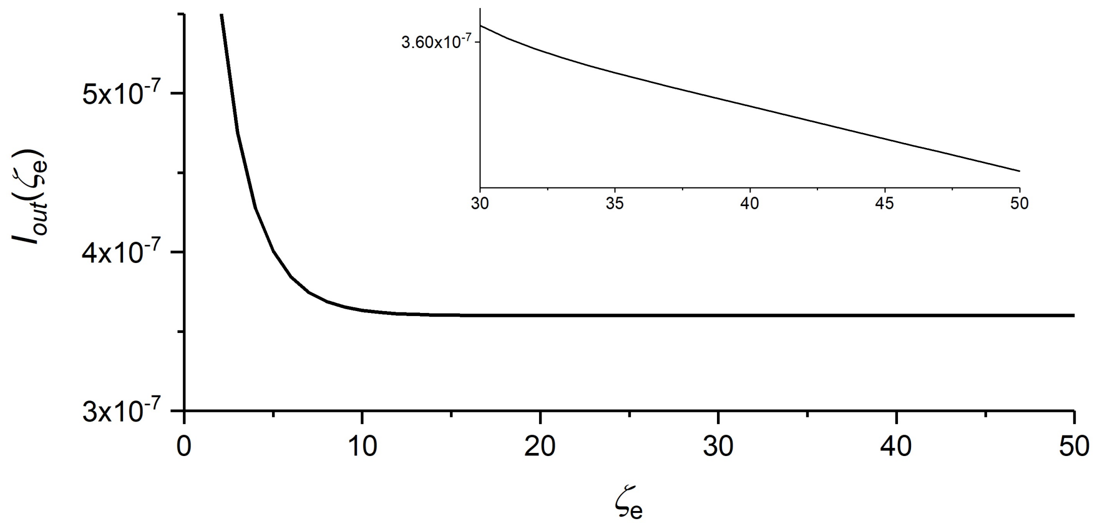

Figure 4.4: Output intensity for a single emitter as a function of emission time ζ_{e} (for $\tilde{\mathcal{E}} = 0.001$, $\beta_{\mathrm{R}} = 0.2$). To evaluate output intensity, ζ_{e} has to be chosen sufficiently large, so that a nearly steady-state is reached. Inset – on a smaller scale it can be seen that intensity slowly decays with order of $O(\mathcal{E}^6)$, which appears due to truncation up to two excitations (the system can decay to states with three excitations, which are not included in the wavefunction ansatz, as was shown in Appendix B.2).

4.2 Workaround for the Initial Dynamics of the System

As discussed in the previous section, to evaluate output intensity (eq. (4.23), (4.24) and (4.25)), we need to integrate the two-photon probability amplitudes over one of the two photons being emitted before ζ_{e}. In order to be able to do this, we need to numerically calculate evolution of probability amplitudes for each emission time with a sufficiently small step, so that the numerical integration would be precise. It is clear that this process is computationally demanding, since the calculation would have to be repeated multiple times with different initial conditions. To avoid this, we would like to do something similar to what was done in the second-order coherence calculation. In that instance, we only had to consider one emission time large enough so that the emitter probability amplitudes reach a nearly steady-state. In a nearly steady-state, the probability amplitudes only decay with a higher order of the input field, which can be discarded for $\tilde{\mathcal{E}} \ll 1$. However, to calculate output intensity, we need to consider that a photon can be emitted at any time before ζ_{e} from the time that the input field starts exciting the system. i.e. from $\zeta = 0$. So we have to perform integration backwards for two-photon probability amplitudes as $\int_0^{\zeta_{\mathrm{e}}+\varepsilon} \mathrm{d}\zeta_{\mathrm{e}}'$

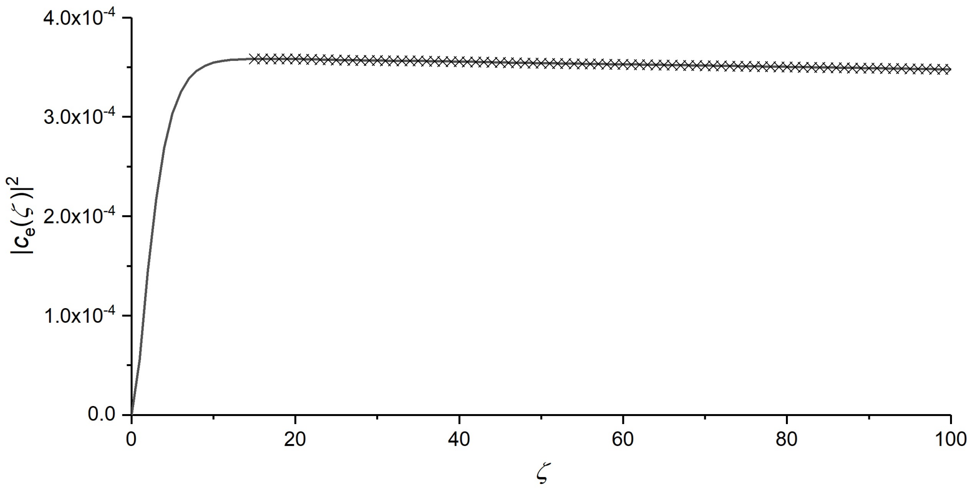

Figure 4.5: Probability of excited emitter state for a single emitter as a function of evolution time ζ ($\tilde{\mathcal{E}} = 0.001$, $\beta_R = 0.2$). Crossed region indicates a nearly steady-state, where it is enough to consider just one emission time, since the slow linear decay is of a higher order of the input field than the rest of dynamics. Initial dynamics before the steady-state, however, cannot be ignored.

and $\int_0^{\zeta_e+\varepsilon} d\zeta_s$ in eq. (4.23), (4.24) and (4.25). Note that such integration was not present for the second-order coherence. At integration times close to $\zeta = 0$, the initial dynamics of the excited emitter probability amplitudes are present, as illustrated in fig. 4.5. Since the initial condition for state amplitudes containing emitted photons is dependent on the excited emitter states (eq. (3.53), (3.54)), these initial dynamics of the system cannot be ignored, since this would result in data fit errors using eq. (4.26).

The initial dynamics of the system can be overcome using the following workaround. We first evolve the emitter states sufficiently long time (until some time ζ_{ss}), so that a nearly steady-state is reached. Then we renormalize emitter state amplitudes as:

$$\begin{aligned}
\tilde{c}_g &= \frac{1}{\sqrt{C}} c_g(\zeta_{ss}), \\
\tilde{c}_e^i &= \frac{1}{\sqrt{C}} c^i{}_e(\zeta_{ss}), \\
\tilde{c}_{ee}^{ij} &= \frac{1}{\sqrt{C}} c^{ij}{}_e(\zeta_{ss}),
\end{aligned} \tag{4.27}$$

where

$$C = |c_g|^2 + \sum_{i=1}^{N} \left| c^i{}_e \right|^2 + \sum_{i<j}^{N} \left| c^{ij}{}_e \right|^2 . \tag{4.28}$$

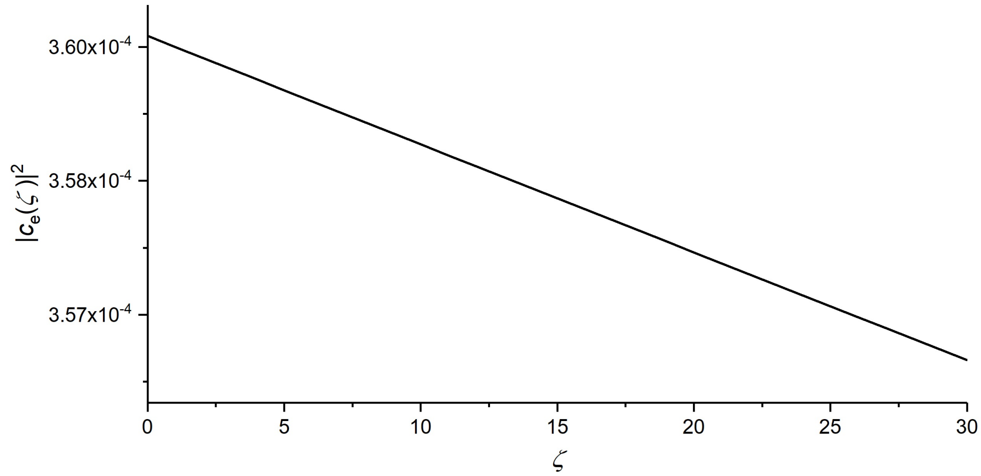

Figure 4.6: Probability of excited emitter state for a single emitter as a function of evolution time ζ ($\tilde{\mathcal{E}} = 0.001$, $\beta_\mathrm{R} = 0.2$). After using a different initial condition (eq. (4.27)), initial system dynamics are overcome and only higher order decay is observed, which can be treated as a steady-state.

We use these renormalized emitter probability amplitudes as a new initial condition for emitter states, instead of $c_\mathrm{g} = 1$. The emitter state amplitudes with these new initial conditions then evolve as shown in fig. 4.6. Initial dynamics are subdued – time-evolution shows only a higher-order decay. It is now enough to simulate system dynamics for one emission time ζ_e. Probability amplitudes at different emission times $\zeta_\mathrm{e} + \zeta'$ are then given by:

$$\tilde{\phi}^i_{\mathrm{eR}}(\zeta, \zeta_\mathrm{e} + \zeta') = \tilde{\phi}^i_{\mathrm{eR}}(\zeta - \zeta', \zeta_\mathrm{e}), \tag{4.29}$$

with the same relation for other probability amplitudes containing emitted photons.

4.3 Simulation Results

In this section, we present output intensity simulation results for multiple emitters. The output intensity was calculated at lower input fields and fitted to eq. (4.26) – transmission coefficients A and B were extracted. In fig. 4.7, output intensity was extrapolated for an input field of 1 MHz in photons per second and a total decay rate (Γ) of $2\pi \cdot 5$ MHz: $\left|\tilde{\mathcal{E}}\right|^2 = I_{in}/\Gamma = 1/10\pi$. The results were checked against analytical results [21]. As was expected, we see exponential decay of linear transmission, which matches the optical depth relation. For higher number of emitters, transmission of the two-photon state is dominant,

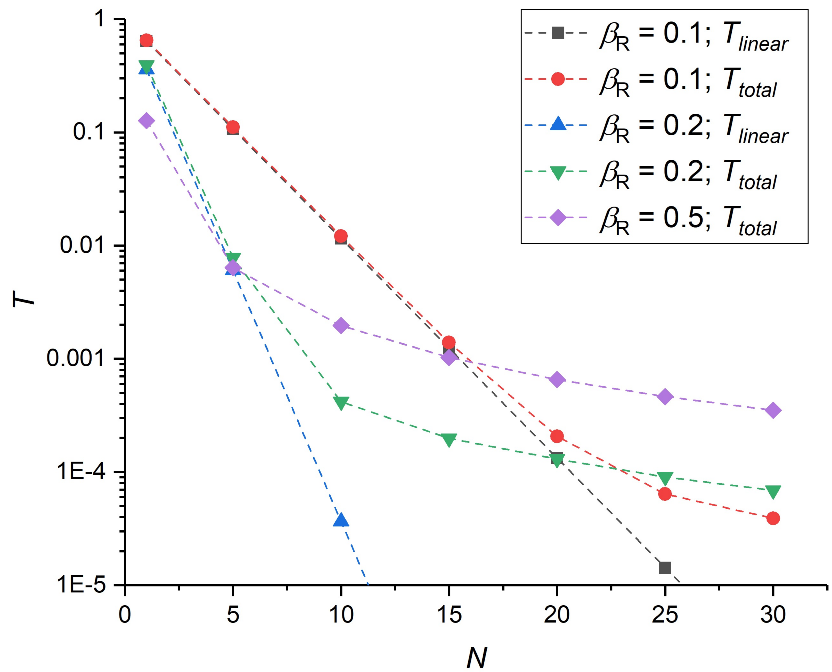

Figure 4.7: Transmission dependence on number of emitters in a chiral waveguide with different coupling factors ($\left|\tilde{\mathcal{E}}\right|^2 = 1/10\pi$, $\Delta = 0$). T_{linear} corresponds to a single-photon transmission from the coherent field expansion (coefficient A in eq. (4.26)), T_{total} is transmission of the total output field: $T_{total} = I_{out}/I_{in}$, where I_{out} is given by eq. (4.26). For higher number of emitters, two-photon number state transmission is dominant. Numerical simulation results were checked against analytical results [21].

which can be seen as an effective interaction between photons mediated by emitters. This is further encouraged by the increase of nonlinear transmission with the coupling factor β_{R}. However, nonlinear transmission consists of probability amplitudes of different states (for example, two emitted right propagating photons; one emitted left and one emitted as right-propagating; one photon passing through and another emitted as right-propagating; etc.) which interfere, so it is non-trivial to investigate which of the states is dominant at the output. It is interesting to note, though, that for $\beta_{\mathrm{R}} = 0.5$, linear transmission coefficient $A \to 0$. This shows that for $\beta_{\mathrm{R}} = 0.5$, single photons are completely lost, but pairs of photons can still be transmitted.

In fig. 4.8, simulation results for a non-chiral waveguide with uniform atom placement are shown. For $\beta_{\mathrm{L}} < \beta_{\mathrm{R}}$ (fig. 4.8, panels (a) and (b)), we find that transmission coefficients are not strongly dependent on the distance between emitters, with an exception of $k_0\Delta z = \pi$. In this case, a slight increase in linear transmission and a slight decrease in

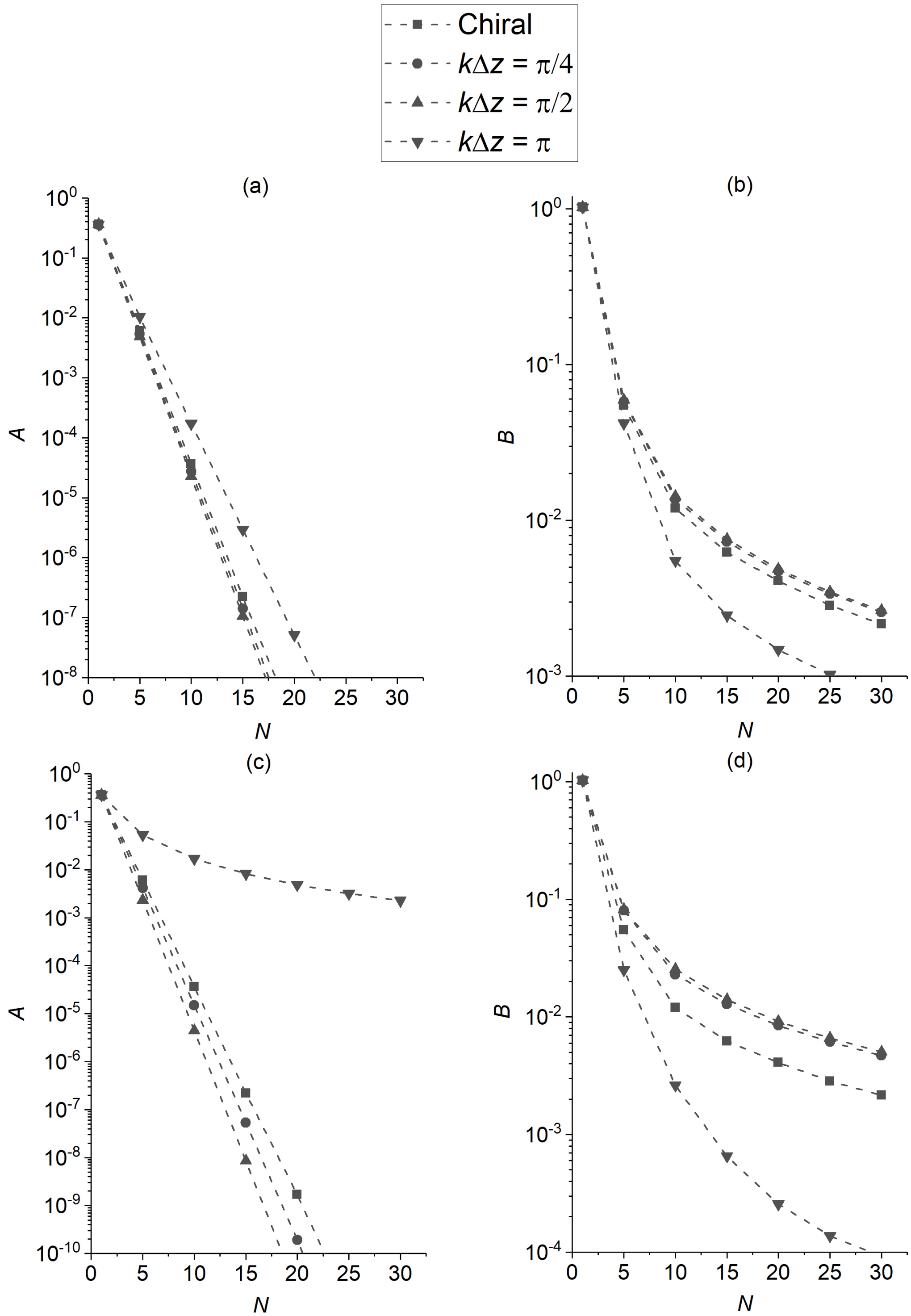

Figure 4.8: Dependence of transmission coefficients A and B on the number of emitters for $\beta_{\mathrm{R}} = 0.2$ with uniform emitter placement ($\Delta = 0$). Panels (a) and (b) – $\beta_{\mathrm{L}} = 0.05$; panels (c) and (d) – $\beta_{\mathrm{L}} = 0.2$. For $k_0\Delta z = \pi$, linear transmission is strongly enhanced, while nonlinear transmission is decreased. An opposite dependence is seen for $k_0\Delta z = \pi/2$. This suggests that output intensity can be strongly influenced by emitter placement.

the nonlinear transmission is observed. As was mentioned in Chapter 3, emitted photons interfere constructively when emitters are placed with distance $k_0\Delta z = \pi$ between them and then the system behaves as an atomic Bragg mirror [20]. Since $\beta_{\mathrm{L}} < \beta_{\mathrm{R}}$, the interference effect is partial and only slight changes are observed.

For equal coupling factors in both directions ($\beta_{\mathrm{L}} = \beta_{\mathrm{R}}$), emitter placement strongly influences output intensity (fig. 4.8, panels (c) and (d)). For $k_0\Delta z = \pi$, linear transmission does not seem to follow the optical depth relation with a strong increase in amplitude, which shows that for full constructive interference effects between emitted photons, the system completely changes its behaviour and the linear transmission is dominant. For $k_0\Delta z \leq \pi/2$, however, an opposite effect is observed – linear tranmission decreases, while nonlinear increases (the effect peaks at $k_0\Delta z = \pi/2$).

In conclusion, we see that for a large number of emitters, the nonlinear transmission is dominant most cases – in a chiral waveguide and a reciprocal waveguide with $k_0\Delta z \leq \pi/2$ distance between emitters, pairs of photons are more likely to transmit, while single photons are mostly lost. Only in the case of a reciprocal waveguide with $k_0\Delta z = \pi$ is the linear transmission is higly dominant. In comparison with the second-order coherence results discussed in Chapter 3 (fig. 3.5 and 3.6), we see that in the cases where nonlinear transmission is dominant, strong initial bunching of photons is observed, while for the linear transmission dominant case an antibunching results. However, this still shows that it is possible to change between linear and nonlinear transmission dominant output intensities by considering a reciprocal waveguide with different emitter placements.

Chapter 5

Experimental System With Multiple Emitters

In this chapter, we present simulation results for currently available multiple emitter systems which are experimentally viable [17, 16]. The waveguide-emitter systems in such experiments are typically formed by an optical glass fiber stretched across a glass chamber with a gas of cesium atoms. The fiber has subwavelength diameter and acts as a 1D waveguide for the incoming field. Since the diameter is smaller than the wavelength of light, an evanescent field is present outside the waveguide. When cooling of cesium atoms is performed, they submerge on the fiber and couple to the evanescent field. In this way, interaction with ~2000 atoms can be achieved. Nearly chiral properties of this system are possible ($\beta_{\mathrm{R}} \sim 5\%$, $\beta_{\mathrm{L}} \sim 0.5\%$, [22]), so it is in particular interesting to see how chiral properties are preserved under weak coupling to the other direction and random emitter placement. It should be noted that so far we only considered uniform emitter placement.

In fig. 5.1, we present our findings for the second-order correlation function with random emitter placements. Average results over 100 runs of the simulation are shown in the figure. $\beta_{\mathrm{R}} = 0.05$ for all simulations and several coupling factors for the other direction were considered: $\beta_{\mathrm{L}} = 0.005$ (panel (a)), $\beta_{\mathrm{L}} = 0.025$ (panel (b)) and $\beta_{\mathrm{L}} = 0.05$ (panel (c)). In fig. 5.1, we also show the random deviations of the second-order coherence with maximum and minimum results obtained during the runs of the simulation. It can be seen that for all values of β_{L}, the average results closely match the chiral behaviour of the second-order correlation function. Also, as expected, for higher values of β_{L}, the random deviations in amplitude compared to the chiral case are found to increase. However, behaviour of the oscillations was found to be the same in all cases, which suggests that the coupling β_{L} averages out for a large number of emitters with random placement, so that it can be treated as an effective decay outside the waveguide.

Nonlinear transmission was extracted for $N = 50$ and $\Delta = 0$ by calculating output intensity for different input fields and fitting the data to eq. (4.26). The fit parameters were found to depend on β_{L} as presented below.

1) For $\beta_{\mathrm{L}} = 0.005$: linear transmission coefficient A was found to deviate in the range of $2.68 \cdot 10^{-5} \leq A \leq 2.91 \cdot 10^{-5}$ with the average of $A = 2.68 \cdot 10^{-5}$ (in the chiral case $A = 2.66 \cdot 10^{-5}$); nonlinear transmission coefficient B deviated in the range $3.24 \cdot 10^{-4} \leq B \leq 3.6 \cdot 10^{-4}$ with the average of $3.49 \cdot 10^{-4}$ (in the chiral case $B = 3.5 \cdot 10^{-4}$).

2) For $\beta_{\mathrm{L}} = 0.025$: A was in the range of $2.32 \cdot 10^{-5} \leq A \leq 3.86 \cdot 10^{-5}$ with the average of $A = 2.74 \cdot 10^{-5}$; B was in the range $2.48 \cdot 10^{-4} \leq B \leq 3.93 \cdot 10^{-4}$ with the average of $B = 3.56 \cdot 10^{-4}$.

3) For $\beta_{\mathrm{L}} = 0.05$: A was in the range of $2.08 \cdot 10^{-5} \leq A \leq 5 \cdot 10^{-5}$ with the average of $A = 2.84 \cdot 10^{-5}$; B was in the range $2.01 \cdot 10^{-4} \leq B \leq 4.68 \cdot 10^{-4}$ with the average of $B = 3.76 \cdot 10^{-4}$.

The summary of above results is the same as for the second-order correlation function: average values closely match the chiral properties of linear and nonlinear transmission, while there is an increase in deviations for higher values of β_{L}. In conclusion, $g^{(2)}$ and output intensity results suggest that effective chiral behaviour is observed for a high number of emitters and random emitter placement even if the waveguide is reciprocal. Since experimentally ~2000 cesium atoms can be coupled [17], we can expect that the shown deviations would be negligible for such a large number of emitters.

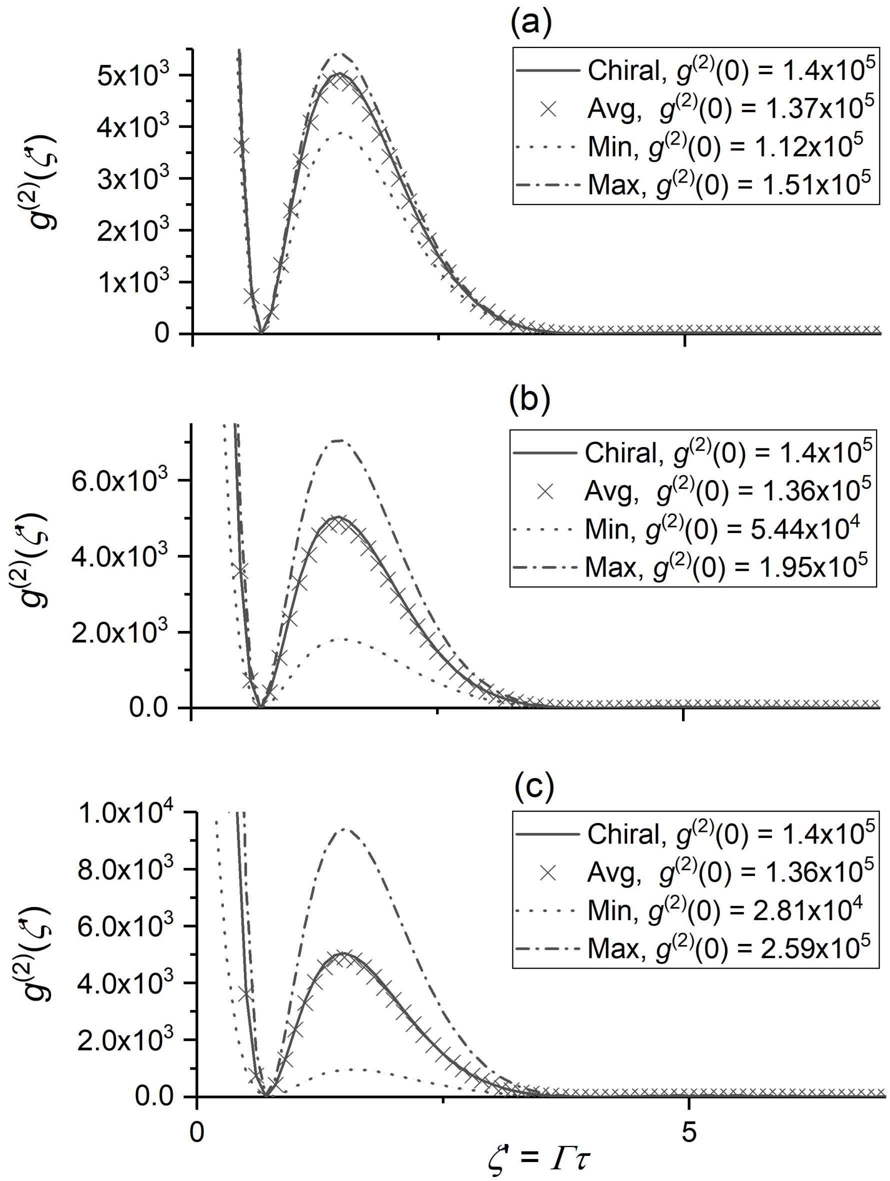

Figure 5.1: $g^{(2)}$ simulation results with random emitter placement for $N = 50$ ($\Delta = 0$). (a) – $\beta_{\mathrm{R}} = 0.05$, $\beta_{\mathrm{L}} = 0.005$; (b) – $\beta_{\mathrm{R}} = 0.05$, $\beta_{\mathrm{L}} = 0.025$; (a) – $\beta_{\mathrm{R}} = 0.05$, $\beta_{\mathrm{L}} = 0.05$. 100 simulations were performed and average, minimum and maximum results with respect to the amplitude of second-order correlation function are shown. Average dynamics closely match the chiral case. In general, the behaviour of $g^{(2)}$ is preserved over all runs, with changes only in amplitudes of oscillations. This suggests that for random emitter placement left-propagating photon coupling averages out and can be treated as effective decay outside the waveguide.

Chapter 6

Conclusions and Outlook

6.1 Conclusions

In this thesis, we developed a method to investigate nonlinear photon interactions in a system of multiple quantum emitters coupled to a waveguide. At its core, this method is designing a wavefunction ansatz and modifying it for a specific purpose. Any number of emitters, combination of coupling factors and emitter separations can be described, as well as detuning of the input field with respect to the transition frequency of the emitters. In particular, the second-order correlation function and nonlinear transmission for a weak coherent input field were calculated.

The second-order coherence at the output of a reciprocal waveguide was found to show that the emitter placement strongly influences nonlinear properties of the system. For uniform separation between emitters with $k_0\Delta z = \pi$, constructive interferences between emitted photons result in an effective single-emitter behaviour of the second-order coherence. The largest bunching of photons was found to be for distances between emitters $k_0\Delta z \leq \pi/2$. In all cases, larger number of emitters resulted in higher frequency oscillations of the second-order correlation function, which shows that collectively, emitters more effectively "squeeze" photons in time. Also, it was found that chiral waveguides are sensitive to small couplings in the other propagation direction if the emitters are placed uniformly.

Output intensity gave additional insight into the nonlinear properties of the system. It was shown that nonlinear transmission is mostly dominant when the number of emitters is large. This suggests that single photons incident on the waveguide are lost, while a two-photon state can propagate through. The only case when linear transmission is dominant was found for $k_0\Delta z = \pi$, which agrees with the second-order coherence results. Also, a method to speed up numerical simulations was developed.

Finally, we investigated the rigidness of a chiral waveguide. It was found that random emitter placement helps preserve the chiral behaviour of the system when couplings to the other propagation direction are present. This shows that non-chiral interference effects average out due to random phases that photons acquire while propagating between randomly placed emitters. Thus, the coupling to the other propagation direction can be treated as an effective decay outside the waveguide.

6.2 Outlook

Many interesting nonlinear properties of the system were found in this work with the formalism that we introduced. It would be interesting to see this work carried further. In this section, we present some directions of what could be investigated next.

First of all, the robustness of waveguides could be investigated further. Experimentally, it is a challenge to align emitters in a way that they would feel the same local electric field. This results in broadening of the emitter transition frequencies, known as inhomogeneous broadening. Our method can be used to investigate how limited the system is under this effect.

Secondly, it would be interesting to see more details regarding output intensity. As was shown, output intensity is mostly dominated by nonlinear transmission. However, part of the nonlinearly transmitted field is a state with one photon lost to the environment. A ratio between such states and states with pairs of photons could give more insight into the system. Parameters could potentially be found, for which the transmitted field consists of only photon pairs. This would be of interest, as a system with such properties could be used as an efficient two-photon filter.

Finally, there are two straightforward ways that the formalism itself could be expanded. Either emitters with more levels could be considered, or truncation of the wavefunction ansatz with up to three excitations could be examined. It can only be imagined what richness of effective nonlinear photon interactions that would give.

Appendix A

Details of the Second-Order Coherence Derivation

A.1 Interaction Picture Transformation

The Schrödinger picture Hamiltonian for a single emitter coupled to a 1D waveguide was introduced in Chapter 3 and is given by eq. (3.2). We transform to an interaction picture with respect to the free energy terms of the Hamiltonian, that is, $\hat{H}_{\mathrm{a}}$ and $\hat{H}_{\mathrm{f}}$, which are respectively given by eq. (3.4) and (3.5). The corresponding unitary transformation operator is then given by:

$$\hat{U}(t) = \mathrm{e}^{-\frac{i}{\hbar}(\hat{H}_{\mathrm{a}}+\hat{H}_{\mathrm{f}})t}.$$

As was shown in Chapter 2, the Hamiltonian describing the dynamics of the system in the interaction picture then is:

$$\hat{\tilde{H}} = \hat{U}^{\dagger}(t)\left(\hat{H}_{\mathrm{side}} + \hat{H}_{\mathrm{int}}\right)\hat{U}(t),$$

where $\hat{H}_{\mathrm{side}}$ and $\hat{H}_{\mathrm{int}}$ are respectively given by eq. (3.3) and (3.1). The Hamiltonian term $\hat{H}_{\mathrm{side}}$ commutes with the unitary operator $\hat{U}(t)$ and is thus unchanged under this transformation. To transform the interaction term of the Hamiltonian $\hat{H}_{\mathrm{int}}$, we use the Baker-Haussdorf lemma [18]:

$$\begin{aligned}
\mathrm{e}^{i\hat{G}\lambda}\hat{A}\mathrm{e}^{-i\hat{G}\lambda} &= \hat{A} + i\lambda\left[\hat{G},\hat{A}\right] + \left(\frac{i^2\lambda^2}{2!}\right)\left[\hat{G},\left[\hat{G},\hat{A}\right]\right] \\
&+ \ldots + \left(\frac{i^n\lambda^n}{n!}\right)\left[\hat{G},\left[\hat{G},\left[\hat{G},\ldots\left[\hat{G},\hat{A}\right]\right]\right]\ldots\right] + \ldots,
\end{aligned}$$

where $\hat{A}$ and $\hat{G}$ are some Hermitian operators and λ is a real number. This lemma can be immediately applied to transform the interaction term of the Hamiltonian by using $\hat{A} = \hat{H}_{\text{int}}$, $\hat{G} = \hat{H}_{\text{a}} + \hat{H}_{\text{f}}$ and $\lambda = t$. Using

$$\int \mathrm{d}k \int \mathrm{d}k' \left[\hat{a}_k^\dagger \hat{a}_k, \hat{a}_{k'}^{(\dagger)}\right] = \mp \int \mathrm{d}k \hat{a}_k^{(\dagger)}$$

and

$$\left[\hat{\sigma}_{\text{ee}}, \hat{\sigma}_{\text{eg(ge)}}\right] = \pm \hat{\sigma}_{\text{eg(ge)}},$$

the transformation results in:

$$\begin{aligned}
\mathrm{e}^{\frac{i}{\hbar}(\hat{H}_{\text{a}}+\hat{H}_{\text{f}})t} \hat{H}_{\text{int}} \mathrm{e}^{-\frac{i}{\hbar}(\hat{H}_{\text{a}}+\hat{H}_{\text{f}})t} =& -\hbar g \int \mathrm{d}k \left(\hat{\sigma}_{\text{eg}} \hat{a}_k \mathrm{e}^{ikz_{\text{a}}} + \hat{a}_k^\dagger \hat{\sigma}_{\text{ge}} \mathrm{e}^{-ikz_{\text{a}}}\right) - \\
& - \hbar g \int \mathrm{d}k \left(\hat{\sigma}_{\text{eg}} \hat{a}_k \mathrm{e}^{ikz_{\text{a}}} \left(-i\Delta_k t\right) + \hat{a}_k^\dagger \hat{\sigma}_{\text{ge}} \mathrm{e}^{-ikz_{\text{a}}} \left(i\Delta_k t\right)\right) \\
& - \hbar g \int \mathrm{d}k \left(\hat{\sigma}_{\text{eg}} \hat{a}_k \mathrm{e}^{ikz_{\text{a}}} \frac{\left(-i\Delta_k t\right)^2}{2!} + \hat{a}_k^\dagger \hat{\sigma}_{\text{ge}} \mathrm{e}^{-ikz_{\text{a}}} \frac{\left(i\Delta_k t\right)^2}{2!}\right) \\
& - \ldots \\
& - \hbar g \int \mathrm{d}k \left(\hat{\sigma}_{\text{eg}} \hat{a}_k \mathrm{e}^{ikz_{\text{a}}} \frac{\left(-i\Delta_k t\right)^n}{n!} + \hat{a}_k^\dagger \hat{\sigma}_{\text{ge}} \mathrm{e}^{-ikz_{\text{a}}} \frac{\left(i\Delta_k t\right)^n}{n!}\right) \\
=& \hbar g \int \mathrm{d}k \left(\hat{\sigma}_{\text{eg}} \hat{a}_k \mathrm{e}^{-i\Delta_k t + ikz_{\text{a}}} + \hat{a}_k^\dagger \hat{\sigma}_{\text{ge}} \mathrm{e}^{i\Delta_k t - ikz_{\text{a}}}\right),
\end{aligned}$$

where $\Delta_k = \omega_k - \omega_0$.

A.2 Rotating Frame of the Displacement Operator

We perform a rotating frame transformation of the interaction picture Hamiltonian in real space with respect to the displacement operator, given by eq. (3.15). As was presented in Chapter 2, the rotating frame Hamiltonian is then given by:

$$\hat{\tilde{H}} = i\hbar \dot{\hat{D}}^\dagger(\alpha_k) \hat{D}(\alpha_k) + \hat{D}^\dagger(\alpha_k) \hat{H} \hat{D}(\alpha_k),$$

where $\hat{H}$ is given by eq. (3.13). We consider a steady input coherent field, so the first term on the right-hand side of the above equation is zero, since $\dot{\hat{D}}(\alpha_k) = 0$. For the second term, we use the property of the displacement operator introduced in Chapter 2, which "displaces" the annihilation operator and gives:

$$\hat{D}^\dagger(\alpha_{k'}) \int \mathrm{d}k \hat{a}_k^{(\dagger)} \hat{D}(\alpha_{k'}) = \int \mathrm{d}k \left(\hat{a}_k + \alpha_k^{(*)}\right).$$

Defining $\mathcal{E} = \int \mathrm{d}k\alpha_k \mathrm{e}^{i(k-k_0)z}$, the resulting Hamiltonian is:

$$\begin{aligned}\hat{\tilde{H}} &= -\hbar\frac{i\Gamma'}{2}\hat{\sigma}_{\mathrm{ee}} - \hbar\sqrt{2\pi}\int \mathrm{d}z\delta(z-z_{\mathrm{a}})\Bigg[\hat{\sigma}_{\mathrm{eg}}\Bigg(g_{\mathrm{R}}\hat{E}_{\mathrm{R}}(z)\mathrm{e}^{-i\Delta t+ik_0z} \\ &+ g_{\mathrm{R}}\mathcal{E}\mathrm{e}^{-i\Delta t+ik_0z} + g_{\mathrm{L}}\hat{E}_{\mathrm{L}}(z)\mathrm{e}^{-i\Delta t-ik_0z}\Bigg) + \Bigg(g_{\mathrm{R}}\hat{E}^{\dagger}_{\mathrm{R}}(z)\mathrm{e}^{i\Delta t-ik_0z} \\ &+ g_{\mathrm{R}}\mathcal{E}^*\mathrm{e}^{i\Delta t-ik_0z} + g_{\mathrm{L}}\hat{E}^{\dagger}_{\mathrm{L}}(z)\mathrm{e}^{i\Delta t+ik_0z}\Bigg)\hat{\sigma}_{\mathrm{ge}}\Bigg].\end{aligned}$$

A.3 Equations of Motion for a Single Emitter With Dimensionless Variables

$$\begin{aligned}\dot{c}_{\mathrm{g}}(\zeta) =& i\sqrt{\beta_{\mathrm{R}}}\tilde{\mathcal{E}}^*\mathrm{e}^{i\tilde{\Delta}\zeta}c_{\mathrm{e}}(\zeta),\\ \dot{c}_{\mathrm{e}}(\zeta) =& i\sqrt{\beta_{\mathrm{R}}}\tilde{\mathcal{E}}\mathrm{e}^{-i\tilde{\Delta}\zeta}c_{\mathrm{g}}(\zeta) - \frac{\beta_{side}}{2}c_{\mathrm{e}}(\zeta) + i\sqrt{\beta_{\mathrm{R}}}\tilde{\phi}_{\mathrm{gR}}(\zeta,\zeta)\mathrm{e}^{-i\tilde{\Delta}\zeta}\\ &+ i\sqrt{\beta_{\mathrm{L}}}\tilde{\phi}_{\mathrm{gL}}(\zeta,\zeta)\mathrm{e}^{-i\tilde{\Delta}\zeta},\end{aligned}$$

$$\begin{aligned}\dot{\tilde{\phi}}_{\mathrm{gR}}(\zeta,\zeta_{\mathrm{e}}) =& i\sqrt{\beta_{\mathrm{R}}}c_{\mathrm{e}}(\zeta_{\mathrm{e}})\delta(\zeta-\zeta_{\mathrm{e}})\mathrm{e}^{i\tilde{\Delta}\zeta_{\mathrm{e}}} + i\sqrt{\beta_{\mathrm{R}}}\tilde{\mathcal{E}}^*\mathrm{e}^{i\tilde{\Delta}\zeta}\tilde{\phi}_{\mathrm{eR}}(\zeta,\zeta_{\mathrm{e}}),\\ \dot{\tilde{\phi}}_{\mathrm{eR}}(\zeta,\zeta_{\mathrm{e}}) =& i\sqrt{\beta_{\mathrm{R}}}\tilde{\mathcal{E}}\mathrm{e}^{-i\tilde{\Delta}\zeta}\tilde{\phi}_{\mathrm{gR}}(\zeta,\zeta_{\mathrm{e}}) - \frac{\beta_{side}}{2}\tilde{\phi}_{\mathrm{eR}}(\zeta,\zeta_{\mathrm{e}})\\ &+ i\sqrt{\beta_{\mathrm{R}}}\tilde{\phi}_{\mathrm{RR}}(\zeta,\zeta,\zeta_{\mathrm{e}})\mathrm{e}^{-i\tilde{\Delta}\zeta} + i\sqrt{\beta_{\mathrm{R}}}\tilde{\phi}_{\mathrm{RR}}(\zeta,\zeta_{\mathrm{e}},\zeta)\mathrm{e}^{-i\tilde{\Delta}\zeta}\\ &+ i\sqrt{\beta_{\mathrm{L}}}\tilde{\phi}_{\mathrm{RL}}(\zeta,\zeta_{\mathrm{e}},\zeta)\mathrm{e}^{-i\tilde{\Delta}\zeta} + i\sqrt{\beta_{\mathrm{L}}}\tilde{\phi}_{\mathrm{LR}}(\zeta,\zeta,\zeta_{\mathrm{e}})\mathrm{e}^{-i\tilde{\Delta}\zeta},\\ \dot{\tilde{\phi}}_{\mathrm{gL}}(\zeta,\zeta_{\mathrm{e}}) =& i\sqrt{\beta_{\mathrm{L}}}c_{\mathrm{e}}(\zeta_{\mathrm{e}})\delta(\zeta-\zeta_{\mathrm{e}})\mathrm{e}^{i\tilde{\Delta}\zeta_{\mathrm{e}}} + i\sqrt{\beta_{\mathrm{R}}}\tilde{\mathcal{E}}^*\mathrm{e}^{i\tilde{\Delta}\zeta}\tilde{\phi}_{\mathrm{eL}}(\zeta,\zeta_{\mathrm{e}}),\\ \dot{\tilde{\phi}}_{\mathrm{eL}}(\zeta,\zeta_{\mathrm{e}}) =& i\sqrt{\beta_{\mathrm{R}}}\tilde{\mathcal{E}}\mathrm{e}^{-i\tilde{\Delta}\zeta}\tilde{\phi}_{\mathrm{gL}}(\zeta,\zeta_{\mathrm{e}}) - \frac{\beta_{side}}{2}\tilde{\phi}_{\mathrm{eL}}(\zeta,\zeta_{\mathrm{e}})\\ &+ i\sqrt{\beta_{\mathrm{L}}}\tilde{\phi}_{\mathrm{LL}}(\zeta,\zeta,\zeta_{\mathrm{e}})\mathrm{e}^{-i\tilde{\Delta}\zeta} + i\sqrt{\beta_{\mathrm{L}}}\tilde{\phi}_{\mathrm{LL}}(\zeta,\zeta_{\mathrm{e}},\zeta)\mathrm{e}^{-i\tilde{\Delta}\zeta}\\ &+ i\sqrt{\beta_{\mathrm{R}}}\tilde{\phi}_{\mathrm{RL}}(\zeta,\zeta,\zeta_{\mathrm{e}})\mathrm{e}^{-i\tilde{\Delta}\zeta} + i\sqrt{\beta_{\mathrm{R}}}\tilde{\phi}_{\mathrm{LR}}(\zeta,\zeta_{\mathrm{e}},\zeta)\mathrm{e}^{-i\tilde{\Delta}\zeta},\end{aligned}$$

$$\begin{aligned}\dot{\tilde{\phi}}_{\mathrm{RR}}(\zeta,\zeta_{\mathrm{e2}},\zeta_{\mathrm{e1}}) =& i\sqrt{\beta_{\mathrm{R}}}\tilde{\phi}_{\mathrm{eR}}(\zeta_{\mathrm{e2}},\zeta_{\mathrm{e1}})\delta(\zeta-\zeta_{\mathrm{e2}})\mathrm{e}^{i\tilde{\Delta}\zeta_{\mathrm{e2}}},\\ \dot{\tilde{\phi}}_{\mathrm{LR}}(\zeta,\zeta_{\mathrm{e2}},\zeta_{\mathrm{e1}}) =& i\sqrt{\beta_{\mathrm{L}}}\tilde{\phi}_{\mathrm{eR}}(\zeta_{\mathrm{e2}},\zeta_{\mathrm{e1}})\delta(\zeta-\zeta_{\mathrm{e2}})\mathrm{e}^{i\tilde{\Delta}\zeta_{\mathrm{e2}}},\\ \dot{\tilde{\phi}}_{\mathrm{RL}}(\zeta,\zeta_{\mathrm{e2}},\zeta_{\mathrm{e1}}) =& i\sqrt{\beta_{\mathrm{R}}}\tilde{\phi}_{\mathrm{eL}}(\zeta_{\mathrm{e2}},\zeta_{\mathrm{e1}})\delta(\zeta-\zeta_{\mathrm{e2}})\mathrm{e}^{i\tilde{\Delta}\zeta_{\mathrm{e2}}},\\ \dot{\tilde{\phi}}_{\mathrm{LL}}(\zeta,\zeta_{\mathrm{e2}},\zeta_{\mathrm{e1}}) =& i\sqrt{\beta_{\mathrm{L}}}\tilde{\phi}_{\mathrm{eL}}(\zeta_{\mathrm{e2}},\zeta_{\mathrm{e1}})\delta(\zeta-\zeta_{\mathrm{e2}})\mathrm{e}^{i\tilde{\Delta}\zeta_{\mathrm{e2}}}.\end{aligned}$$

A.4 Coupled Equations of Motion for a Multiple Emitter System

Keeping in mind that we use dimensionless variables in the same way that we did in the single emitter case and omitting "∼" which was used to indicate that, the equations of motion for the probability amplitudes of a system with N emitters are given by:

$$
\begin{aligned}
\dot{c}_{\mathrm{g}}(\zeta) \;=& i\sqrt{\beta_{\mathrm{R}}}\sum_{i=1}^{N}\mathcal{E}^{*}\mathrm{e}^{i\Delta\zeta-ik_0z_i}c_{\mathrm{e}}^{i}(\zeta),\\
\dot{c}_{\mathrm{e}}^{i}(\zeta) \;=& i\sqrt{\beta_{\mathrm{R}}}\mathcal{E}\mathrm{e}^{-i\Delta\zeta+ik_0z_i}c_{\mathrm{g}}(\zeta)-\frac{\beta_{side}}{2}c_{\mathrm{e}}^{i}(\zeta)+i\sqrt{\beta_{\mathrm{R}}}\sum_{j<i}^{N}\mathcal{E}^{*}\mathrm{e}^{i\Delta\zeta-ik_0z_j}c_{\mathrm{ee}}^{ji}(\zeta)\\
&+i\sqrt{\beta_{\mathrm{R}}}\sum_{i<j}^{N}\mathcal{E}^{*}\mathrm{e}^{i\Delta\zeta-ik_0z_j}c_{\mathrm{ee}}^{ij}(\zeta)+i\sqrt{\beta_{\mathrm{R}}}\int\mathrm{d}z_{\mathrm{e}}\phi_{\mathrm{gR}}(\zeta,\zeta+\mathit{\Gamma}\frac{z_{\mathrm{e}}-z_i}{v_{\mathrm{g}}},z_{\mathrm{e}})\mathrm{e}^{-i\Delta\zeta+ik_0z_i}\\
&+i\sqrt{\beta_{\mathrm{R}}}\int\mathrm{d}z_{\mathrm{e}}\phi_{\mathrm{gL}}(\zeta,\zeta-\mathit{\Gamma}\frac{z_{\mathrm{e}}-z_i}{v_{\mathrm{g}}},z_{\mathrm{e}})\mathrm{e}^{-i\Delta\zeta-ik_0z_i},\\
\dot{c}_{\mathrm{ee}}^{ij}(\zeta) =& i\sqrt{\beta_{\mathrm{R}}}\mathcal{E}\mathrm{e}^{-i\Delta\zeta+ik_0z_j}c_{\mathrm{e}}^{i}(\zeta)+i\sqrt{\beta_{\mathrm{R}}}\mathcal{E}\mathrm{e}^{-i\Delta\zeta+ik_0z_i}c_{\mathrm{e}}^{j}(\zeta)-\beta_{side}c_{\mathrm{ee}}^{ij}(\zeta)\\
&+i\sqrt{\beta_{\mathrm{R}}}\int\mathrm{d}z_{\mathrm{e}}\phi_{\mathrm{eR}}^{i}(\zeta,\zeta+\mathit{\Gamma}\frac{z_{\mathrm{e}}-z_j}{v_{\mathrm{g}}},z_{\mathrm{e}})\mathrm{e}^{-i\Delta\zeta+ik_0z_j}\\
&+i\sqrt{\beta_{\mathrm{R}}}\int\mathrm{d}z_{\mathrm{e}}\phi_{\mathrm{eR}}^{j}(\zeta,\zeta+\mathit{\Gamma}\frac{z_{\mathrm{e}}-z_i}{v_{\mathrm{g}}},z_{\mathrm{e}})\mathrm{e}^{-i\Delta\zeta+ik_0z_i}\\
&+i\sqrt{\beta_{\mathrm{L}}}\int\mathrm{d}z_{\mathrm{e}}\phi_{\mathrm{eL}}^{i}(\zeta,\zeta-\mathit{\Gamma}\frac{z_{\mathrm{e}}-z_j}{v_{\mathrm{g}}},z_{\mathrm{e}})\mathrm{e}^{-i\Delta\zeta-ik_0z_j}\\
&+i\sqrt{\beta_{\mathrm{L}}}\int\mathrm{d}z_{\mathrm{e}}\phi_{\mathrm{eL}}^{j}(\zeta,\zeta-\mathit{\Gamma}\frac{z_{\mathrm{e}}-z_i}{v_{\mathrm{g}}},z_{\mathrm{e}})\mathrm{e}^{-i\Delta\zeta-ik_0z_i},
\end{aligned}
$$

$$
\begin{aligned}
\dot{\phi}_{\mathrm{gR}}(\zeta,\zeta_{\mathrm{e}},z_{\mathrm{e}}) =& i\sqrt{\beta_{\mathrm{R}}}\sum_{i=1}^{N}c_{\mathrm{e}}^{i}(\zeta_{\mathrm{e}})\delta(\zeta-\zeta_{\mathrm{e}})\delta(z_{\mathrm{e}}-z_i)\mathrm{e}^{i\Delta\zeta_{\mathrm{e}}-ik_0z_e}\\
&+i\sqrt{\beta_{\mathrm{R}}}\sum_{i=1}^{N}\mathcal{E}^{*}\mathrm{e}^{i\Delta\zeta-ik_0z_i}\phi_{\mathrm{eR}}^{i}(\zeta,\zeta_{\mathrm{e}},z_{\mathrm{e}}),\\
\dot{\phi}_{\mathrm{eR}}^{i}(\zeta,\zeta_{\mathrm{e}},z_{\mathrm{e}}) =& i\sqrt{\beta_{\mathrm{R}}}\sum_{j<i}^{N}c_{\mathrm{ee}}^{ji}(\zeta_{\mathrm{e}})\delta(\zeta-\zeta_{\mathrm{e}})\delta(z_{\mathrm{e}}-z_j)\mathrm{e}^{i\Delta\zeta_{\mathrm{e}}-ik_0z_e}\\
&+i\sqrt{\beta_{\mathrm{R}}}\sum_{j>i}^{N}c_{\mathrm{ee}}^{ij}(\zeta_{\mathrm{e}})\delta(\zeta-\zeta_{\mathrm{e}})\delta(z_{\mathrm{e}}-z_j)\mathrm{e}^{i\Delta\zeta_{\mathrm{e}}-ik_0z_e}\\
&+i\sqrt{\beta_{\mathrm{R}}}\mathcal{E}\mathrm{e}^{-i\Delta\zeta+ik_0z_i}\phi_{\mathrm{gR}}(\zeta,\zeta_{\mathrm{e}},z_{\mathrm{e}})-\frac{\beta_{side}}{2}\phi_{\mathrm{eR}}^{i}(\zeta,\zeta_{\mathrm{e}},z_{\mathrm{e}})
\end{aligned}
$$

$$
\begin{aligned}
&+ i\sqrt{\beta_{\mathrm{R}}}\int \mathrm{d}z'_{\mathrm{e}}\phi_{\mathrm{RR}}(\zeta,\zeta+\mathit{\Gamma}\frac{z'_{\mathrm{e}}-z_i}{v_{\mathrm{g}}},\zeta_{\mathrm{e}},z'_{\mathrm{e}},z_{\mathrm{e}})\mathrm{e}^{-i\Delta\zeta+ik_0z_i}\\
&+ i\sqrt{\beta_{\mathrm{R}}}\int \mathrm{d}z'_{\mathrm{e}}\phi_{\mathrm{RR}}(\zeta,\zeta_{\mathrm{e}},\zeta+\mathit{\Gamma}\frac{z'_{\mathrm{e}}-z_i}{v_{\mathrm{g}}},z_{\mathrm{e}},z'_{\mathrm{e}})\mathrm{e}^{-i\Delta\zeta+ik_0z_i}\\
&+ i\sqrt{\beta_{\mathrm{L}}}\int \mathrm{d}z'_{\mathrm{e}}\phi_{\mathrm{LR}}(\zeta,\zeta-\mathit{\Gamma}\frac{z'_{\mathrm{e}}-z_i}{v_{\mathrm{g}}},\zeta_{\mathrm{e}},z'_{\mathrm{e}},z_{\mathrm{e}})\mathrm{e}^{-i\Delta\zeta-ik_0z_i}\\
&+ i\sqrt{\beta_{\mathrm{L}}}\int \mathrm{d}z'_{\mathrm{e}}\phi_{\mathrm{RL}}(\zeta,\zeta_{\mathrm{e}},\zeta-\mathit{\Gamma}\frac{z'_{\mathrm{e}}-z_i}{v_{\mathrm{g}}},z_{\mathrm{e}},z'_{\mathrm{e}})\mathrm{e}^{-i\Delta\zeta-ik_0z_i},
\end{aligned}
$$

$$
\begin{aligned}
\dot{\phi}_{\mathrm{gL}}(\zeta,\zeta_{\mathrm{e}},z_{\mathrm{e}}) =& i\sqrt{\beta_{\mathrm{L}}}\sum_{i=1}^{N} c^i_{\mathrm{e}}(\zeta_{\mathrm{e}})\delta(\zeta-\zeta_{\mathrm{e}})\delta(z_{\mathrm{e}}-z_i)\mathrm{e}^{i\Delta\zeta_{\mathrm{e}}+ik_0z_e}\\
&+ i\sqrt{\beta_{\mathrm{R}}}\sum_{i=1}^{N}\mathcal{E}^*\mathrm{e}^{i\Delta\zeta-ik_0z_i}\phi^i_{\mathrm{eL}}(\zeta,\zeta_{\mathrm{e}},z_{\mathrm{e}}),\\
\dot{\phi}^i_{\mathrm{eL}}(\zeta,\zeta_{\mathrm{e}},z_{\mathrm{e}}) =& i\sqrt{\beta_{\mathrm{L}}}\sum_{j<i}^{N} c^{ji}_{\mathrm{ee}}(\zeta_{\mathrm{e}})\delta(\zeta-\zeta_{\mathrm{e}})\delta(z_{\mathrm{e}}-z_j)\mathrm{e}^{i\Delta\zeta_{\mathrm{e}}+ik_0z_e}\\
&+ i\sqrt{\beta_{\mathrm{L}}}\sum_{j>i}^{N} c^{ij}_{\mathrm{ee}}(\zeta_{\mathrm{e}})\delta(\zeta-\zeta_{\mathrm{e}})\delta(z_{\mathrm{e}}-z_j)\mathrm{e}^{i\Delta\zeta_{\mathrm{e}}+ik_0z_e}\\
&+ i\sqrt{\beta_{\mathrm{R}}}\mathcal{E}\mathrm{e}^{-i\Delta\zeta+ik_0z_i}\phi_{\mathrm{gL}}(\zeta,\zeta_{\mathrm{e}},z_{\mathrm{e}})-\frac{\beta_{side}}{2}\phi^i_{\mathrm{eL}}(\zeta,\zeta_{\mathrm{e}},z_{\mathrm{e}})\\
&+ i\sqrt{\beta_{\mathrm{L}}}\int \mathrm{d}z'_{\mathrm{e}}\phi_{\mathrm{LL}}(\zeta,\zeta+\mathit{\Gamma}\frac{z'_{\mathrm{e}}-z_i}{v_{\mathrm{g}}},\zeta_{\mathrm{e}},z'_{\mathrm{e}},z_{\mathrm{e}})\mathrm{e}^{-i\Delta\zeta-ik_0z_i}\\
&+ i\sqrt{\beta_{\mathrm{L}}}\int \mathrm{d}z'_{\mathrm{e}}\phi_{\mathrm{LL}}(\zeta,\zeta_{\mathrm{e}},\zeta+\mathit{\Gamma}\frac{z'_{\mathrm{e}}-z_i}{v_{\mathrm{g}}},,z_{\mathrm{e}},z'_{\mathrm{e}})\mathrm{e}^{-i\Delta\zeta-ik_0z_i}\\
&+ i\sqrt{\beta_{\mathrm{R}}}\int \mathrm{d}z'_{\mathrm{e}}\phi_{\mathrm{RL}}(\zeta,\zeta_{\mathrm{e}},\zeta-\mathit{\Gamma}\frac{z'_{\mathrm{e}}-z_i}{v_{\mathrm{g}}},z_{\mathrm{e}},z'_{\mathrm{e}})\mathrm{e}^{-i\Delta\zeta+ik_0z_i}\\
&\ i\sqrt{\beta_{\mathrm{R}}}\int \mathrm{d}z'_{\mathrm{e}}\phi_{\mathrm{LR}}(\zeta,\zeta-\mathit{\Gamma}\frac{z'_{\mathrm{e}}-z_i}{v_{\mathrm{g}}},\zeta_{\mathrm{e}},z'_{\mathrm{e}},z_{\mathrm{e}})\mathrm{e}^{-i\Delta\zeta+ik_0z_i},
\end{aligned}
$$

$$
\begin{aligned}
\dot{\phi}_{\mathrm{RR}}(\zeta,\zeta_{\mathrm{e2}},\zeta_{\mathrm{e1}},z_{\mathrm{e2}},z_{\mathrm{e1}}) =& i\sqrt{\beta_{\mathrm{R}}}\sum_{i=1}^{N}\phi^i_{\mathrm{eR}}(\zeta_{\mathrm{e2}},\zeta_{\mathrm{e1}},z_{\mathrm{e1}})\delta(\zeta-\zeta_{\mathrm{e2}})\delta(z_{\mathrm{e2}}-z_i)\mathrm{e}^{i\Delta\zeta_{\mathrm{e2}}-ik_0z_{e2}},\\
\dot{\phi}_{\mathrm{LR}}(\zeta,\zeta_{\mathrm{e2}},\zeta_{\mathrm{e1}},z_{\mathrm{e2}},z_{\mathrm{e1}}) =& i\sqrt{\beta_{\mathrm{L}}}\sum_{i=1}^{N}\phi^i_{\mathrm{eR}}(\zeta_{\mathrm{e2}},\zeta_{\mathrm{e1}},z_{\mathrm{e1}})\delta(\zeta-\zeta_{\mathrm{e2}})\delta(z_{\mathrm{e2}}-z_i)\mathrm{e}^{i\Delta\zeta_{\mathrm{e2}}+ik_0z_{e2}},\\
\dot{\phi}_{\mathrm{RL}}(\zeta,\zeta_{\mathrm{e2}},\zeta_{\mathrm{e1}},z_{\mathrm{e2}},z_{\mathrm{e1}}) =& i\sqrt{\beta_{\mathrm{R}}}\sum_{i=1}^{N}\phi^i_{\mathrm{eL}}(\zeta_{\mathrm{e2}},\zeta_{\mathrm{e1}},z_{\mathrm{e1}})\delta(\zeta-\zeta_{\mathrm{e2}})\delta(z_{\mathrm{e2}}-z_i)\mathrm{e}^{i\Delta\zeta_{\mathrm{e2}}-ik_0z_{e2}},\\
\dot{\phi}_{\mathrm{LL}}(\zeta,\zeta_{\mathrm{e2}},\zeta_{\mathrm{e1}},z_{\mathrm{e2}},z_{\mathrm{e1}}) \quad& i\sqrt{\beta_{\mathrm{L}}}\sum_{i=1}^{N}\phi^i_{\mathrm{eL}}(\zeta_{\mathrm{e2}},\zeta_{\mathrm{e1}},z_{\mathrm{e1}})\delta(\zeta-\zeta_{\mathrm{e2}})\delta(z_{\mathrm{e2}}-z_i)\mathrm{e}^{i\Delta\zeta_{\mathrm{e2}}+ik_0z_{e2}}.
\end{aligned}
$$

As in the single emitter case, we define two time windows $0 < \zeta < \zeta_\mathrm{e}+\varepsilon$ and $\zeta_\mathrm{e}+\varepsilon < \zeta < \infty$, to uncouple some of the equations. For $0 < \zeta < \zeta_\mathrm{e}+\varepsilon$ we can formally integrate the equations for ϕ_{gR}, ϕ_{gL}, ϕ^i_{eR} and ϕ^i_{eL}:

$$
\begin{aligned}
\phi_{\mathrm{gR}}(\zeta,\zeta_\mathrm{e},z_\mathrm{e}) =& i\sqrt{\beta_\mathrm{R}}\sum_{i=1}^{N} c^i_\mathrm{e}(\zeta)\theta(\zeta-\zeta_\mathrm{e})\theta(z_\mathrm{e}-z_i)\mathrm{e}^{i\Delta\zeta-ik_0z_i},\\
\phi_{\mathrm{gL}}(\zeta,\zeta_\mathrm{e},z_\mathrm{e}) =& i\sqrt{\beta_\mathrm{L}}\sum_{i=1}^{N} c^i_\mathrm{e}(\zeta)\theta(\zeta-\zeta_\mathrm{e})\theta(z_\mathrm{e}-z_i)\mathrm{e}^{i\Delta\zeta+ik_0z_i},\\
\phi^i_{\mathrm{eR}}(\zeta,\zeta_\mathrm{e},z_\mathrm{e}) =& i\sqrt{\beta_\mathrm{R}}\sum_{j<i}^{N} c^{ji}_\mathrm{ee}(\zeta)\theta(\zeta-\zeta_\mathrm{e})\theta(z_\mathrm{e}-z_j)\mathrm{e}^{i\Delta\zeta-ik_0z_j}\\
&+ i\sqrt{\beta_\mathrm{R}}\sum_{j>i}^{N} c^{ij}_\mathrm{ee}(\zeta)\theta(\zeta-\zeta_\mathrm{e})\theta(z_\mathrm{e}-z_j)\mathrm{e}^{i\Delta\zeta-ik_0z_j},\\
\phi^i_{\mathrm{eL}}(\zeta,\zeta_\mathrm{e},z_\mathrm{e}) =& i\sqrt{\beta_\mathrm{L}}\sum_{j<i}^{N} c^{ji}_\mathrm{ee}(\zeta)\theta(\zeta-\zeta_\mathrm{e})\theta(z_\mathrm{e}-z_j)\mathrm{e}^{i\Delta\zeta+ik_0z_j}\\
&+ i\sqrt{\beta_\mathrm{L}}\sum_{j>i}^{N} c^{ij}_\mathrm{ee}(\zeta)\theta(\zeta-\zeta_\mathrm{e})\theta(z_\mathrm{e}-z_j)\mathrm{e}^{i\Delta\zeta+ik_0z_j}.
\end{aligned}
$$

Plugging this in to equations of motion for c^i_e and c^{ij}_ee, we get the following:

$$
\begin{aligned}
\dot{c}^i_\mathrm{e}(\zeta) =& i\sqrt{\beta_\mathrm{R}}\mathcal{E}\mathrm{e}^{-i\Delta\zeta+ik_0z_i}c_\mathrm{g}(\zeta) - \frac{\beta_{side}}{2}c^i_\mathrm{e}(\zeta) + i\sqrt{\beta_\mathrm{R}}\sum_{j<i}^{N}\mathcal{E}^*\mathrm{e}^{i\Delta\zeta-ik_0z_j}c^{ji}_\mathrm{ee}(\zeta)\\
&+ i\sqrt{\beta_\mathrm{R}}\sum_{i<j}^{N}\mathcal{E}^*\mathrm{e}^{i\Delta\zeta-ik_0z_j}c^{ij}_\mathrm{ee}(\zeta) - \beta_\mathrm{R}\sum_{j\leq i}c^j_\mathrm{e}(\zeta)\theta(\mathit{\Gamma}\frac{z_i-z_j}{v_\mathrm{g}})\mathrm{e}^{ik_0(z_i-z_j)}\\
&- \beta_\mathrm{L}\sum_{j\geq i}c^j_\mathrm{e}(\zeta)\theta(\mathit{\Gamma}\frac{z_j-z_i}{v_\mathrm{g}})\mathrm{e}^{ik_0(z_j-z_i)},\\
\dot{c}^{ij}_\mathrm{ee}(\zeta) =& i\sqrt{\beta_\mathrm{R}}\mathcal{E}\mathrm{e}^{-i\Delta\zeta+ik_0z_j}c^i_\mathrm{e}(\zeta) + i\sqrt{\beta_\mathrm{R}}\mathcal{E}\mathrm{e}^{-i\Delta\zeta+ik_0z_i}c^j_\mathrm{e}(\zeta) - \mathit{\Gamma}'c^{ij}_\mathrm{ee}(\zeta)\\
&- \beta_\mathrm{R}\sum_{j'<i}^{N}c^{j'i}_\mathrm{ee}(\zeta)\theta(\mathit{\Gamma}\frac{z_j-z_{j'}}{v_\mathrm{g}})\mathrm{e}^{ik_0(z_j-z_{j'})} - \beta_\mathrm{R}\sum_{j'>i}^{N}c^{ij'}_\mathrm{ee}(\zeta)\theta(\mathit{\Gamma}\frac{z_\mathrm{j}-z_{j'}}{v_\mathrm{g}})\mathrm{e}^{ik_0(z_j-z_{j'})}\\
&- \beta_\mathrm{R}\sum_{i'<j}^{N}c^{i'j}_\mathrm{ee}(\zeta)\theta(\mathit{\Gamma}\frac{z_i-z_{i'}}{v_\mathrm{g}})\mathrm{e}^{ik_0(z_i-z_{i'})} - \beta_\mathrm{L}\sum_{j'>i}^{N}c^{ij'}_\mathrm{ee}(\zeta)\theta(\mathit{\Gamma}\frac{z_{j'}-z_j}{v_\mathrm{g}})\mathrm{e}^{ik_0(z_{j'}-z_j)}\\
&- \beta_\mathrm{L}\sum_{i'<j}^{N}c^{i'j}_\mathrm{ee}(\zeta)\theta(\mathit{\Gamma}\frac{z_{i'}-z_i}{v_\mathrm{g}})\mathrm{e}^{ik_0(z_{i'}-z_i)} - \beta_\mathrm{L}\sum_{i'>j}^{N}c^{ji'}_\mathrm{ee}(\zeta)\theta(\mathit{\Gamma}\frac{z_{i'}-z_i}{v_\mathrm{g}})\mathrm{e}^{ik_0(z_{i'}-z_i)}.
\end{aligned}
$$

Using the above derivation, the equations of motion that completely describe the dynamics of the system in the time window $0 < \zeta < \zeta_{\mathrm{e}} + \varepsilon$ are given by:

$$
\begin{aligned}
\dot{c}_{\mathrm{g}}(\zeta) \; =& i\sqrt{\beta_{\mathrm{R}}}\sum_{i=1}^{N}\mathcal{E}^{*}\mathrm{e}^{i\Delta\zeta-ik_0z_i}c_{\mathrm{e}}^{i}(\zeta),\\
\dot{c}_{\mathrm{e}}^{i}(\zeta) \; =& i\sqrt{\beta_{\mathrm{R}}}\mathcal{E}\mathrm{e}^{-i\Delta\zeta+ik_0z_i}c_{\mathrm{g}}(\zeta)-\frac{1}{2}c_{\mathrm{e}}^{i}(\zeta)+i\sqrt{\beta_{\mathrm{R}}}\sum_{j<i}\mathcal{E}^{*}\mathrm{e}^{i\Delta\zeta-ik_0z_j}c_{\mathrm{ee}}^{ji}(\zeta)\\
&+i\sqrt{\beta_{\mathrm{R}}}\sum_{i<j}\mathcal{E}^{*}\mathrm{e}^{i\Delta\zeta-ik_0z_j}c_{\mathrm{ee}}^{ij}(\zeta)-\beta_{\mathrm{R}}\sum_{j<i}c_{\mathrm{e}}^{j}(\zeta)\mathrm{e}^{ik_0(z_i-z_j)}-\beta_{\mathrm{L}}\sum_{j>i}c_{\mathrm{e}}^{j}(\zeta)\mathrm{e}^{ik_0(z_j-z_i)},\\
\dot{c}_{\mathrm{ee}}^{ij}(\zeta) =& i\sqrt{\beta_{\mathrm{R}}}\mathcal{E}\mathrm{e}^{-i\Delta\zeta+ik_0z_j}c_{\mathrm{e}}^{i}(\zeta)+i\sqrt{\beta_{\mathrm{R}}}\mathcal{E}\mathrm{e}^{-i\Delta\zeta+ik_0z_i}c_{\mathrm{e}}^{j}(\zeta)-c_{\mathrm{ee}}^{ij}(\zeta)\\
&-\beta_{\mathrm{R}}\sum_{j'<i}c_{\mathrm{ee}}^{j'i}(\zeta)\mathrm{e}^{ik_0(z_j-z_{j'})}-\beta_{\mathrm{R}}\sum_{j'<j,j'>i}c_{\mathrm{ee}}^{ij'}(\zeta)\mathrm{e}^{ik_0(z_j-z_{j'})}\\
&-\beta_{\mathrm{R}}\sum_{i'<i,}c_{\mathrm{ee}}^{i'j}(\zeta)\mathrm{e}^{ik_0(z_i-z_{i'})}-\beta_{\mathrm{L}}\sum_{j'>j}c_{\mathrm{ee}}^{ij'}(\zeta)\mathrm{e}^{ik_0(z_{j'}-z_j)}\\
&-\beta_{\mathrm{L}}\sum_{i'>i,i'<j}^{N}c_{\mathrm{ee}}^{i'j}(\zeta)\mathrm{e}^{ik_0(z_{i'}-z_i)}-\beta_{\mathrm{L}}\sum_{i'>j}^{N}c_{\mathrm{ee}}^{ji'}(\zeta)\mathrm{e}^{ik_0(z_{i'}-z_i)}.
\end{aligned}
$$

Appendix B

Details of the Output Intensity Derivation

B.1 Emitter Probability Amplitudes With Decay Outside the Waveguide

Using eq. (4.1), (4.3) and (4.4), time-evolution of the probability amplitudes for the excited emitters states (ground emitter state has no dependence on states that have photons emitted outside the waveguide, so its equation of motion is unchanged) are given by:

$$
\begin{aligned}
\dot{c}_{\mathrm{e}}^{i}(\zeta) =& i\sqrt{\beta_{\mathrm{R}}}\mathcal{E}\mathrm{e}^{-i\tilde{\Delta}\zeta+ik_0z_i}c_{\mathrm{g}}(\zeta)+i\sqrt{\beta_{\mathrm{side}}}\tilde{\phi}_{\mathrm{gS},i}(\zeta,\zeta)\mathrm{e}^{-i\tilde{\Delta}\zeta}\\
&+i\sqrt{\beta_{\mathrm{R}}}\sum_{j<i}^{N}\mathcal{E}^{*}\mathrm{e}^{i\tilde{\Delta}\zeta-ik_0z_j}c_{\mathrm{ee}}^{ji}(\zeta)\\
&+i\sqrt{\beta_{\mathrm{R}}}\sum_{i<j}^{N}\mathcal{E}^{*}\mathrm{e}^{i\tilde{\Delta}\zeta-ik_0z_j}c_{\mathrm{ee}}^{ij}(\zeta)\\
&+i\sqrt{\beta_{\mathrm{R}}}\int\mathrm{d}z_{\mathrm{e}}\tilde{\phi}_{\mathrm{gR}}(\zeta,\zeta+\Gamma\frac{z_{\mathrm{e}}-z_i}{v_{\mathrm{g}}},z_{\mathrm{e}})\mathrm{e}^{-i\tilde{\Delta}\zeta+ik_0z_i}\\
&+i\sqrt{\beta_{\mathrm{R}}}\int\mathrm{d}z_{\mathrm{e}}\tilde{\phi}_{\mathrm{gL}}(\zeta,\zeta-\Gamma\frac{z_{\mathrm{e}}-z_i}{v_{\mathrm{g}}},z_{\mathrm{e}})\mathrm{e}^{-i\tilde{\Delta}\zeta-ik_0z_i},\\
\dot{c}_{\mathrm{ee}}^{ij}(\zeta) =& i\sqrt{\beta_{\mathrm{R}}}\mathcal{E}\mathrm{e}^{-i\tilde{\Delta}\zeta+ik_0z_j}c_{\mathrm{e}}^{i}(\zeta)\\
&+i\sqrt{\beta_{\mathrm{side}}}\tilde{\phi}_{\mathrm{eS},j}^{i}(\zeta,\zeta)\mathrm{e}^{-i\tilde{\Delta}\zeta}+i\sqrt{\beta_{\mathrm{side}}}\tilde{\phi}_{\mathrm{eS},i}^{j}(\zeta,\zeta)\mathrm{e}^{-i\tilde{\Delta}\zeta}\\
&+i\sqrt{\beta_{\mathrm{R}}}\mathcal{E}\mathrm{e}^{-i\tilde{\Delta}\zeta+ik_0z_i}c_{\mathrm{e}}^{j}(\zeta)\\
&+i\sqrt{\beta_{\mathrm{R}}}\int\mathrm{d}z_{\mathrm{e}}\tilde{\phi}_{\mathrm{eR}}^{i}(\zeta,\zeta+\Gamma\frac{z_{\mathrm{e}}-z_j}{v_{\mathrm{g}}},z_{\mathrm{e}})\mathrm{e}^{-i\tilde{\Delta}\zeta+ik_0z_j}
\end{aligned}
$$

$$
\begin{aligned}
&+ i\sqrt{\beta_{\mathrm{R}}}\int \mathrm{d}z_{\mathrm{e}}\tilde{\phi}^{j}_{\mathrm{eR}}(\zeta,\zeta+\mathit{\Gamma}\frac{z_{\mathrm{e}}-z_i}{v_{\mathrm{g}}},z_{\mathrm{e}})\mathrm{e}^{-i\tilde{\Delta}\zeta+ik_0z_i}\\
&+ i\sqrt{\beta_{\mathrm{L}}}\int \mathrm{d}z_{\mathrm{e}}\tilde{\phi}^{i}_{\mathrm{eL}}(\zeta,\zeta-\mathit{\Gamma}\frac{z_{\mathrm{e}}-z_j}{v_{\mathrm{g}}},z_{\mathrm{e}})\mathrm{e}^{-i\tilde{\Delta}\zeta-ik_0z_j}\\
&+ i\sqrt{\beta_{\mathrm{L}}}\int \mathrm{d}z_{\mathrm{e}}\tilde{\phi}^{j}_{\mathrm{eL}}(\zeta,\zeta-\mathit{\Gamma}\frac{z_{\mathrm{e}}-z_i}{v_{\mathrm{g}}},z_{\mathrm{e}})\mathrm{e}^{-i\tilde{\Delta}\zeta-ik_0z_i}.
\end{aligned}
$$

For $0<\zeta<\zeta_{\mathrm{s}}+\varepsilon$, we can formally integrate equations of motion for probability amplitudes $\tilde{\phi}_{\mathrm{gS},i}$ and $\tilde{\phi}^{i}_{\mathrm{eS},m}(\zeta,\zeta)$, which are given by eq. (4.5) and (4.6), respectively. Integration gives

$$
\begin{aligned}
\tilde{\phi}_{\mathrm{gS},i}(\zeta,\zeta_{\mathrm{s}}) &= i\sqrt{\beta_{\mathrm{side}}}c^{i}_{\mathrm{e}}(\zeta)\theta(\zeta-\zeta_{\mathrm{s}})\mathrm{e}^{i\tilde{\Delta}\zeta},\\
\tilde{\phi}^{i}_{\mathrm{eS},m}(\zeta,\zeta_{\mathrm{s}}) &= i\sqrt{\beta_{\mathrm{side}}}c^{im}_{\mathrm{ee}}(\zeta)\delta(\zeta-\zeta_{\mathrm{s}})\mathrm{e}^{i\tilde{\Delta}\zeta}.
\end{aligned}
$$

Plugging this back in to above equations of motion for c^{i}_{e} and c^{ij}_{ee}, we get

$$
\begin{aligned}
\dot{c}^{i}_{\mathrm{e}}(\zeta) &= i\sqrt{\beta_{\mathrm{R}}}\mathcal{E}\mathrm{e}^{-i\tilde{\Delta}\zeta+ik_0z_i}c_{\mathrm{g}}(\zeta)-\frac{\beta_{side}}{2}c^{i}_{\mathrm{e}}(\zeta)\\
&+ i\sqrt{\beta_{\mathrm{R}}}\sum_{j<i}^{N}\mathcal{E}^{*}\mathrm{e}^{i\tilde{\Delta}\zeta-ik_0z_j}c^{ji}_{\mathrm{ee}}(\zeta)\\
&+ i\sqrt{\beta_{\mathrm{R}}}\sum_{i<j}^{N}\mathcal{E}^{*}\mathrm{e}^{i\tilde{\Delta}\zeta-ik_0z_j}c^{ij}_{\mathrm{ee}}(\zeta)\\
&+ i\sqrt{\beta_{\mathrm{R}}}\int \mathrm{d}z_{\mathrm{e}}\tilde{\phi}_{\mathrm{gR}}(\zeta,\zeta+\mathit{\Gamma}\frac{z_{\mathrm{e}}-z_i}{v_{\mathrm{g}}},z_{\mathrm{e}})\mathrm{e}^{-i\tilde{\Delta}\zeta+ik_0z_i}\\
&+ i\sqrt{\beta_{\mathrm{R}}}\int \mathrm{d}z_{\mathrm{e}}\tilde{\phi}_{\mathrm{gL}}(\zeta,\zeta-\mathit{\Gamma}\frac{z_{\mathrm{e}}-z_i}{v_{\mathrm{g}}},z_{\mathrm{e}})\mathrm{e}^{-i\tilde{\Delta}\zeta-ik_0z_i},\\
\dot{c}^{ij}_{\mathrm{ee}}(\zeta) &= i\sqrt{\beta_{\mathrm{R}}}\mathcal{E}\mathrm{e}^{-i\tilde{\Delta}\zeta+ik_0z_j}c^{i}_{\mathrm{e}}(\zeta)-\beta_{side}c^{ij}_{\mathrm{ee}}(\zeta)\\
&+ i\sqrt{\beta_{\mathrm{R}}}\mathcal{E}\mathrm{e}^{-i\tilde{\Delta}\zeta+ik_0z_i}c^{j}_{\mathrm{e}}(\zeta)-\beta_{side}c^{ij}_{\mathrm{ee}}(\zeta)\\
&+ i\sqrt{\beta_{\mathrm{R}}}\int \mathrm{d}z_{\mathrm{e}}\tilde{\phi}^{i}_{\mathrm{eR}}(\zeta,\zeta+\mathit{\Gamma}\frac{z_{\mathrm{e}}-z_j}{v_{\mathrm{g}}},z_{\mathrm{e}})\mathrm{e}^{-i\tilde{\Delta}\zeta+ik_0z_j}\\
&+ i\sqrt{\beta_{\mathrm{R}}}\int \mathrm{d}z_{\mathrm{e}}\tilde{\phi}^{j}_{\mathrm{eR}}(\zeta,\zeta+\mathit{\Gamma}\frac{z_{\mathrm{e}}-z_i}{v_{\mathrm{g}}},z_{\mathrm{e}})\mathrm{e}^{-i\tilde{\Delta}\zeta+ik_0z_i}\\
&+ i\sqrt{\beta_{\mathrm{L}}}\int \mathrm{d}z_{\mathrm{e}}\tilde{\phi}^{i}_{\mathrm{eL}}(\zeta,\zeta-\mathit{\Gamma}\frac{z_{\mathrm{e}}-z_j}{v_{\mathrm{g}}},z_{\mathrm{e}})\mathrm{e}^{-i\tilde{\Delta}\zeta-ik_0z_j}\\
&+ i\sqrt{\beta_{\mathrm{L}}}\int \mathrm{d}z_{\mathrm{e}}\tilde{\phi}^{j}_{\mathrm{eL}}(\zeta,\zeta-\mathit{\Gamma}\frac{z_{\mathrm{e}}-z_i}{v_{\mathrm{g}}},z_{\mathrm{e}})\mathrm{e}^{-i\tilde{\Delta}\zeta-ik_0z_i},
\end{aligned}
$$

which matches the equations of motion derived with an effective decay to the side Hamiltonian, given in Appendix A.4.

B.2 Steady-State Output Intensity

For $\zeta_T \geq \zeta_e + \varepsilon$, the derivative of ouput intensity gives (considering a chiral waveguide and a single emitter for simplification):

$$
\begin{aligned}
\frac{\mathrm{d}}{\mathrm{d}\zeta_T}\tilde{I}_{\mathcal{E}\mathcal{E}} &= \frac{\mathrm{d}}{\mathrm{d}\zeta_T}\left|\mathcal{E}\right|^2 = 0, \\
\frac{\mathrm{d}}{\mathrm{d}\zeta_T}\tilde{I}_{E_\mathrm{R}E_\mathrm{R}}(\zeta_\mathrm{e}) &= -i\sqrt{\beta_\mathrm{R}}\mathcal{E}\mathrm{e}^{-i\tilde{\Delta}\zeta_T}\tilde{\phi}^*_{\mathrm{eR}}(\zeta_T,\zeta_\mathrm{e})\tilde{\phi}_{\mathrm{gR}}(\zeta_T,\zeta_\mathrm{e}) \\
&+ \tilde{\phi}^*_{\mathrm{gR}}(\zeta,\zeta_\mathrm{e})i\sqrt{\beta_\mathrm{R}}\mathcal{E}^*\mathrm{e}^{i\tilde{\Delta}\zeta_T}\tilde{\phi}_{\mathrm{eR}}(\zeta_T,\zeta_\mathrm{e}) \\
&+ \left(-i\sqrt{\beta_\mathrm{R}}\mathcal{E}^*\mathrm{e}^{i\tilde{\Delta}\zeta_T}\tilde{\phi}^*_{\mathrm{gR}}(\zeta_T,\zeta_\mathrm{e}) - \frac{1}{2}\tilde{\phi}^*_{\mathrm{eR}}(\zeta_T,\zeta_\mathrm{e})\right)\tilde{\phi}_{\mathrm{eR}}(\zeta_T,\zeta_\mathrm{e}) \\
&+ \tilde{\phi}^*_{\mathrm{eR}}(\zeta_T,\zeta_\mathrm{e})\left(i\sqrt{\beta_\mathrm{R}}\tilde{\mathcal{E}}\mathrm{e}^{-i\tilde{\Delta}\zeta_T}\tilde{\phi}_{\mathrm{gR}}(\zeta_T,\zeta_\mathrm{e}) - \frac{1}{2}\tilde{\phi}_{\mathrm{eR}}(\zeta_T,\zeta_\mathrm{e})\right) \\
&- i\sqrt{\beta_\mathrm{R}}\int \mathrm{d}\zeta'_\mathrm{e}\tilde{\phi}^*_{\mathrm{eR}}(\zeta'_\mathrm{e},\zeta_\mathrm{e})\delta(\zeta_T-\zeta'_\mathrm{e})\mathrm{e}^{-i\tilde{\Delta}\zeta'_\mathrm{e}}\tilde{\phi}_{\mathrm{RR}}(\zeta_T,\zeta'_\mathrm{e},\zeta_\mathrm{e}) \\
&+ \tilde{\phi}^*_{\mathrm{RR}}(\zeta_T,\zeta'_\mathrm{e},\zeta_\mathrm{e})i\sqrt{\beta_\mathrm{R}}\int \mathrm{d}\zeta'_\mathrm{e}\tilde{\phi}_{\mathrm{eR}}(\zeta'_\mathrm{e},\zeta_\mathrm{e})\delta(\zeta_T-\zeta'_\mathrm{e})\mathrm{e}^{i\tilde{\Delta}\zeta'_\mathrm{e}} \\
&- i\sqrt{\beta_\mathrm{side}}\int \mathrm{d}\zeta_\mathrm{s}\tilde{\phi}^*_{\mathrm{eR}}(\zeta_\mathrm{s},\zeta_\mathrm{e})\delta(\zeta_T-\zeta_\mathrm{s})\mathrm{e}^{-i\tilde{\Delta}\zeta_\mathrm{s}}\tilde{\phi}_{\mathrm{RS}}(\zeta_T,\zeta_\mathrm{s},\zeta_\mathrm{e}) \\
&+ i\sqrt{\beta_\mathrm{side}}\int \mathrm{d}\zeta_\mathrm{s}\tilde{\phi}_{\mathrm{eR}}(\zeta_\mathrm{s},\zeta_\mathrm{e})\delta(\zeta_T-\zeta_\mathrm{s})\mathrm{e}^{i\tilde{\Delta}\zeta_\mathrm{s}}\tilde{\phi}^*_{\mathrm{RS}}(\zeta_T,\zeta_\mathrm{s},\zeta_\mathrm{e}) \\
&= 0,
\end{aligned}
$$

where $i\sqrt{\beta_\mathrm{R}}\int \mathrm{d}\zeta'_\mathrm{e}\tilde{\phi}^*_{\mathrm{eR}}(\zeta'_\mathrm{e},\zeta_\mathrm{e})\delta(\zeta_T-\zeta'_\mathrm{e})\mathrm{e}^{-i\tilde{\Delta}\zeta'_\mathrm{e}}\tilde{\phi}_{\mathrm{RR}}(\zeta_T,\zeta'_\mathrm{e},\zeta_\mathrm{e}) = \frac{\beta_\mathrm{R}}{2}\left|\tilde{\phi}_{\mathrm{eR}}(\zeta_T,\zeta_\mathrm{e})\right|^2$, $i\sqrt{\beta_\mathrm{side}}\int \mathrm{d}\zeta_\mathrm{s}\tilde{\phi}^*_{\mathrm{eR}}(\zeta_\mathrm{s},\zeta_\mathrm{e})\delta(\zeta_T-\zeta_\mathrm{s})\mathrm{e}^{-i\tilde{\Delta}\zeta_\mathrm{s}}\tilde{\phi}_{\mathrm{RS}}(\zeta_T,\zeta_\mathrm{s},\zeta_\mathrm{e}) = \frac{\beta_\mathrm{side}}{2}\left|\tilde{\phi}_{\mathrm{eR}}(\zeta_T,\zeta_\mathrm{e})\right|^2$ and $\beta_\mathrm{side}+\beta_\mathrm{R} = 1$ (for a chiral waveguide there is no coupling to the left-propagating photons) was used. Also,

$$
\begin{aligned}
\frac{\mathrm{d}}{\mathrm{d}\zeta_T}\tilde{I}_{E_\mathrm{R}\mathcal{E}}(\zeta_\mathrm{e}) &= -i\sqrt{\beta_\mathrm{R}}\mathcal{E}\mathrm{e}^{-i\tilde{\Delta}\zeta_T}\tilde{\phi}^*_{\mathrm{eR}}(\zeta_T,\zeta_\mathrm{e})\mathcal{E}c_\mathrm{g}(\zeta_T) + \tilde{\phi}^*_{\mathrm{gR}}(\zeta,\zeta_\mathrm{e})i\sqrt{\beta_\mathrm{R}}\mathcal{E}^*\mathrm{e}^{i\tilde{\Delta}\zeta_T}c_\mathrm{e}(\zeta_T) \\
&+ \left(-i\sqrt{\beta_\mathrm{R}}\mathcal{E}^*\mathrm{e}^{i\tilde{\Delta}\zeta_T}\tilde{\phi}^*_{\mathrm{gR}}(\zeta_T,\zeta_\mathrm{e}) - \frac{1}{2}\tilde{\phi}^*_{\mathrm{eR}}(\zeta_T,\zeta_\mathrm{e})\right)\mathcal{E}c_\mathrm{e}(\zeta_T) \\
&+ \tilde{\phi}^*_{\mathrm{eR}}(\zeta_T,\zeta_\mathrm{e})\mathcal{E}\left(i\sqrt{\beta_\mathrm{R}}\mathcal{E}\mathrm{e}^{-i\tilde{\Delta}\zeta_T}c_\mathrm{g}(\zeta_T) - \frac{1}{2}c_\mathrm{e}(\zeta_T)\right) \\
&- i\sqrt{\beta_\mathrm{R}}\int \mathrm{d}\zeta'_\mathrm{e}\tilde{\phi}^*_{\mathrm{eR}}(\zeta'_\mathrm{e},\zeta_\mathrm{e})\delta(\zeta_T-\zeta'_\mathrm{e})\mathrm{e}^{-i\tilde{\Delta}\zeta'_\mathrm{e}}\mathcal{E}\tilde{\phi}_{\mathrm{gR}}(\zeta_T,\zeta'_\mathrm{e}) \\
&+ \int \mathrm{d}\zeta'_\mathrm{e}\tilde{\phi}^*_{\mathrm{RR}}(\zeta_T,\zeta'_\mathrm{e},\zeta_\mathrm{e})\mathcal{E}i\sqrt{\beta_\mathrm{R}}\mathcal{E}^*\mathrm{e}^{i\tilde{\Delta}\zeta_T}\tilde{\phi}_{\mathrm{eR}}(\zeta_T,\zeta_\mathrm{e}) \\
&- i\sqrt{\beta_\mathrm{side}}\int \mathrm{d}\zeta_\mathrm{s}\tilde{\phi}^*_{\mathrm{eR}}(\zeta_\mathrm{s},\zeta_\mathrm{e})\delta(\zeta_T-\zeta_\mathrm{s})\mathrm{e}^{-i\tilde{\Delta}\zeta_\mathrm{s}}\mathcal{E}\tilde{\phi}_{\mathrm{gS}}(\zeta_T,\zeta_\mathrm{s})
\end{aligned}
$$

$$
\begin{aligned}
&+ \quad \int \mathrm{d}\zeta_{\mathrm{s}} \tilde{\phi}^{*}_{\mathrm{RS}}(\zeta_T, \zeta_{\mathrm{s}}, \zeta_{\mathrm{e}}) \mathcal{E} i \sqrt{\beta_{\mathrm{R}}} \tilde{\mathcal{E}}^{*} \mathrm{e}^{i\tilde{\Delta}\zeta_T} \tilde{\phi}_{\mathrm{eS}}(\zeta_T, \zeta_{\mathrm{s}}) \\
&= \quad \int \mathrm{d}\zeta'_{\mathrm{e}} \tilde{\phi}^{*}_{\mathrm{RR}}(\zeta_T, \zeta'_{\mathrm{e}}, \zeta_{\mathrm{e}}) \mathcal{E} i \sqrt{\beta_{\mathrm{R}}} \mathcal{E}^{*} \mathrm{e}^{i\tilde{\Delta}\zeta_T} \tilde{\phi}_{\mathrm{eR}}(\zeta_T, \zeta_{\mathrm{e}}) \\
&+ \quad \int \mathrm{d}\zeta_{\mathrm{s}} \tilde{\phi}^{*}_{\mathrm{RS}}(\zeta_T, \zeta_{\mathrm{s}}, \zeta_{\mathrm{e}}) \mathcal{E} i \sqrt{\beta_{\mathrm{R}}} \tilde{\mathcal{E}}^{*} \mathrm{e}^{i\tilde{\Delta}\zeta_T} \tilde{\phi}_{\mathrm{eS}}(\zeta_T, \zeta_{\mathrm{s}}),
\end{aligned}
$$

where $i\sqrt{\beta_{\mathrm{R}}} \int \mathrm{d}\zeta'_{\mathrm{e}} \tilde{\phi}^{*}_{\mathrm{eR}}(\zeta'_{\mathrm{e}}, \zeta_{\mathrm{e}}) \delta(\zeta_T - \zeta'_{\mathrm{e}}) \mathrm{e}^{-i\tilde{\Delta}\zeta'_{\mathrm{e}}} \mathcal{E} \tilde{\phi}_{\mathrm{gR}}(\zeta_T, \zeta'_{\mathrm{e}}) = \beta_{\mathrm{R}} \tilde{\phi}^{*}_{\mathrm{eR}}(\zeta_T, \zeta_{\mathrm{e}}) \mathcal{E} c_{\mathrm{e}}(\zeta_T)$ and $i\sqrt{\beta_{\mathrm{side}}} \int \mathrm{d}\zeta_{\mathrm{s}} \tilde{\phi}^{*}_{\mathrm{eR}}(\zeta_{\mathrm{s}}, \zeta_{\mathrm{e}}) \delta(\zeta_T - \zeta_{\mathrm{s}}) \mathrm{e}^{-i\tilde{\Delta}\zeta_{\mathrm{s}}} \mathcal{E} \tilde{\phi}_{\mathrm{gS}}(\zeta_T, \zeta_{\mathrm{s}}) = \beta_{\mathrm{side}} \tilde{\phi}^{*}_{\mathrm{eR}}(\zeta_T, \zeta_{\mathrm{e}}) \mathcal{E} c_{\mathrm{e}}(\zeta_T)$ and $\beta_{\mathrm{side}} + \beta_{\mathrm{R}} = 1$ was used.

We see that the derivative is non-zero for $\tilde{I}_{E_{\mathrm{R}}\mathcal{E}}$. However, notice that the leftover terms are of the order $O(\tilde{\mathcal{E}}^6)$. The most we can investigate with this formalism is $O(\tilde{\mathcal{E}}^4)$, since we truncate our wavefunction up to two excitations. These leftover terms are most likely due to the truncation, since some states can decay to a higher order, which is not included in our description. For $\tilde{\mathcal{E}} \ll 1$, we can in any case discard terms of order $O(\tilde{\mathcal{E}}^6)$ and approximate $\frac{\mathrm{d}}{\mathrm{d}\zeta_T} I_{E_{\mathrm{R}}\mathcal{E}}(\zeta_{\mathrm{e}}) = 0$. Similarly, since $\tilde{I}_{\mathcal{E}E_{\mathrm{R}}}(\zeta_{\mathrm{e}}) = \tilde{I}^{*}_{E_{\mathrm{R}}\mathcal{E}}$, the same description holds and we can treat the total output intensity as steady for $\zeta_T \geq \zeta_{\mathrm{e}} + \varepsilon$.

Bibliography

[1] Darrick E. Chang, Anders S. Sørensen, Eugene A. Demler, and Mikhail D. Lukin. A single-photon transistor using nanoscale surface plasmons. *Nat Phys*, 3(11):807–812, November 2007.

[2] L.-M. Duan and H. J. Kimble. Scalable photonic quantum computation through cavity-assisted interactions. *Phys. Rev. Lett.*, 92:127902, Mar 2004.

[3] David d'Enterria and Gustavo G. da Silveira. Observing light-by-light scattering at the large hadron collider. *Phys. Rev. Lett.*, 111:080405, Aug 2013.

[4] Robert W. Boyd. *Nonlinear Optics, Third Edition.* Academic Press, 3rd edition, 2008.

[5] Peter Lodahl, Sahand Mahmoodian, and Søren Stobbe. Interfacing single photons and single quantum dots with photonic nanostructures. *Rev. Mod. Phys.*, 87:347–400, May 2015.

[6] T. G. Tiecke, J. D. Thompson, N. P. de Leon, L. R. Liu, V. Vuletic, and M. D. Lukin. Nanophotonic quantum phase switch with a single atom. *Nature*, 508(7495):241–244, April 2014.

[7] Bastian Hacker, Stephan Welte, Gerhard Rempe, and Stephan Ritter. A photon-photon quantum gate based on a single atom in an optical resonator. *Nature*, 536(7615):193–196, August 2016.

[8] M. Arcari, I. Söllner, A. Javadi, S. Lindskov Hansen, S. Mahmoodian, J. Liu, H. Thyrrestrup, E. H. Lee, J. D. Song, S. Stobbe, and P. Lodahl. Near-unity coupling efficiency of a quantum emitter to a photonic crystal waveguide. *Phys. Rev. Lett.*, 113:093603, Aug 2014.

[9] A. Javadi, I. Söllner, M. Arcari, S. Lindskov Hansen, L. Midolo, S. Mahmoodian, G. Kiršanskė, T. Pregnolato, E. H. Lee, J. D. Song, S. Stobbe, and P. Lodahl. Single-photon non-linear optics with a quantum dot in a waveguide. 6:8655, October 2015.

[10] D. Witthaut and A. S. Sørensen. Photon scattering by a three-level emitter in a one-dimensional waveguide. *New Journal of Physics*, 12(4):043052, 2010.

[11] Sumanta Das, Vincent E. Elfving, Sanli Faez, and Anders S. Sørensen. Interfacing superconducting qubits and single optical photons using molecules in waveguides. *Phys. Rev. Lett.*, 118:140501, 2017.

[12] Yao-Lung L. Fang, Huaixiu Zheng, and Harold U. Baranger. One-dimensional waveguide coupled to multiple qubits: photon-photon correlations. *EPJ Quantum Technology*, 1(1):3, January 2014.

[13] Sahand Mahmoodian, Kasper Prindal-Nielsen, Immo Söllner, Søren Stobbe, and Peter Lodahl. Engineering chiral light-matter interaction in photonic crystal waveguides with slow light. *Opt. Mater. Express*, 7(1):43–51, January 2017.

[14] Peter Lodahl, Sahand Mahmoodian, Søren Stobbe, Arno Rauschenbeutel, Philipp Schneeweiss, Jürgen Volz, Hannes Pichler, and Peter Zoller. Chiral quantum optics. *Nature*, 541(7638):473–480, January 2017.

[15] Sahand Mahmoodian, Peter Lodahl, and Anders S. Sørensen. Quantum networks with chiral-light-matter interaction in waveguides. *Phys. Rev. Lett.*, 117(24):240501, December 2016.

[16] H. L. Sørensen, J.-B. Béguin, K. W. Kluge, I. Iakoupov, A. S. Sørensen, J. H. Müller, E. S. Polzik, and J. Appel. Coherent backscattering of light off one-dimensional atomic strings. *Phys. Rev. Lett.*, 117:133604, Sep 2016.

[17] C. Østfeldt, J.-B. Béguin, F. T. Pedersen, E. S. Polzik, J. Helge Müller, and J. Appel. Dipole force free optical control and cooling of nanofiber trapped atoms. *ArXiv e-prints*, August 2017.

[18] J.J. Sakurai and J. Napolitano. *Modern Quantum Mechanics*. Addison-Wesley, 2011.

[19] C. Gerry and P. Knight. *Introductory Quantum Optics*. Cambridge University Press, 2005.

[20] D E Chang, L Jiang, A V Gorshkov, and H J Kimble. Cavity QED with atomic mirrors. *New Journal of Physics*, 14(6):063003, 2012.

[21] Private communication with Sahand Mahmoodian.

[22] Private communication with Jörg Helge Müller.